Frequency characteristics of lower limb muscle responses to proprioceptive perturbations evoked by Achilles tendon vibration during standing and the influence of age and stroke

by

Robyn Lynne Mildren

M.Sc., The University of Guelph, 2015

B.Sc., The University of Guelph, 2013

A THESIS SUBMITTED IN PARTIAL FULFILLMENT OF

THE REQUIREMENTS FOR THE DEGREE OF

DOCTOR OF PHILOSOPHY

in

THE FACULTY OF GRADUATE AND POSTDOCTORAL STUDIES

(Kinesiology)

THE UNIVERSITY OF BRITISH COLUMBIA

(Vancouver)

July 2020

The following individuals certify that they have read, and recommend to the Faculty of Graduate and Postdoctoral Studies for acceptance, the dissertation entitled:

Frequency characteristics of lower limb muscle responses to proprioceptive perturbations evoked by Achilles tendon vibration during standing and the influence of age and stroke

submitted by Robyn L. Mildren in partial fulfillment of the requirements for

the degree of Doctor of Philosophy

in Kinesiology

Examining Committee:

Dr. J. Timothy Inglis, Professor, School of Kinesiology, University of British Columbia

Supervisor

Dr. Jean-Sébastien Blouin, Professor, School of Kinesiology, University of British Columbia

Supervisory Committee Member

Dr. Mark Carpenter, Professor, School of Kinesiology, University of British Columbia

Supervisory Committee Member

Dr. Chris McNeil, Associate Professor, School of Health and Exercise Sciences, University of British Columbia

University Examiner

Dr. Alex Scott, Professor, Department of Physical Therapy, University of British Columbia

University Examiner

Abstract

There are many structures within the nervous system that, as a whole, are responsible for the control of movement and balance. The spinal cord plays an important role in sensorimotor processing, it integrates sensory signals from the periphery as well as signals from the brain to control muscle activation. The purpose of this thesis was to characterize the short latency (spinally mediated) lower limb muscle responses to proprioceptive perturbations during standing, and examine how they are influenced by ageing and chronic stroke. Chapter 2 develops an innovative methodology to characterize muscle responses to proprioceptive perturbations during standing. Here, we examined the association between noisy (10-115 Hz) suprathreshold Achilles tendon vibration and ongoing triceps surae muscle activity. We observed responses in soleus across a broad frequency bandwidth (~10-80 Hz). Consistent responses were obtained with short trial durations (<60 s); furthermore, responses did not habituate, and the stimulus did not noticeably perturb standing balance.

Chapter 3 demonstrates differences in single motor unit responses to noisy and sinusoidal vibration between two plantar flexor muscles – soleus and medial gastrocnemius. These experiments revealed soleus motor units had stronger responses relative to medial gastrocnemius, and single motor units showed minimal non-linear phase locking. Chapter 4 illustrates how cutaneous feedback from the foot sole interacts with the soleus vibration responses. Foot sole cutaneous stimuli were found to modulate the vibration responses in a spatially organized manner, where heel stimuli suppressed and metatarsal stimuli enhanced responses. Finally, Chapters 5 and 6 examine the influences of age and chronic stroke on the characteristics of the soleus vibration responses. We found a narrowing of the frequency bandwidth, and a decrease in

gain, amplitude, and scaling of soleus responses with age. On the affected side post-stroke, we found evidence of altered soleus vibration responses, along with changes in postural control and mechanical admittance of the muscle-tendon unit. Collectively, these studies contribute to our understanding of the proprioceptive system and how changes associated with ageing and stroke may contribute to impaired balance and falls. These findings have implications for rehabilitation strategies and the development of neuroprostheses.

Lay Summary

Sensory receptors in muscles provide information about the position and movement of body segments (proprioception), and can evoke reflexive responses. This thesis examines the characteristics of leg muscle responses to proprioceptive stimuli generated by vibration of the Achilles tendon during standing. We found the soleus muscle, in particular, responds to vibration across a broad frequency range (up to 100 Hz) – frequencies that may be naturally generated by postural sway, walking, and balance perturbations. Information from skin on the foot sole tuned soleus responses; heel stimuli suppressed and metatarsal stimuli enhanced responses. Ageing was associated with weaker soleus responses across a smaller frequency range, and chronic stroke altered soleus response characteristics, mechanical properties of the muscle-tendon, and the control of balance. These studies enhance our understanding of how muscles respond to proprioceptive information and how changes in response characteristics contribute to impaired balance and mobility associated with ageing and stroke.

Preface

In the studies included in this thesis, all data were collected by Robyn Mildren (Mildren, RL), with assistance where outlined below, in the Human Neurophysiology Lab at the University of British Columbia (Vancouver campus). All methods were approved by the University of British Columbia Research Ethics Board (IDs: H12-01698 and H18-01466), and all participants provided written informed consent prior to participating in each study.

Chapter 2 is published in The Journal of Applied Physiology [Mildren RL, Peters RM, Hill AJ, Blouin JS, Carpenter MG, Inglis JT. Frequency characteristics of human muscle and cortical responses evoked by noisy Achilles tendon vibration. *J Appl Physiol*. (1985) 2017;122:1134-1144]. Mildren RL was responsible for the conception and experimental design, data collection and analyses, interpretation of results, and manuscript drafting and revisions. Hill AJ assisted with data collection, and Peters RM, Blouin JS, Carpenter MG, and Inglis JT assisted with experimental design, interpretation of results, and manuscript revisions. Dr. Romeo Chua also provided guidance with the electroencephalography portion of this study.

Chapter 3 is published in The Journal of Neurophysiology [Mildren RL, Peters RM, Carpenter MG, Blouin JS, and Inglis JT. Soleus single motor units show stronger coherence with Achilles tendon vibration across a broad bandwidth relative to medial gastrocnemius units while standing. *J Neurophysiol.* 2019;122:2119-2129]. Mildren RL was responsible for the conception and experimental design, data collection and analyses, interpretation of results, and manuscript drafting and revisions. Inglis JT supervised portions of data collection, and Peters RM, Carpenter MG, Blouin JS, and Inglis JT assisted with experimental design, interpretation of results, and manuscript revisions.

Chapter 4 is being prepared for submission to a peer-reviewed journal. Mildren RL was responsible for the conception and experimental design, data collection and analyses, interpretation of results, and manuscript drafting and revisions. Eschelmuller G assisted with data collection. Carpenter MG, Blouin JS, and Inglis JT assisted with experimental design, interpretation of results, and manuscript revisions.

Chapter 5 is under review for a peer-reviewed journal. Mildren RL was responsible for the conception and experimental design, data collection and analyses, interpretation of results, and manuscript drafting and revisions. Schmidt ME assisted with participant recruitment and data collection, and Eschelmuller G also assisted with data collection. Carpenter MG, Blouin JS, and Inglis JT assisted with experimental design, interpretation of results, and manuscript revisions.

Chapter 6 is a pilot study in a clinical population. Mildren RL was responsible for the conception and experimental design, data collection and analyses, and interpretation of results. Pollock CL and Lim SB assisted with study design, clinical assessments, and participant recruitment. Schmidt ME and Eschelmuller G assisted with data collection, and Carpenter MG, Blouin JS, and Inglis JT assisted with experimental design and interpretation of results.

Data for these studies were collected in the order they are presented in this thesis.

Table of Contents

List of Tables

List of Figures

List of Abbreviations

ANOVA – analysis of variance
AP – anteroposterior
CF – common fibular
CI – confidence interval
CNS – central nervous system
COP – centre of pressure
DOC – difference of coherence
EEG – electroencephalography
EMG – electromyography
EPSP – excitatory post synaptic potential
FA – fast adapting
GABA – gamma-aminobutyric acid
GTO – Golgi tendon organ
H-reflex – Hoffman reflex
Ia – primary spindle afferent nerve
II – secondary spindle afferent nerve
Ib – Golgi tendon organ afferent nerve
LGas – lateral gastrocnemius
MPF – mean-power-frequency
MPT – monofilament perceptual threshold
MGas – medial gastrocnemius
NTV – noisy tendon vibration
P2P – peak-to-peak
PAD – primary afferent depolarization
PIC – persistent inward current
PSTH – peristimulus time histogram
RMS – root-mean-square
SA – slowly adapting
SD – standard deviation
SCI – spinal cord injury
SOL – soleus
TVR – tonic vibration reflex

Acknowledgements

I am incredibly grateful to my supervisor Tim for making an exception to take me on as a student after he had said he wouldn't take on any more PhD students. I felt that Tim had a huge amount of confidence in me and my work, and that helped get the best out of me. Tim and my committee, comprised of Jean-Sébastien Blouin and Mark Carpenter, have very high standards for research quality, and they always pushed me to take my research a few steps farther. Despite the struggles, I am thankful that I was able to produce research that was rigorous and interesting. I would also like to thank Romeo Chua for helping me with some technical bits, he always managed to pull out the right little piece of electronic equipment that I needed to finish my experimental setup. I would like to thank Courtney Pollock and Shannon Lim for their assistance with the stroke project; this research couldn't have been done without their collaboration. My lab mates Ryan Peters, Margot Schmidt, and Gregg Eschelmuller were instrumental in assisting me with my thesis studies, and also made working in the lab fun (even though it was a cold dark place that sometimes lacked a functioning roof). Lastly, I would like to thank my family and friends for their love and support. I especially would like to thank my partner Marty and our furry quadrupedal child Levi for being the best emotional support team I could have ever asked for.

To my fellow grad students

Chapter 1: Introduction

The control of movement and balance involves the interplay between many different structures in the nervous system. Somatosensory receptors in muscles, tendon, and skin continuously provide the central nervous system (CNS) with information about body position and movement. This sensory feedback is processed in spinal and supraspinal structures for accurate perception and motor control. In the legs, somatosensory receptors in the foot sole provide information about pressure distribution, ground contact, and slips, while somatosensory receptors in muscles provide information about muscle length and stretch induced by movement. Ageing and disorders that affect either sensory feedback (e.g., peripheral neuropathy) or sensorimotor processing in the CNS (e.g., stroke, Parkinson's disease, cerebellar disorders) can impair mobility and increase the risk of falls. Therefore, research that advances our understanding of sensorimotor processing in a healthy nervous system, as well as how it is influenced by ageing and disorders of the nervous system, has implications for improving balance, mobility, and motor recovery in addition to informing the design of neuroprostheses.

This thesis primarily aims to characterize one somatosensory feedback pathway – short latency spinally mediated responses to proprioceptive stimuli – and examine the influences of ageing and chronic stroke on this pathway during standing. First, the following literature review is provided to contextualize the subsequent experiments described in Chapters 2-6.

1.1 An overview of α-motoneurons

α-motoneurons integrate information from numerous sources and provide the final common pathway to the muscle for the control of force and movement (Sherrington, 1904). The

cell bodies of α-motoneurons reside in the spinal cord and their axons project through the ventral horn to innervate their target muscle fibres. A motor unit refers to an α-motoneuron and all of the muscle fibres it innervates; the activation of a single motor unit represents the smallest quantum of contractile force that can be generated by the CNS (Rothwell, 1994, p. 35). Each α-motoneuron has an extensive dendritic tree; this allows it to receive and integrate information from thousands of inputs. This is in line with Charles Sherrington's view that some neurons produce outcomes through a process of a million fold democracy (Sherrington, 1940). Either directly or indirectly, α-motoneurons receive a vote from many peripheral afferents (that arise from receptors in skin, muscles, tendons, and joints) and descending pathways from supraspinal structures.

Signals to α-motoneurons can generate either excitatory or inhibitory post-synaptic potentials. Post-synaptic potentials are local and graded in magnitude, and their summation determines whether the membrane potential is depolarized enough to reach the threshold to generate an action potential. Action potentials, in contrast, are typically considered "all or none"; i.e., if threshold is reached, the amplitude of the action potential is consistent. (However, action potentials can be shunted at later stages of transmission along the axon; Eccles et al., 1962.) Importantly, α-motoneurons receive extensive neuromodulatory input that influences how they respond to peripheral or descending input. Descending pathways from the brainstem are an extensive source of monoaminergic neuromodulatory input. Specifically, these monoaminergic inputs can depolarize the membrane potential, hyperpolarize firing threshold, reduce afterhyperpolarization, and facilitate persistent inward currents (PICs) that can amplify and sustain α-motoneuron activity in response to excitatory input (Heckman et al., 2003; Hultborn et

al., 2004; Powers and Binder, 2001). This descending drive from the brainstem plays one role in setting the state of neural circuits in the spinal cord.

1.1.1 Measuring α-motoneuron responses to sensory stimuli

When an action potential is sent down a motor unit, the motor unit action potential can be recorded using surface or indwelling electromyography (EMG) as it travels across the sarcolemma of the muscle fibres. These motor unit action potentials can provide a glimpse of the output of the nervous system to the muscle. Methodologically, one way to probe the effects of a sensory input on motor output is to provide a large number of stimuli and trigger-average the evoked EMG response or motor unit spike probability. This stimulus trigger-averaging approach will lead to cancellation of other random "noise" unrelated to the stimulus (i.e, the effects of other inputs or spontaneous activity), and thus allow for the identification of responses tied to one particular stimulus or input.

Another way to probe the effects of a sensory input is to add suprathreshold noise to one system (e.g., muscle spindle afferents) and use a correlation approach to determine to what extent that same noise appears in the output at appropriate transmission delays. This noisy stimulus approach has been effectively used to map connections in several sensory systems (visual; Jones and Palmer, 1987, auditory; Fritz et al., 2003, and vestibular; Dakin et al., 2007). Correlations can be applied at different lags between the input and output signals to account for transmission delays (termed cross-correlations), and can also be examined in the frequency domain (termed coherence). In addition, the phase and the gain of the input-output relationship can provide information about the time delays across frequencies and the amplitude of the response relative to the stimulus. In the following thesis studies (Chapters 2-6) we leverage this noisy stimulus and

linear systems analysis approach to examine responses in postural muscles to proprioceptive stimuli during standing.

1.2 An overview of the somatosensory system

There are four main classes of somatosensory receptors in humans: Golgi tendon Organs (GTO), joint receptors, muscle spindles, and cutaneous mechanoreceptors. GTOs are situated in the muscle-tendon junction and are primarily sensitive to actively generated muscle tension (Binder et al., 1977). The activation of Ib afferents that innervate GTOs typically produces autogenic inhibition (i.e., inhibition of the homonymous muscle) through Ib inhibitory interneurons, as well as reciprocal facilitation of the antagonist muscle. However, many other sources (descending and peripheral) also project to Ib inhibitory interneurons. Thus, Ib interneurons serve as a neural integrator at a pre-motoneuron level in the spinal cord. Relative to the other somatosensory receptors, joint receptors are less well understood. A prominent view is that they have a limited ability to transduce physiologically relevant movement information since they tend to fire ambiguously at end ranges of motion, and provide minimal graded feedback throughout the natural joint range of motion (Burgess and Clark, 1969).

Muscle spindles can be subdivided into two classes, primary and secondary, that preferentially provide muscle dynamic and static information, respectively. Both the larger diameter primary (Ia) and smaller secondary (II) spindle afferents have direct excitatory connections onto α-motoneurons as well as connections onto other spinal pathways (e.g., propriospinal neurons, Ia inhibitory interneurons) and ascending projections to supraspinal structures (Jankowska, 2015; Pierrot-Deseilligny and Burke, 2012). Cutaneous

mechanoreceptors are subdivided into four classes; Meissner's and Pacinian corpuscles preferentially signal dynamic events at the skin and are innervated by fast adapting afferents (FAI and FAII, respectively) while Merkel disks and Ruffini endings preferentially signal pressure and skin stretch and are innervated by slowly adapting afferents (SAI and SAII, respectively) (Kennedy and Inglis, 2002; Strzalkowski et al., 2015). This review will primarily focus on muscle spindle and cutaneous afferents since these are the somatosensory channels primarily studied in this thesis.

1.2.1 Cutaneous mechanoreceptors and cutaneous reflexes

In the foot sole, the two slowly adapting cutaneous afferents primarily signal the magnitude and distribution of pressure under the feet while the two fast adapting receptors primarily signal contact and release from the ground and translations across the skin (Kennedy and Inglis, 2002; Strzalkowski et al., 2015). Cutaneous reflexes can be evoked by electrical stimuli applied either to cutaneous nerves or directly to the skin. The resulting cutaneous reflexes evoked by electrical stimuli are spatially organized. For example, stimulation under the heel evokes initial excitation of plantar flexor α-motoneurons while stimulation under the metatarsals evokes an initial inhibition (Aniss et al., 1992; Nakajima et al., 2006). Cutaneous reflexes are also adaptable; reflex gain can change with posture (while controlling for background EMG level; Aniss et al., 1990), and reflex polarity can reverse between different phases of the gait cycle (Zehr et al., 1997, 2012, 2014). Cutaneous afferents also have widespread connections spanning segments of the spinal cord; for example, coupling between the activity of single cutaneous afferents from the foot and α-motoneurons of both leg (Fallon et al., 2005) and arm (Bent and Lowrey, 2013) muscles has been demonstrated. Cutaneous reflexes are often complex

and multiphasic, which likely reflects the dispersed nature of cutaneous input to different neuronal populations in the spinal cord. Specifically, cutaneous afferents have been shown to provide input to primary afferent depolarization (PAD) interneurons, γ-motoneurons, and Ia and Ib inhibitory interneurons (Hunt et al., 1951; Alnaes et al., 1965; Appelberg et al., 1977; Lundberg et al., 1977; Pierrot-Deseilligny et al., 1981; Bergego et al., 1981; Rossi and Mazzocchio, 1988; Aniss et al., 1988, 1990; Iles, 1996). Some of the cutaneous afferent connections to spinal interneurons are depicted in Fig. 1-1.

1.2.2 Muscle spindles and short latency stretch responses

Primary (Ia) and secondary (II) muscle spindle afferents innervate the central region of the intrafusal fibres of muscle spindles and convey information about muscle stretch and rate of stretch to the CNS. The intrafusal fibres of muscle spindles lie in parallel with the force generating extrafusal fibres, and their stretch opens mechanically gated ion channels on the afferent axons to convey proprioceptive information to the spinal cord. There are three types of intrafusal fibres: dynamic bag 1, static bag II, and chain. Ia afferents have a large diameter and wrap around the centre of all three types of intrafusal fibres, and are primarily sensitive to the velocity of muscle stretch. Meanwhile, II afferents are smaller in diameter and typically innervate only bag II and chain fibres slightly off centre, and are primarily sensitive to muscle length. However, the fidelity of the velocity and length feedback from Ia and II afferents is degraded by muscle thixotropic effects. Blum et al. (2017) demonstrated that the firing rate of spindle afferents were better explained by muscle force related variables (force and its first derivative – yank) rather than length related variables to account for muscle history dependent effects. In addition to history dependent effects, spindle sensitivity is also influenced by an

efferent (fusimotor) system (*see section 1.2.3*), and the maintenance of stretch sensitivity relies upon the release of glutamate from synaptic-like vesicles at the mechanosensory nerve terminals (reviewed in Bewick, 2015). The control of spindle sensitivity via these mechanisms, and how they are influenced by ageing and disorders of the nervous system, is still not well understood in humans.

In most muscles, spindle afferents have direct excitatory projections to α-motoneurons of the same (homonymous) muscle, synergistic muscles, as well as muscles with actions at different joints (Jankowska, 2015; Eschemuller et al. 2019). For example, Ia afferents from the soleus will project to nearly all of the α-motoneurons that innervate the soleus, as well as α-motoneurons that innervate the quadricep and hamstring muscles. The divergent connections from proprioceptive afferents can form the basis of muscle synergies (Ting et al., 2015), and can be leveraged to evoke coordinated movement patterns through electrical stimulation over the spinal cord (Capogrosso et al., 2016, 2018). This highlights some of the clinical implications for understanding the characteristics of proprioceptive evoked muscle responses in a healthy nervous system as well as after an injury to the nervous system.

Stretch responses are mediated by excitatory input from spindle afferents to α-motoneurons and function to help maintain muscle length in response to perturbations. In decerebrate cats, stretch responses have been shown to linearize the resistance to muscle stretch and compensate for yielding (Nichols and Houk, 1976). Stretch responses have also been suggested to play a role in compensating for small, rapid irregularities in movement speed (Burke et al., 1978) and damping mechanical oscillations (Cathers et al., 1999).

The initial portion of the muscle response to stretch can be attributed to monosynaptic connections between muscle spindle afferents and α-motoneurons, while it is possible that polysynaptic pathways contribute to later portions of the response (Burke et al., 1983). In addition to their monosynaptic excitatory projections to α-motoneurons, spindle afferents also project to different spinal interneurons. These spindle connections include PAD interneurons that mediate presynaptic inhibition, Ia inhibitory interneurons that mediate reciprocal inhibition, propriospinal neurons that span multiple segments of the spinal cord, and neurons involved in the flexor reflex afferent pathway (Pierrot-Deseilligny and Burke, 2012). This thesis will focus on the short latency muscle responses primarily evoked by excitatory Ia afferent input to α-motoneurons.

Short latency responses evoked by input from muscle spindles can be modulated at three locations along the pathway *1)* sensory receptor level via fusimotor drive, *2)* sensory axon level via depolarizing input, and *3)* spinal interneuron and/or α-motoneuron level. The modulation of transmission at all three of these levels is important so muscle responses to proprioceptive perturbations are appropriate for the particular posture or motor task. Importantly, ageing and neurological disorders could alter the transmission of information via alterations at these three locations. The modulation of α-motoneurons has already been discussed above (*see section 1.1*), and the control of fusimotor drive and primary afferent depolarization will be discussed in more detail in the following two sections (*see sections 1.2.3 and 1.2.4*).

1.2.3 Fusimotor drive to muscle spindles

Muscle spindles are unique from other somatosensory receptors (cutaneous, joint, and GTO) because their sensitivity can be influenced by an efferent (fusimotor) system that

innervates contractile elements at the polar regions of intrafusal muscle fibres (first demonstrated by Leksell, 1945). It is still not fully understood what system(s) control(s) the activity of the fusimotor system, and what the teleological reasons for having independent control over extrafusal and intrafusal fibres are. There are many theories centred around roles of the fusimotor system in the prevention of spindle unloading during muscle shortening (Vallbo, 1971), as well as more complex functions in motor learning and forward models that rely upon spindle feedback to predict future sensory states (Dmitriou and Edin, 2010).

The fusimotor system encompasses two classes of γ-motoneurons, as well as the β-system which simultaneously innervates both extra- and intra-fusal muscle fibres. There are two types of γ-motoneurons (γ-static and γ-dynamic); where γ-dynamic fibres primarily innervate the contractile elements of the dynamic bag 1 intrafusal fibres, and thus accentuate dynamic coding from Ia spindle afferents. Conversely, γ-static fibres primarily innervate contractile elements of the bag 2 and chain fibres and thus accentuate length coding from II spindle afferents. Within the spindle sensory system, there is a lot of divergence and convergence. For example, one γ-motoneuron will branch to innervate multiple intrafusal muscle fibres, and one Ia afferent will branch to innervate many α-motoneurons. Overall, this means that a single α-motoneuron will receive feedback from many Ia afferents that are under the influence of many γ-motoneurons. While the setup of this system likely weakens the coupling between single spindle afferents and single α-motoneurons, it likely serves to provide a more integrative signal based on the overall activity of a population of spindle afferents under some bias from a population of γ-motoneurons.

While the control of the fusimotor system is not well understood, it has been shown that fusimotor drive in spinal cats is supported by sensory input to the dorsal horn of the spinal cord

(Hunt, 1951; Alnaes et al., 1965) (depicted in Fig. 1-1). In animals, cutaneous input has been shown to have strong effects on fusimotor drive (Appelberg et al., 1977; Eldred and Hagbarth, 1954). Overall, cutaneous-fusimotor interactions have been found to be easily evoked in animal experiments and at a lower threshold than corresponding cutaneous-α-motoneuron interactions (Eldred and Hagbarth, 1954); i.e., reflexive changes in fusimotor drive can be observed in the absence of a change in α-motoneuron activity. Generally this system seems to be organized such that stimulation of skin overlying a muscle facilitates both α- and γ-motoneurons that innervate that muscle, while the opposite effect is seen in antagonistic muscles (Eldred and Hagbarth, 1954). However, these cutaneous-γ-motoneuron connections have been difficult to demonstrate in humans (Aniss et al., 1988). The lack of corroborating evidence in human experiments, in part, may be due to methodological difficulties (small diameter γ nerve fibres cannot be recorded from directly using microneurography) and/or the potential that the input from cutaneous afferents to γ-motoneurons is task dependent. There is some indirect evidence in humans of cutaneous modulation of γ-motoneuron activity (modulation of spindle afferent discharge independent of muscle stretch) in a small sample of recordings from the radial nerve during stimulation of skin on the hand (Gandevia et al., 1994). Similarly, there is indirect evidence of cutaneous modulation of γ-motoneuron activity in a small sample of recordings from spindle afferents innervating ankle dorsiflexor muscles while subjects were standing (Aniss et al., 1990). Therefore, it is possible that cutaneous-γ-motoneuron interactions in lower limb muscles manifest in humans when the nervous system is engaged in a sensorimotor task such as balance control.

1.2.4 Presynaptic inhibition

Many different factors, including temperature, action potential frequency, membrane channels, and axo-axonal connections, can influence the propagation (or blockage) of an action potential through an axon and its branch points. Presynaptic inhibition from primary afferent depolarization (PAD) is the most commonly discussed mechanism in the literature that can control the transmission of action potentials through afferent axons. It was first identified in animal experiments that excitatory postsynaptic potentials (EPSPs) in α-motoneurons could be depressed in the absence of a change in α-motoneuron membrane potential or conductance (Frank and Fuortes, 1957). This depression was associated with PAD and later attributed to inhibitory interneurons with axo-axonal connections onto Ia afferent terminals (Eccles et al., 1962) (depicted in Fig. 1-1). Control of afferent transmission through PAD likely has important roles in movement control. In mice, the genetic ablation of the interneurons that contact sensory afferent terminals was found to result in a forelimb motor oscillation during goal-directed reaching (Fink et al., 2014). Furthermore, a model of the consequences of high proprioceptive feedback gain was able to mimic this oscillation (Fink et al., 2014). Overall, these findings illustrate that the inability to modulate reflex transmission via PAD can be detrimental to smooth control of movement. However, the control of a hind limb motor task (horizontal ladder stepping) in mice was not noticeably affected by the ablation of PAD interneurons (Fink et al., 2014); which suggests there is some task selectivity in the roles of PAD during movement.

Some electrophysiological characteristics of presynaptic inhibition include: a) a change in Ia reflex transmission not simply related to α-motoneuron excitability, b) a long duration of action, c) preferential gating of low frequency Ia input, and d) long central delay (~5 ms)

(Pierrot-Deseilligny and Burke, 2012). The organization of presynaptic inhibition tends to favour the overall depression of plantar flexor relative to dorsiflexor muscle activation. Specifically, group I (Ia and Ib) afferents from both plantar flexor and dorsiflexor muscles project to PAD interneurons of plantar flexor Ia afferents (which suppresses plantar flexor Ia input) (Rudomin and Schmidt, 1999). In contrast, dorsiflexor Ia afferents primarily receive PAD input from dorsiflexor group I afferents (Rudomin and Schmidt, 1999). Therefore, the excitability of PAD interneurons is often tested by applying a conditioning stimulus to the deep branch of the common fibular (CF) nerve ~1-1.5 × M-wave threshold in tibialis anterior, prior to applying a test stimulus to the posterior tibial nerve to evoke the soleus H-reflex. The conditioning stimulus to the CF nerve typically evokes two phases of inhibition of the soleus H-reflex, the first (termed D1) phase occurs with condition-test intervals of ~15-20 ms, and the second (termed D2 phase) occurs with condition-test intervals of ~70-200 ms (Capaday et al., 1995). It is suggested that there is a single long lasting presynaptic inhibition that is masked in the middle by a facilitation that could originate from other input such as from cutaneous afferents (Hultborn et al., 1987).

In addition to the D1-D2 inhibition approach, another method to assess tonic levels of PAD is to measure the amount of heteronymous facilitation of the soleus H-reflex from femoral nerve stimulation. The level of facilitation of the soleus H-reflex presumably reflects the tonic level of presynaptic inhibition onto the femoral Ia afferents that project to soleus α-motoneurons. This heteronymous facilitation method is often used in conjunction with the D1-D2 inhibition method because it is not affected by potential saturation of PAD interneurons, which will affect D1-D2 inhibition.

During voluntary movement, presynaptic inhibition was shown to be modulated in a way that served to reinforce agonist contraction and dampen antagonist stretch responses (Morita et al., 2001). Specifically, inhibition onto plantar flexor Ia afferents was increased at the onset of dorsiflexion and decreased at the onset of plantar flexion (Morita et al., 2001). Interestingly, this modulation during voluntary movement was less pronounced in multiple sclerosis patients with spasticity, and it was postulated that the lack of ability to modulate stretch responses during voluntary movement could contribute to excessive co-contraction and antagonist stretch responses (Morita et al., 2001). Levels of presynaptic inhibition have also been investigated in paraplegic and hemiplegic patients with spasticity (Faist et al., 1994). The paraplegic group was found to have lower levels of presynaptic inhibition, although surprisingly the hemiplegic group was not different from controls despite presenting with worse spasticity (Faist et al., 1994). Studies have suggested that ageing is associated with either an accentuated (Baudry and Duchateau, 2012) or impaired (Koceja and Mynark, 2000) ability to modulate presynaptic inhibition with changes in posture and task. Overall, our current understanding of the functions of presynaptic inhibition in motor control in humans and the effects of ageing and neurological disorders is limited.

Cutaneous afferents have been found to reduce presynaptic inhibition (i.e., enhance Ia transmission) in animals and humans (Iles, 1996); however, the effects of cutaneous input from different locations has not been explored comprehensively. Iles (1996) stimulated nerves or skin across multiple sites (the lateral border of the foot, arch, and forefoot) and always observed facilitation (decreased presynaptic inhibition); however, the heel region was not examined. It is possible that in humans, cutaneous input from different functional locations of the foot sole

might have different effects on presynaptic inhibition given the known differences in cutaneous reflex polarity between the heel (excitatory) relative to the metatarsals (inhibitory) (Aniss et al., 1992; Nakajima et al., 2006).

A limitation of previous research is that presynaptic inhibition has almost exclusively been explored using H-reflex techniques. While Morita et al. (1998) found that the H-reflex is strongly suppressed by PAD input from flexor afferents (by ~50%), the tendon tap response was only weakly depressed (by ~10% maximum), while the stretch response was not significantly depressed. Similar findings were replicated in cats (Enríquez-Denton et al., 2002), and it was suggested that the differential effects of PAD on the H-reflex vs. tendon tap and stretch responses could be attributed to the greater number of afferent spikes evoked by tendon taps and muscle stretches relative to the H-reflex, whereby PAD preferentially affects lower frequency transmission (<30 Hz) (Morita et al., 2001). Therefore, the strong influence of PAD on the artificial afferent input that mediates the H-reflex may not reflect its influence on more dispersed afferent input generated by mechanotransduction.

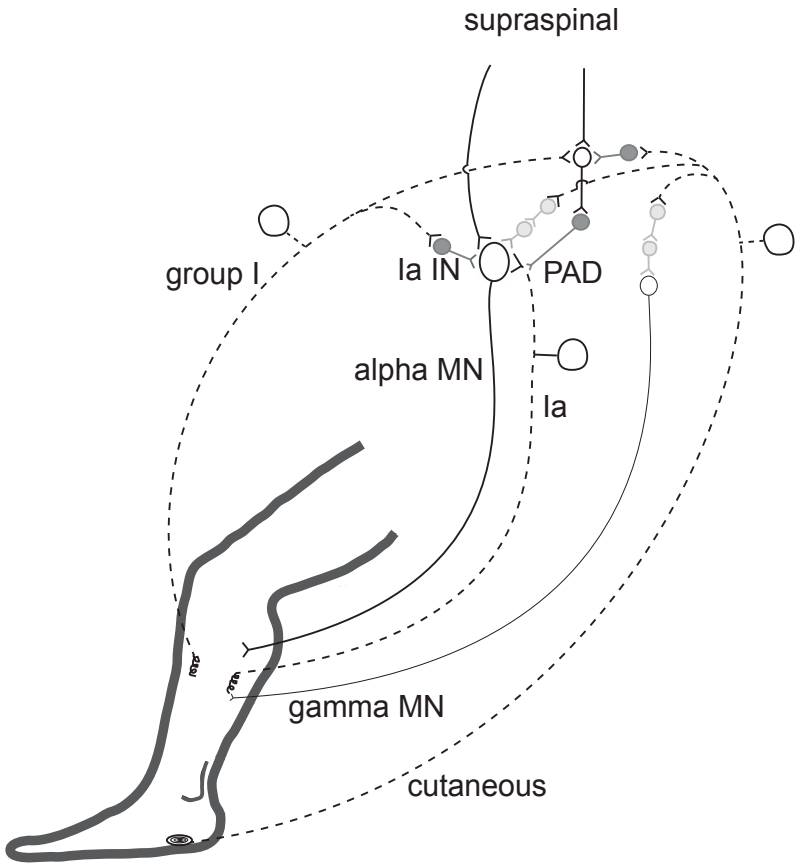

Figure 1-1 Diagram of some connections in the spinal cord

Diagram of cutaneous afferent connections to PAD interneurons and α- and γ-motoneurons, along with the Ia afferent connections to spinal α-motoneurons and group I connections that mediate reciprocal and presynaptic inhibition. MN = motoneuron, IN = interneuron, PAD = primary afferent depolarization. Darker grey cell bodies indicate inhibitory interneurons.

1.3 Age-related changes in muscle stretch responses

Ageing has been shown to affect many components of the stretch response pathway, including spindle receptors, afferent nerves, synaptic connections, α-motoneuron somas and axons, and neuromuscular junctions (Swallow, 1966; Swash and Fox, 1972; Morales et al., 1987; Boxer et al., 1988; Lexell and Downham, 1991; Zhang et al., 1996; Liu et al., 2005: Hepple and Rice, 2016; Vaughan et al., 2017). Ageing may also affect the mechanical properties of the muscle and tendon (Karamanidis and Arampatzis, 2005; Stenroth et al., 2012; Delabastita et al., 2018), which could influence the transmission of mechanical stimuli to sensory receptors. Changes in human muscle spindle morphology with age include an increase in capsular thickness and denervation (Swash and Fox, 1972). Muscle spindles in old rats were shown to have a lower discharge rate and lower dynamic index during ramp stretches (Miwa et al., 1995). Demyelination of sensory and motor axons with age can also affect transmission capacity and velocity, and this effect seems to begin earlier in sensory afferent relative to motor efferent fibres (Morales et al., 1987).

There is an ongoing process of loss and remodelling of motor units with age that results in a larger innervation ratio (muscle fibre to motor unit ratio) (Scaglioni et al., 2003). However, this remodelling does not occur to the same extent across all muscles, where some muscles are more resistant to age-related changes possibly due to their fibre composition or habitual activity (e.g., the diaphragm; Nguyen et al., 2019, trapezius; Kirk et al., 2019, and soleus; Dalton et al. 2008, 2009). The soma of motoneurons have been found to shrink with age, and EPSPs from Ia input were found to become prolonged (Boxer et al., 1988). Lastly, changes in contact between axons and muscle fibres and abnormalities in the neuromuscular junction with age generally lead

to a less effective motor end plate (Hepple and Rice, 2016). Altogether, most of these age-related changes would be expected to decrease the amplitude and prolong the onset latency of the muscle response to proprioceptive stimuli. However, some of the aforementioned changes (e.g., increased input resistance and reinnervation) might help maintain the muscle response to proprioceptive stimuli.

The ability to appropriately modulate responses to proprioceptive perturbations for specific contexts or tasks is critical for motor control. Koceja and Mynark (2000) suggest old adults have higher tonic levels of presynaptic inhibition in the supine position; this was based on the finding of lower heteronymous facilitation of the soleus H-reflex from femoral nerve conditioning stimuli. Higher tonic levels of presynaptic inhibition were suggested to contribute to a lack of ability to further modulate (dampen) the H-reflex when going from a supine to standing posture (Koceja and Mynark, 2000). Morita et al., (1995), using the heteronymous facilitation method, similarly found a linear decrease in heteronymous facilitation (evidence of increased tonic presynaptic inhibition) with age. In contrast to the findings of these studies (Koceja and Mynark 2000; Morita et al., 1995), using the common fibular nerve conditioning stimulus method Earles et al., (2001) found old adults demonstrated lower levels of presynaptic inhibition, and less of an ability to modulate presynaptic inhibition with background EMG. Surprisingly, Mynark and Koceja (2002) found old adults maintain the ability to dampen their H-reflex with training (via H-reflex induced balance perturbations) to a comparable degree as young adults. Moreover, Baudry and Duchateau (2012) suggest old adults actually have a greater ability to modulate the H-reflex through presynaptic inhibition with changes in balance difficulty during standing (eye closure and standing on foam). Although the functional implications of the

changes in stretch responses with age are unclear, correlations have been found between standing postural control and reflex gain (Angulo-Kinzler et al., 1998) as well as the ability to modulate reflex gain with changes in posture (Koceja et al., 1995).

The H-reflex has been the primary technique used to probe changes in proprioceptive responses associated with ageing. However, the interpretation of H-reflex results may be limited when comparisons are made between muscles or populations due to confounds created by antidromic potentials. Specifically, it has been suggested that the afferent and efferent excitability thresholds to electrical stimulation may become more homogeneous with age (Scaglioni et al., 2003). This relative axon excitability shift could contribute to a smaller H-reflex due to a larger proportion of antidromic potentials in old age. The use of mechanical stimuli to examine responses could avoid some confounds related to differences in axon excitability and also incorporates the assessment of mechanotransduction.

1.4 Sensorimotor changes post-stroke

Injury to neural tissue caused by lack of blood supply during a stroke can cause sensorimotor symptoms such as muscle weakness and spasticity. Spasticity is commonly defined as a velocity dependent increase in tonic stretch responses, along with enhanced tendon tap responses (Lance, 1980). A stroke usually produces symptoms primarily on one side of the body (hemiparesis). Changes in the sensorimotor system induced by a stroke can impair mobility and increase the risk of falls (Maeda et al., 2009; Mansfield et al., 2018).

1.4.1 Motor unit properties post-stroke

Paradoxically, motor units in the upper limb tend to show high excitability at rest (based on evidence of spontaneous discharge and exaggerated reflexes), yet reduced firing rates and abnormal rate coding during voluntary movement (Mottram et al., 2014). Hand muscles affected by stroke were found to demonstrate greater motor unit synchronization, which was suggested to reflect stronger common drive to motor units that originated from fewer sources (Dai et al., 2017). Coherence between motor units was found to be particularly strong in the α-band (8-12 Hz; Dai et al., 2017), which was suggested to reflect greater input from muscle spindles and the actions of rhythmic reflex loops (Semmler et al., 2002; Erimaki et al., 2007).

Upper limb muscles are generally more affected by a stroke relative to lower limb muscles, and changes in motor unit properties may differ between the upper and lower limbs. Whereas in the upper limb there is evidence of an increase in common drive (Dai et al., 2017), in the lower limb Garland et al. (2014) found slightly diminished common drive to medial gastrocnemius motor units on the affected side of chronic stroke survivors during a postural task.

Intrinsic changes in motor units have also been shown post-stroke, such as prolonged afterhyperpolarization (Garland et al., 2014) and increased excitability via PICs (McPherson et al., 2008). PICs are a depolarizing inward ion flux that can generate self-sustained activation of α-motoneurons and amplify α-motoneuron activation in response to excitatory input. PICs are enhanced by monoaminergic input (norepinephrine and serotonin); it has been suggested that PICs are enhanced post-stroke due to a disrupted balance of brainstem pathways to the spinal cord (Li et al., 2015). In chronic stroke, vibration of the biceps brachii tendon resulted in an exaggerated tonic vibration reflex (TVR) and persistent contraction after the vibration was turned

off; this was suggested to be mediated by enhanced activation of PICs by somatosensory feedback that amplified and sustained motor unit firing (Gorassini et al., 1998; McPherson et al., 2008).

1.4.2 Changes in descending drive and spinal cord circuitry post-stroke

The most common scientific definition of spasticity adopted in the literature is "a velocity dependent increase in tonic stretch reflexes with exaggerated tendon jerks, resulting from hyperexcitability of the stretch reflexes as one component of the upper motoneuron syndrome" (Lance, 1980). Spasticity is believed to be a part of abnormal plasticity that manifests during recovery from stroke. Initially after a stroke, patients typically present with weakness and hyporeflexia (Florman et al., 2013); when reflexes return they often become exaggerated in muscles at rest (Bruunstrom, 1970; Lance, 1980). Exaggerated reflexes could be caused by altered descending drive to the spinal cord (Li et al., 2014, 2015; Miller et al., 2014, 2016), or intrinsic changes in spinal cord circuitry and tissue mechanical properties that result from the altered descending drive over time (Gao et al., 2009; Zhao et al., 2015).

Altered brainstem pathways may influence both motoneurons and interneurons. For example, there is evidence that motor inhibition from the medullary reticulospinal tract is mediated by parallel input onto α- and γ-motoneurons as well as interneurons of Ib and flexor reflex afferent pathways in cats (Takakusaki et al., 2001). Therefore, a change in the excitability of α-motoneurons as well as spinal pathways that mediate somatosensory evoked responses could contribute to impaired motor control. Increased tonic excitatory input could also arise from enhanced vestibulospinal input to the spinal cord. There is evidence of both abnormal reticulospinal and vestibulospinal drive; acoustic startle reflexes (likely mediated by the

reticulospinal tract) were found to be enhanced in stroke survivors with spasticity (Li et al., 2014), but were normal in individuals who showed full recovery. Similarly, Miller et al. (2014, 2016) observed that vestibular evoked myogenic potentials were asymmetrically enhanced (typically in the more affected side) in stroke survivors.

Although spasticity is commonly assessed in muscles at rest, it is important to examine proprioceptive evoked responses during voluntary movement to help understand mechanisms that underly impaired motor control. In patients that exhibited abnormal tonic stretch responses in plantar flexor muscles at rest, Ada et al. (1998) found no evidence of exaggerated tonic stretch responses during a sustained background contraction. The plantar flexor muscle stretches were specifically designed to mimic the dorsiflexion experienced during the gait cycle (Ada et al., 1998). Similarly, Burne et al. (2005) did not find enhanced stretch responses in stroke survivors relative to controls during low levels of background contraction; these authors suggest that enhanced stretch responses at rest might be explained by the impaired ability to relax excitatory drive to α-motoneurons. Therefore, enhanced stretch responses at rest in chronic stroke survivors could be related to increased resting excitability of motoneurons (Matthews et al., 1986) as well as some potential removal of slack in intra- and extra-fusal fibres (Hagbarth et al., 1995).

It has been debated whether spasticity contributes to motor impairment and should be treated pharmacologically (O'Dwyer et al., 1996; Burke et al., 2013). Anti-spasticity medications often exert effects by reducing afferent input to the spinal cord (e.g., baclofen, tizanidine, clonidine, and diazepam work on GABA receptors or monoamine receptors to increase presynaptic inhibition), reducing motoneuron excitability (e.g., cyproheptadine), or blocking acetylcholine release from neuromuscular junctions (e.g., botulinum toxin). Overall, more

studies should examine the characteristics of stretch responses in stroke survivors during voluntary movement and postural tasks to develop a better understanding of the reorganization of spinal cord pathways and how they may contribute to impaired motor control. An alternative approach to pharmacological treatment is to provide assistive movements along with artificial sensory input through electrical stimulation to try to stimulate plasticity and aid motor recovery (D'Amico et al., 2014).

One limitation of current research on proprioceptive evoked muscle responses post-stroke is that the H-reflex has been primarily used as an experimental method. Mixed nerve stimulation evokes synchronous activation of all large diameter afferent and efferent fibres, and the motor response may not reflect the processing of more natural patterns of afferent input. However, H-reflex studies have provided some insight into changes in several spinal pathways post-stroke. Specifically, there is some evidence of a small reduction in reciprocal inhibition post-stroke (Crone et al., 1994), mixed evidence related to changes in presynaptic inhibition (Faist et al., 1994), and consistent evidence of reduced homosynaptic post activation depression (Grey et al., 2008; Yang et al., 2015). With the exception of homosynaptic depression, no correlations have been found between alterations in spinal pathways and the level of spasticity or disability (reviewed in Pierrot-Deseilligny and Burke, 2012, Chapter 14).

Homosynaptic post activation depression was first described by Curtis and Eccles (1960) when they observed that the size of EPSPs from Ia afferents varied with the frequency of input [facilitation at short intervals (<50 ms, or 20 Hz), and depression at longer intervals (>1 s, or 1 Hz)]. The frequency dependence of the amount of neurotransmitter release is primarily related to mechanisms in the presynaptic nerve terminal, such as calcium signalling and different pools of

vesicles (reviewed by Regehr, 2012). Most synapses demonstrate a mixture of depression or potentiation depending on the frequency of input; these forms of short-term synaptic plasticity have important functions in sensory adaptation and gradation of responses. Thus, altered homosynaptic depression post-stroke has the potential to contribute to motor impairment. In healthy individuals, homosynaptic depression lasts up to 10 s in muscles at rest, but homosynaptic depression is weak or absent during a background contraction (Hultborn et al., 1996). Homosynaptic depression of the soleus H-reflex and stretch reflex is consistently reduced in patients with spasticity as a result of different injuries (stroke, SCI, multiple sclerosis) (Grey et al., 2008; Yang et al., 2015). In stroke survivors, the reduction in homosynaptic depression is correlated with the degree of spasticity (Yang et al., 2015).

Although the mechanisms underlying the change in homosynaptic depression post-stroke are not fully known, it is possible a lesion interrupts descending sources that modulate short-term synaptic plasticity. However, it should be noted that it is difficult for stroke survivors to relax drive to motoneurons at rest, and background contraction reduces homosynaptic depression (Crone and Nielsen, 1989). It is possible that the inability to fully relax the muscle being examined could confound measures of homosynaptic depression at rest post-stroke.

There is some evidence that a CNS lesion disrupts the integration of cutaneous sensory feedback into spinal cord circuitry. Although effects of a stroke has not been studied specifically, the capacity of foot sole cutaneous feedback to modulate the soleus H-reflex has been examined in patients with disrupted descending drive from a SCI. It was observed that stimulation under the metatarsals reduced the soleus H-reflex in healthy controls, but conversely facilitated the H-reflex in SCI patients (across condition-test intervals of 15-90 ms) (Knikou et al., 2007).

Similarly, conditioning cutaneous stimulation of the medial plantar nerve during quiet standing tended to produce soleus H-reflex facilitation in patients with spasticity yet inhibition in controls (Fung and Barbeau, 1994). However, tonic pressure applied to the foot sole reduced the soleus H-reflex in SCI patients as well as controls (Knikou and Conway, 2001). Foot sole cutaneous stimuli was also shown to modulate the soleus H-reflex during assisted stepping in SCI patients in a phase-dependent manner (facilitation during mid-stance and inhibition during mid-swing) (Knikou et al., 2010). Fung and Barbeau (1994) similarly found conditioning the H-reflex with cutaneous stimuli promoted a more natural phasic modulation of the H-reflex throughout the gait cycle in patients with spasticity. Overall, these studies suggest cutaneous functional electrical stimulation could be used to promote appropriate modulation of proprioceptive evoked responses after an injury to the nervous system.

1.4.3 Effects of spasticity and clonus on fusimotor drive and spindle behaviour

Another mechanism that has the potential to contribute to altered stretch responses post-stroke is impaired control over the fusimotor system. During controlled dorsiflexion steps, Hagbarth et al. (1973) found a larger proportion of single spindle afferents from triceps surae muscles with spasticity became active in a less dorsiflexed position (before the ankle reached 90° relative to the shank); whereas most spindles of healthy controls did not have a background discharge until the ankle was dorsiflexed beyond 90°. This finding could be due to changes in fusimotor drive, or mechanical changes in the tissue such as shortening and stiffening of the muscle (Gao et al., 2009; Zhao et al., 2015). Hagbarth et al. (1973) also observed spindle afferent firing rates increased with dorsiflexion steps with a slightly higher slope in patients with spasticity relative to controls (2.5 Hz/step vs. 1.9 Hz/step). The highest static firing rates

observed (~30 Hz) and dynamic indexes were similar between groups. While this study provides minimal evidence that increased fusimotor drive could explain the enhanced stretch responses that characterize spasticity (Hagbarth et al., 1973), it should be noted that only two heterogeneous patients with spasticity were examined.

Similarly, Wilson et al. (1999) quantified background muscle spindle firing rates and reflex activation from cutaneous stimuli in elbow extensor muscles of hemiplegic stroke survivors. They observed no difference in background firing rates relative to controls, and neither group (control nor stroke) displayed evidence of reflex changes in fusimotor drive (Wilson et al., 1999). Altogether, the change in fusimotor drive and how it might contribution to spasticity has not been thoroughly investigated. The involvement of the fusimotor system could also differ depending on the motor task or neurological symptoms. Interestingly, in patients with Parkinson's disease, clonus (~5-8 Hz contractions) was attributed to stretch responses purely affecting α-motoneuron activity (Ia afferents were active during the stretch but not contraction phase), whereas tremor (~3-7 Hz contractions) was associated with both α and γ activation similar to rapid voluntary movements in healthy controls (Ia afferents fired during both muscle stretch and contraction phases) (Hagbarth et al., 1975). Therefore, the organization and involvement of the α- and γ-systems may vary according to different motor symptoms and the neural structures involved in the movement.

1.4.4 Muscle synergies and heteronymous responses post-stroke

In the upper limb of stroke survivors with spasticity, muscle synergies (groups of muscles activated together) become more pronounced (Bruunstrom, 1970). For example, voluntary elbow flexion becomes accompanied by shoulder adduction (Sangani et al., 2009). Abnormal

heteronymous responses to proprioceptive perturbations in the upper limb have also been described; elbow extension perturbations were found to evoke enhanced homonymous responses (elbow and shoulder flexion torque generated by the biceps brachii) as well as adduction torque at the shoulder generated by other muscles (Sangani et al., 2007).

Less research has examined the expression of heteronymous responses in lower limb muscles post-stroke. The leg extensor synergy often observed post-stroke includes extension, internal rotation, and adduction at the hip, along with extension of the knee and extension and inversion of the ankle (Sanchez and Dewald, 2014). The strength of this synergy in chronic hemiparetic stroke can result in difficulty generating movements outside of the extensor synergy (e.g., hip abduction during hip extension) (Sanchez and Dewald, 2014). In the lower limb, heteronymous connections from the quadriceps to soleus have been examined by electrical stimulation of the femoral nerve to evoke changes in the soleus background EMG or H-reflex amplitude (Dyer et al., 2009, 2011). Dyer et al., (2009) found increased heteronymous facilitation of the soleus H-reflex on the paretic side of stroke survivors relative to the non-paretic side and control participants in a seated posture. Moreover, the amplitude and duration of heteronymous facilitation on the paretic side were correlated to poorer clinical measures of lower limb coordination and motor recovery (Dyer et al., 2009). Increased heteronymous facilitation of the soleus H-reflex from quadriceps afferents aligns with the observation of an overactive extensor synergy in the leg, and parallels the findings in the upper limb of increased heteronymous responses along with pronounced flexion/adduction synergies (Sangani et a. 2007, 2009). Similarly, Dyer et al., (2011) found increased heteronymous facilitation of soleus EMG in stroke survivors, which was correlated with the abnormal leg extension synergy (voluntary

extension of the knee paired with plantar flexion). The abnormal expression of muscle synergies is thought to contribute to impairments to stance and gait; however, whether these abnormal heteronymous responses manifest during these specific tasks has not been directly tested.

Altogether, there are many potential changes that may occur within spinal cord circuitry that could affect movement control post-stroke. However, there is a limited description of response characteristics post-stroke in muscles engaged in sensorimotor tasks. Improvements in the assessment of responses to proprioceptive stimuli in engaged postural muscles post-stroke may help provide insight into mechanisms behind impaired motor control and may be useful to monitor the efficacy of therapy and pharmacological treatments.

1.5 Bridging Summary

The goal of the study described in the following chapter was to develop an innovative methodology to examine the characteristics of responses to proprioceptive stimuli in active postural muscles. Specifically, we aimed to develop an approach that involved a continuous noisy perturbation to the Achilles tendon and a linear correlation analysis to characterize muscle and cortical responses to proprioceptive stimuli. This methodology may be useful for subsequent studies to investigate integration with other somatosensory channels (e.g., cutaneous) and to examine changes associated with ageing and neurological disorders such as chronic stroke.

Chapter 2: Frequency characteristics of human muscle and cortical responses evoked by noisy Achilles tendon vibration

2.1 Abstract

Noisy stimuli, along with linear systems analysis, have proven to be effective for mapping functional neural connections. We explored the use of noisy (10–115 Hz) Achilles tendon vibration to examine somatosensory reflexes in the triceps surae muscles in standing healthy young adults (n = 8). We also examined the association between noisy vibration and electrical activity recorded over the sensorimotor cortex using electroencephalography. We applied 2 min of vibration and recorded ongoing muscle activity of the soleus and gastrocnemii using surface electromyography (EMG). Vibration amplitude was varied to characterize reflex scaling and to examine how different stimulus levels affected postural sway. Muscle activity from the soleus and gastrocnemii was significantly correlated with the tendon vibration across a broad frequency range (~10–80 Hz), with a peak located at ~40 Hz. Vibration-EMG coherence positively scaled with stimulus amplitude in all three muscles, with soleus displaying the strongest coupling and steepest scaling. EMG responses lagged the vibration by ~38 ms, a delay that paralleled observed response latencies to tendon taps. Vibration-evoked cortical oscillations were observed at frequencies ~40–70 Hz (peak ~54 Hz) in most subjects, a finding in line with previous reports of sensory-evoked γ-band oscillations. Further examination of the method revealed *1)* accurate reflex estimates could be obtained with <60 s of low-level (root mean square = 10 m/s^2) vibration; *2)* responses did not habituate over 2 min of

exposure; and importantly, *3)* noisy vibration had a minimal influence on standing balance. Our findings suggest noisy tendon vibration is an effective novel approach to characterize somatosensory reflexes during standing.

2.2 Introduction

Charles Sherrington was the first to trace the source of the stretch reflex to muscle spindles and subsequently describe reflexes as a simple expression of the interactive action of the nervous system (Sherrington, 1906). Since then, reflex excitability has been probed by delivering transient tendon taps or electrical nerve stimuli and observing the muscle response (for reviews, see Misiaszek, 2003; Tucker et al., 2007; Voerman et al., 2005). Reflex examinations have enhanced our understanding of the nervous system and have proven beneficial for diagnosing and monitoring rehabilitation efforts for many disorders associated with spasticity or other reflex abnormalities, including stroke, polyneuropathies, spinal cord injury, and cerebral palsy (Hammerstad et al., 1994; Lorentzen et al., 2017; Mezzarane et al., 2014; Nardone et al., 2014; Vieira et al., 2017).

There are, however, some limitations associated with the assessment of reflex pathways using transient stimuli (mechanical or electrical). Generally, many stimuli need to be delivered to obtain a reliable average response (Horslen et al., 2013; Mildren et al., 2016); this can be somewhat inefficient and multiple abrupt stimuli permit the influence of anticipation and habituation effects (Ghanim et al., 2009). Furthermore, due to the large and relatively synchronized volleys of Ia afferent input generated by a tap or nerve stimulation (Burke et al., 1984), sufficient recovery time must be left between stimuli to

allow postactivation depression to dissipate (Crone and Nielsen, 1989; Hultborn et al., 1996). Limitations of previous methods become particularly salient when studying reflex actions in postural muscles during tasks in which they are actively engaged such as standing and walking. During standing, additional recovery time likely must be left between stimuli to allow for recovery of balance following the postural perturbation of each stimulus. Triceps surae reflex responses are also dependent on postural sway, with increased H reflex responses observed during anterior sway and decreased responses during posterior sway (Tokuno et al., 2007). If sway is not accounted for during stimulus delivery, results averaged over a limited number of samples could be skewed or highly variable; this observation is supported by the finding that individuals with greater postural sway demonstrate poor reliability in reflex amplitude (Mynark, 2005).

Suprathreshold white noise stimulation methods have proven effective for assessing the frequency characteristics of human vestibular reflexes in posturally active muscles (stochastic vestibular stimulation; Dakin et al., 2007) and could be adapted to mechanical tendon stimulation to circumvent some of the limitations of traditional tendon tap methods. In general, noisy stimuli delivered to a neural system can be used to assess connectivity through estimates of the amount of frequency variability in ongoing neural activity that can be explained by the frequency content of the stimulus (Fritz et al., 2003; Jones and Palmer, 1987). A suprathreshold noisy tendon vibration (NTV) methodology, along with linear systems analysis, could provide researchers and clinicians with a unique tool to unobtrusively examine reflex excitability in posturally active muscles and gain insight into the frequency characteristics of stretch reflex coupling.

Previous research has probed the frequency characteristics of stretch reflexes by applying continuous sinusoidal stretches (at discrete frequencies between 10 and 50 Hz) to upper limb muscles and subsequently measuring the magnitude of EMG modulation and phase lag between the mechanical stretch and muscle response (Matthews, 1994). The modulation strength and estimated phase delays provided insight into the operation of reflex circuitry at different frequencies, as well as provided an arguably superior measure of the delays inherent in the reflex pathway (Matthews, 1994). The delays measured from the phase estimates take into account the envelope of the response and therefore are more representative of the "average response time of the average unit" (Matthews, 1994), whereas the latency measured to the onset of a response evoked by transient stimuli is likely representative of only the fastest conducting axons. Sinusoidal stimuli can also shed light on motoneuron evoked response properties, such as where their response(s) lie within a given stretch cycle and how susceptible they are to coupling with stimuli close to their firing rate to produce a sharp increase in reflex gain (carrier resonance effect; Matthews, 1997). Although the pure sinusoidal stimulus method imparts numerous benefits, there are several notable drawbacks that include *1)* response contamination from voluntary tracking of the predictable stimulus (Cathers et al., 1999), *2)* the development of movement illusions or tonic vibration reflex, and *3)* the experimental time necessary to test a series of frequencies individually.

Stretch reflexes have also been examined using large amplitude, low-frequency (<25 Hz) pseudorandom joint perturbations (Johnson et al., 1981; Kearney and Hunter, 1983; Kearney and Hunter, 1984; Leao and Burne, 2004). In particular, low-frequency

ankle joint perturbations in humans lying prone have been used to identify the ongoing relationship between ankle movement velocity and muscle activity (Kearney and Hunter, 1983; Kearney and Hunter, 1984). Using pseudorandom stimuli, these authors identified some key differences in reflex organization between the triceps surae and tibialis anterior (Kearney and Hunter, 1983; Kearney and Hunter, 1984). Other researchers who have used a pseudorandom muscle stretching protocol also chose to apply primarily low-frequency stimuli that are relevant to voluntary movement and within motoneuron firing rate limits (Cathers et al., 1996; Johnson et al., 1981; Kearney and Hunter, 1983; Kearney and Hunter, 1984; Leao and Burne, 2004). Human muscle spindles, however, have the capacity to respond and entrain to higher frequency stimuli (exceeding 100 Hz; Fallon and Macefield, 2007), and strong reflex EMG modulation can be observed during high-frequency sinusoidal stretching (50 Hz; Matthews, 1993, 1994). In addition, high-frequency components are present in impulses naturally experienced by the ankle joint, for example, during a trip; therefore, these high-frequency components have functional relevance. Thus we focused our experiment on responses to a broadband noisy mechanical stimulus that contained power up to the highest frequency that could evoke a discernable reflex response.

Similar to spinal stretch reflexes, transient electrical or mechanical stimuli are typically used to evoke cortical potentials to study the ascending transmission of sensory information (Frascarelli et al., 1993; Mauguiére, 1999; Davis et al., 2011). Thus, these methods of evoking cortical activity are subject to similar limitations as tendon tap or H reflexes, such as the potential influence of anticipation, habituation, and postural

interference. Estimates of coherence between noisy peripheral sensory input and somatosensory cortex activity may have the additional benefit of providing a useful alternative approach to probe the frequency characteristics of somatosensory-evoked cortical potentials.

The primary objective of our experiment was to explore the use of Achilles NTV to assess the frequency characteristics of triceps surae reflexes and sensorimotor cortex-evoked potentials during standing. We also aimed to examine the scaling of reflex responses to different vibration amplitudes in the soleus and medial and lateral gastrocnemius muscles. Finally, we aimed to establish trial durations that evoke consistent responses and identify whether stretch reflexes evoked by noisy mechanical stimuli are subject to habituation over 2 mins of stimulus exposure.

2.3 Methods

2.3.1 Participants

Eight healthy young adults (age = 27 ± 5.3 yr, 4 male) free of musculoskeletal and neurological disorders participated. Participants provided written informed consent and all procedures were approved by the University of British Columbia Research Ethics Board.

2.3.2 Experimental setup

Participants stood on a force plate (OR6–7; AMTI, USA) with their stance width normalized to foot length and their gaze directed onto a visual target positioned at eye level ~3 m ahead. A 3-cm diameter probe, attached to a linear motor (model MT-160;

Labworks, USA), was positioned against the right Achilles tendon. The linear motor was secured onto two near-frictionless linear slides and was pulled forward onto the tendon by a weighted pulley system (Fig. 2-1); this setup was decoupled from the force plate and was able to maintain a constant ~1 N preload force on the tendon. A force transducer (model 31; Honeywell, USA) was placed in line with the probe and motor piston and an accelerometer (model 220 – 010; X Tronics, CA) was secured to the back of the motor piston. Acceleration and force signals were differentially amplified (×1 and ×100, respectively) and low-pass analogue filtered at 600 Hz (Brownlee model 440; AutoMate Scientific, USA). All motor command signals were generated using LabVIEW 11 software and output at 5000 Hz from a PXI-6225 multifunctional data acquisition board (running with a PXI-8106 real-time controller in a PXI-1031 chassis). Analogue voltage commands were sent to a motor amplifier (PA-141; Labworks, USA) for open-loop control of tendon stimulation.

Electromyography (EMG) was recorded from the soleus (SOL), medial gastrocnemius (MGas), and lateral gastrocnemius (LGas) muscles using surface electrodes positioned over the muscle bellies in bipolar arrangement (amplified ×2,000, 10 Hz highpass and 1000 Hz lowpass filter; NeuroLog NL824 preamplifier and NL820 Isolator; Digitimer LTD, UK). The ground electrode was placed on the lateral malleolus. Electroencephalography (EEG) was recorded across the sensorimotor cortex using scalp ring electrodes placed over Cz (active), Fpz' (reference), and the right mastoid process (ground) (amplified ×20000; 1 Hz highpass and 1000-Hz lowpass filter; GRASS P511 AC amplifier; Astromed, USA). EEG electrode impedance levels were maintained below

5 kΩ. Ocular and facial muscle artifacts were identified and displayed to participants, and participants were subsequently instructed to minimize these behaviors during trials. Forces and moments from the force plate were amplified (×1000 – 4000) and sampled at 100 Hz, while motor voltage commands, probe acceleration and force, surface EMG, and EEG signals were sampled at 2000 Hz (Power 1401 A/D board and Spike2 software; Cambridge Electronic Design, UK).

2.3.3 Experimental procedures

Participants completed a 2-min quiet stance trial and mean foot center of pressure (COP) positions were calculated in the mediolateral and anteroposterior directions to determine their neutral position. Participants began subsequent trials at their neutral position, and in the case that their COP drifted, experimenters provided verbal feedback to guide them back to neutral. Four 2-min trials of NTV were conducted where a white noise signal low-pass filtered at 100 Hz was delivered to the right Achilles tendon. In the recorded probe acceleration, power below 10 Hz and above 115 Hz was less than or equal to -13 dB (ref. peak plateau of power spectrum); a sample recorded acceleration profile and power spectrum are displayed in Fig. 2-1C. This stimulus bandwidth was chosen based on pilot data that demonstrated the maximum frequency that could contain significant coherence was ~90 Hz even when larger stimulus bandwidths were delivered (e.g., 10–300 Hz). The NTV was delivered at four different amplitudes (vibration root mean square accelerations: 5, 10, 15, and 20 m/s^2); these amplitudes were also chosen based on pilot data that suggested these amplitudes would fall approximately within a steep, ascending portion of the reflex recruitment curve. Two additional trials of 20

tendon taps (30 Hz raised-cosine bell curve pulses at 25 m/s^2; 8 to 12 s interstimulus interval) were conducted to compare the temporal characteristics of the responses elicited by noisy stimulation to the responses elicited by taps. The tendon tap and NTV trials were presented in block-randomized order.

2.3.4 Analyses

Forces and moments from the force plate were digitally low pass filtered at 10 Hz (5th order dual pass Butterworth filter) and COP was calculated from moments (Mx and My) and vertical force (Fz). For tendon stimulation and quiet stance trials, the frequency spectra of COP in the anteroposterior and mediolateral directions was calculated (frequency resolution 0.0122 Hz) and mean power frequency (MPF) were determined as:

$$\mathrm{MPF} = \sum_{j=1}^{n} fjPj / \sum_{j=1}^{n} Pj$$

where f is frequency and P is power. EMG, EEG, force, and acceleration data were digitally low pass filtered at 1000 Hz (5th order dual pass Butterworth filter). For the tendon tap trials, EMG data were full wave rectified and EMG and EEG signals were trigger averaged to the tap stimulus onset within a window from 20 ms preceding to 300 ms following the stimulus. COP was also trigger averaged within a window from 0.5 s preceding to 4.5 s following the tap. For noisy stimulation trials, EMG data were full wave rectified and coherence analysis was performed using the Neuro-Spec2.0 software package developed by Rosenberg, Halliday, and colleagues (Halliday et al., 1995; Rosenberg et al., 1989) for MATLAB (Mathworks, USA). Our approach was similar to that of previous research conducted to establish the time and frequency characteristics of

vestibular responses elicited by stochastic stimuli (Dakin et al., 2007, 2010, 2011). To determine the strength of the linear association between two signals in the frequency domain, coherence functions were calculated between probe acceleration (input signal) and rectified surface EMG of each muscle and EEG (output signals) (Rosenberg et al., 1989; Halliday et al., 1995; Dakin et al., 2007). Coherence was calculated as the magnitude of the input-output signal cross spectra squared divided by the product of the input and output autospectra (Dakin et al., 2007). Thus coherence values provide normative estimates of the frequency coupling strength between two signals. To identify temporal characteristics of coherent frequencies, cross-covariance was calculated using the inverse Fourier transform of the input-output signal cross spectra and normalized by the product of the vector norms of the input and output signals. Therefore, cross-covariance values are bounded by -1 and +1 and provide an estimate of the signal coupling strength in the time domain (Dakin et al., 2010). Our convention was that acceleration toward the tendon and increased (rectified) EMG were assigned positive polarities. For example, a positive correlation would represent acceleration into the tendon is associated with increased EMG, or acceleration away from the tendon is associated with decreased EMG. As described by Halliday et al. (1995), 95% confidence limits for coherence (positive threshold) and cross-covariance (positive and negative thresholds) were constructed under the hypothesis of independence between the two signals. Values exceeding these limits provide evidence of a significant linear relationship between the stimulus and response. Phase was also estimated to infer the temporal relationship between the NTV and EMG at all frequencies containing significant

coherence (Amjad et al., 1997).

To analyze pooled responses, data were concatenated across participants and stimulus amplitudes to compare between the three muscles; this yielded a total of 3,712 disjoint sections (1.024 s/segments; frequency resolution = 0.9765 Hz). Data were also concatenated across participants and muscles for comparisons between stimulus amplitudes; this yielded a total of 2,784 disjoint segments (1.024 s/segments; frequency resolution = 0.9765 Hz). For analysis of individual 2-min trials, data were sectioned into 116 segments to obtain a frequency resolution of 0.9765 Hz (1.024 s/segments). The number of segments used in the analysis is an important factor in determining the 95% confidence limits constructed around coherence and cross-covariance traces. In addition, we divided each 2-min trial in various ways to answer two questions: *1)* what is the minimum trial duration required to obtain reliable reflex measures, and *2)* does the reflex response habituate over the trial? To answer the first question, 10-s portions of data (9–10 segments) were incrementally added and normative error in peak-to-peak cross-covariance was calculated for each duration as:

$$\text{error} = \sum [\sqrt{(}\left|C_{120}\right| - \left|C_n\right|)^2/C_{120}] \times 100\%$$

where C_{120} is cross-covariance for the full trial duration and C_n is cross-covariance for different trial lengths between 10–110 s in 10 s increments (Blouin et al., 2011). Since our segment size was 1.024 s, each 10 s addition of data increased the number of segments by either 9 or 10 segments because incomplete segments were removed from the analysis. Signal to noise ratios were also calculated for each trial duration as peak-to-

peak cross-covariance divided by the width between the 95% confidence limits. To answer the second question, coherence and cross-covariance were calculated and compared between the first ~40 s (39 segments, 39.936 s data used) and the last ~40 s of the trial. Comparisons of different trial durations were conducted for the SOL muscle in response to the 10 m/s^2 RMS acceleration noisy stimulus. We elected to probe trial duration and habituation effects in SOL since it is the most commonly studied lower limb muscle for reflex testing, and we chose the medium-low level NTV based on results that showed this subtle stimulus level evoked strong responses across all participants.

2.3.5 Statistics

To examine if the tendon stimulation affected the frequency content of postural sway, we performed a one-way repeated-measures ANOVA (5 levels: 4 vibration amplitudes and no vibration) on anteroposterior and mediolateral COP MPF. To examine how reflex responses scaled with stimulus amplitude, we conducted a two-way (muscle × NTV amplitude) repeated-measures ANOVA on peak-to-peak cross-covariance. Significant ANOVA effects were followed up with Fisher least significant difference post hoc comparisons. Pooled participant data were concatenated across stimulus amplitudes and a χ^2 extended difference of coherence (DOC) test was performed to determine whether the independent coherence estimates significantly differed between muscles (Amjad et al., 1997). Similarly, pooled participant data were concatenated across muscles and a χ^2 extended DOC test was performed to determine if coherence significantly differed between stimulus amplitudes. Significant main effects were followed up with pairwise DOC tests between successive stimulus amplitudes and between each muscle

combination. Finally, to determine if the SOL muscle response to NTV habituated throughout the trial, we compared peak-to-peak cross-covariance in the first 40 s of the trial to last 40 s of the trial using a paired *t*-test. Effects were considered significant at an α-level of 0.05, all error bars demonstrate standard error (n = 8).

2.4 Results

No participants reported illusory movements in response to the NTV (even when asked to close their eyes) nor did they report any noticeable interference with standing balance. Participants naturally maintained their COP around their neutral position and verbal feedback to correct postural drift was only necessary for two subjects. MPF of COP in both the anteroposterior and mediolateral directions were not affected by the noisy vibration ($p = 0.583$ and 0.773, respectively; Fig. 2-2). Perturbations were observed in participants' COP traces in response to tendon taps; triggered-average anteroposterior COP demonstrated that the taps evoked a directional postural response that required several seconds for recovery (Fig. 2-2C). Meanwhile, the noisy stimulus did not produce any noticeable change in COP relative to quiet stance.

2.4.1 NTV-muscular coherence

In all participants, significant (exceeding 95% confidence limits) muscle responses were observed in the SOL and MGas EMG in the frequency (coherence) and time (cross-covariance) domains for all NTV stimulus amplitudes. Responses were characterized by a significant coherence band generally within ~10–80 Hz (Fig. 2-3), with the peak response observed at ~40 Hz in all muscles (SOL 36 ± 4 Hz; MGas 39 ± 5

Hz; LGas 47 ± 9 Hz). Background activity in the LGas muscle during standing was low or absent in the majority of participants, and significant reflex responses were not always observed in LGas EMG, particularly at the lower levels of stimulation (absent in 50% of participants). For all three muscles, the slope of the phase estimate was generally linear, indicating a fixed reflex delay across frequencies (Fig. 2-4). The magnitude of the slope corresponded to approximately a 40-ms delay. There was, however, a small upward deflection in the phase estimates, accompanied by a reduction in the coherence strength, at ~20 Hz.

The NTV-EMG cross-covariance displayed a short-latency biphasic profile with a positive peak followed by a trough. For the SOL muscle, the first peak in the cross-covariance occurred at a lag of 38.1 ± 0.8 ms (range = 34 to 42 ms), and similar lag times were observed for the MGas (38.5 ± 1.9 ms) and LGas (38.4 ± 3.1 ms) muscles. Lag times observed in the cross-covariance generally corresponded to the latencies of the first peak stimulus-triggered average response to tendon taps (SOL = 41.3 ± 2.4 ms; MGas = 40.5 ± 2.5 ms; LGas = 41.3.7 ± 1.6 ms; Fig. 2-3).

Peak-to-peak cross-covariance positively scaled with NTV amplitude (Fig. 2-5); statistically there was a significant main effect of stimulus amplitude on peak-to-peak cross-covariance [$F_{(3,21)} = 13.135$, $p = 0.001$], main effect of muscle [$F_{(2,14)} = 7.464$, $p = 0.006$], and muscle × stimulus amplitude interaction [$F_{(6,42)} = 2.464$, $p = 0.039$]. These results indicate that overall the SOL muscle had stronger coupling with the noisy stimulus and scaled more with increases in the stimulus amplitude. In contrast, LGas demonstrated the weakest coupling and the shallowest rate of increase with stimulus amplitude. Post

hoc comparisons revealed significant overall differences in peak-to-peak cross-covariance between SOL and LGas at all four stimulus amplitudes (5, 10, 15, and 20 m/s^2; *p-value* range 0.009 – 0.016) and between LGas and MGas at the 5 m/s^2 ($p = 0.041$) and 10 m/s^2 ($p = 0.025$) stimulus amplitudes.

Results for pooled data revealed a general increase in coherence with increases in stimulus amplitude (Fig. 2-6A). The χ^2 extended DOC test demonstrated a significant effect of the stimulus amplitude on coherence at frequencies between ~10 and 60 Hz (Fig. 2-6B). Pairwise DOC tests indicated significant increases in coherence between the 5 and 10 m/s^2 stimulus amplitudes at frequencies ~20–40 Hz, and significant increases in coherence between the 15 and 20 m/s^2 stimulus amplitudes at frequencies ~10–30 Hz. Pooled data also revealed generally stronger NTV-EMG coherence for the SOL and MGas muscle compared with the LGas (Fig. 2-6C). The χ^2 extended DOC test indicated a significant effect of the muscle on coherence at frequencies between ~20–70 Hz (Fig. 2-6D). Pairwise DOC tests demonstrated significantly higher coherence in SOL compared with both MGas and LGas at frequencies ~30–50 Hz and significantly higher coherence in MGas compared with LGas at frequencies ~50–70 Hz.

2.4.2 NTV-cortical coherence

One participant's EEG data were excluded due to facial muscle and blink artifacts. Clear stimulus triggered-average-evoked potentials were observed in the EEG recording across the sensorimotor cortex in all remaining seven participants in response to tendon taps. However, significant NTV-EEG coherence was only observed in five out of the seven participants, and coherence was often absent during the lower stimulus

amplitudes (5 and 10 m/s^2). Significant coherence was observed within a frequency range of ~40–70 Hz (within the γ-band), with the peak coherence located at 54 ± 8 Hz (Fig. 2-3).

The peak EEG response occurred at a slightly longer lag relative to muscle responses, with the trough observed at 50 ± 6 ms and peak observed at 53 ± 6 ms; these latencies generally correspond to early event related potentials from tendon taps in our experiment (peak 47.8 ± 4.5 ms; trough 56.2 ± 8.7) and previous experiments (Davis et al., 2011). EEG responses were subtle relative to muscle responses and characterized by multiple peaks and troughs. Interestingly, there was no prominent EEG activity in the cross-covariance at longer lag times (e.g., ~100 ms and later) that would correspond to later stages of sensory processing.

2.4.3 Trial duration and habituation

Two-minute trials of the 10 m/s^2 NTV were subdivided into 10 s additive sections to determine the minimum trial duration necessary to obtain reasonable reflex estimates in the SOL muscle. With ~10 s of data collection (9 segments), mean normative error in the peak-to-peak cross-covariance was high (~40%) and there was a large amount of between-participant variability in normative error (Fig. 2-7). As expected, confidence intervals and background noise decreased as the trial duration (and number of segments used in the analysis) increased. The decline in the mean and variability of normative error with each addition of ~10 s of data began to plateau at the ~40-s data length, signifying the reflex responses measured with ~40 s of data collection approximated responses measured with 2 min of data collection (10% difference). In addition, the signal to noise

ratio increased with each addition of data segments, and this increase was steeper between 10 and 40 s (Fig. 2-7). The signal to noise ratio approximately doubled between ~10 and ~40 s of data, while further increases in data length up to ~120 s only resulted in an increase in the signal to noise ratio by another 1.7-fold.

There was no evidence that the peak-to-peak cross-covariance amplitude differed between the beginning and end of the trial ($p = 0.417$; Fig. 2-7C), indicating no significant habituation to the NTV over 2 min of stimulus exposure.

2.5 Discussion

The primary objective of our experiment was to examine the frequency responses of triceps surae EMG, and sensorimotor cortex EEG, evoked by noisy (10–115 Hz) Achilles tendon vibration in standing participants. Our results showed surface EMG was significantly coherent with NTV across a broad frequency range, with strong responses observed in the SOL and MGas muscles. Our results also demonstrate that reasonable SOL coherence estimates can be obtained with minimal perturbation to standing balance, and without habituation effects.

2.5.1 NTV-evoked muscle responses

We observed significant coherence between the NTV and surface EMG that extended from ~10–80 Hz. This bandwidth falls within the muscle spindle vibration sensitivity range (Fallon and Macefield, 2007), but exceeds the upper limit of human individual motor unit firing rate capabilities (maximal soleus motor unit rates ~20 Hz; Kallio et al., 2013). In spite of known homosynaptic postactivation depression and

motoneuron afterhyperpolarization effects, high-frequency sine wave vibration bursts (3 cycles at 100 Hz) have previously been shown to generate three distinct reflex responses in SOL surface EMG (Fornari and Kohn, 2008). EMG responses to high-frequency vibration likely reflect that high-frequency spindle input can effectively shift the firing probability of individual triceps surae motor units.

The profile of the reflex response evoked by NTV in the time domain exhibited a short latency peak followed by a trough; the lag time between the NTV and muscle response (~38 ms) approximately corresponded to the latency of the T-reflex in the lower limb observed in our experiment (~41 ms) as well as in previous experiments (Woollacott and Nashner, 1982; Horslen et al., 2013; Mildren et al., 2016). Similar to our tap-evoked responses, there was no evidence of responses in the cross-covariance at longer delays that could parallel the medium or long latency responses observed in ramp-and-hold stretch reflexes (Yavuz et al., 2014). Therefore, we believe our NTV method can be used to characterize the functional short latency reflex coupling between type Ia spindle afferents and lower limb motoneurons. It has previously been shown that an adapted trigger-averaging technique used with sinusoidal stimuli allowed for the identification of a shorter reflex onset latency compared with cross-correlation lag times (Karacan et al., 2014). However, there was no difference between the trigger-averaged latency and cross-correlation lag time measured to the peak of the response (Karacan et al., 2014), as was done in our experiment. This suggests that trigger averaging to either transient or sinusoidal stimuli could provide clearer identification of the earliest reflex onset latency (mediated by the fastest conducting axons) compared with correlational techniques.

However, trigger-averaging techniques do not provide important information about the frequency characteristics of responses, which are obtained through estimates of coherence, gain, and phase using the framework developed by Halliday and colleagues (Rosenberg et al., 1989; Halliday et al., 1995; Amjad et al., 1997).

The slopes of the phase estimates for each muscle were linear and suggested a relatively conserved stimulus-response delay of ~40 ms across frequencies containing significant coherence. There was, however, a slight upward deflection in the phase slope at ~20 Hz, accompanied by a discontinuity in the coherence plot at ~20 Hz. This 20 Hz phenomenon was observed in all three muscles, although it was more prominent at higher stimulus amplitudes and in SOL. This pattern of a decrease in EMG modulation with sinusoidal stimuli around 20–25 Hz, accompanied by an upward deflection in the phase estimate, has previously been observed in the flexor carpi radialis (FCR) muscle (Matthews, 1993). Matthews (1993) suggested that this pattern could arise from the interference between two different latency reflex responses (which traveled through pathways that impart different delays), since the sum of the two responses would create a phase intermediate between them. The appearance of a longer latency interfering response in the FCR was suggested to have a functional role in stabilizing the system to tremor or clonus (Matthews, 1993). The interference pattern that we observed in the triceps surae muscles at ~20 Hz requires more detailed investigation.

The amount of EMG that could be explained by the tendon vibration increased as we increased the amplitude of the NTV, and the overall reflex response and amplitude scaling were strongest in the SOL and weakest in the LGas muscle. DOC tests also

demonstrated stronger NTV coupling in the SOL muscle ~30–50 Hz compared with MGas and LGas. Response differences within the triceps surae group could reflect differences in their spindle density, where SOL houses a higher overall number (~400) and density (0.94 spindles/g) of muscle spindles compared with the gastrocnemius muscles (~150 spindles total, 0.4 spindles/g; Banks, 2006; Voss, 1971). SOL muscle spindles might also experience a higher stimulus intensity compared with gastrocnemius spindles due to dampening of the vibration as it travels through tissue. Reflex coupling strengths could also reflect differences in their relative contributions to standing balance, where SOL generally provides the majority of plantar flexion torque while LGas remains relatively silent (Heckman and Binder, 1988). In addition, the higher proportion of slow twitch fibers in the SOL might favour stronger reflex coupling since animal studies have shown higher efficacy of Ia input to low-threshold motoneurons in a way that accentuates orderly recruitment (Héroux et al., 2014).

2.5.2 Postural and perceptual effects

Across the four stimulus intensities, ~17–34% of the SOL EMG variability could be explained by the tendon stimulation. Despite this strong reflex coupling, there was no notable interference with posture, illusions of forward sway (i.e., illusory muscle lengthening) or presence of a tonic vibration reflex (TVR). Compared with sine wave vibration, the frequency variability of our noisy stimulus (10–115 Hz) seems to impede the generation of illusory movement and TVRs. We speculate that the frequency variability precludes the stimulus from producing a ramping reflex contraction. The absence of any illusory movement or TVR suggests NTV is a more suitable method for

the continuous assessment of reflex excitability. Additionally, tendon taps produce a strong unidirectional postural response, whereas noisy stimulation produces a subtle and more bidirectional postural response; thus NTV circumvents some of the limitations of traditional tendon tap methods. The absence of low-frequency content in the NTV likely causes less interference with postural sway, similar to observations from stochastic vestibular stimulation (Dakin et al., 2010).

2.5.3 Trial duration and reflex habituation

With the use of the RMS = 10 m/s^2 NTV, reasonably accurate reflex excitability estimates could be obtained with a minimum of ~40 s of data collection; the response amplitudes measured with ~40 s of data collection were 10% different from those measured with 2 min of data collection. T-reflex responses between successive stimuli are inherently variable (Horslen et al., 2013; Mildren et al., 2016); therefore, our method of sampling the ongoing association between the stimulus and muscle activity over a sufficient window (e.g., 40–60 s) has advantages over traditional approaches (e.g., T- and H-reflex) that only provide discrete snapshots of reflex excitability.

There was no indication that reflex responses to NTV habituated with continuous stimulus exposure over 2 min. Therefore, measurements obtained using this method are not affected by habituation within the intensity levels and durations necessary for reflex testing.

2.5.4 NTV-evoked cortical potentials

Although tendon tap-evoked potentials were present in all participants throughout the experiment, NTV-cortical coherence was absent in two out of seven participants, and

in two of the remaining participants it was only prominent during the highest stimulus amplitude (20 m/s^2). When significant coherence was present, NTV-EEG peak coherence values were small and scaled with the stimulus amplitude from r^2 ~0.04 to 0.07. Our success rate (71%) in extracting NTV-EEG coherence is similar to the success rate previously reported for extracting corticomuscular coherence during voluntary muscle contraction (50–75%; Mima and Hallett, 1999; Perez et al., 2012; Murnaghan et al., 2014). When present, triceps surae corticomuscular coherence values are also modest (r^2 = 0.06; Mima and Hallett, 1999; Murnaghan et al., 2014). The absence of strong NTV-EEG coherence could be due to nonlinearities between the stimulus and evoked cortical activity and the absence of low-frequency power to associate with the longer latency cortical-evoked responses.

We observed NTV-EEG coherence within the frequency range of ~40–80 Hz, with the peak located at 54 Hz on average. This range corresponds to the γ-band oscillations recorded over the somatosensory cortex induced by mechanical or electrical nerve stimuli (Ihara et al., 2003; Bauer et al., 2006). Specifically, magnetoencephalography recordings have shown that tactile stimulation of the finger evokes γ-oscillations (concentrated around 60–90 Hz) over the sensorimotor cortex ~40–100 ms after stimulus presentation (Bauer et al., 2006). Attention directed toward the spatial features of the stimulus further enhanced these γ-oscillations, which source analysis suggested originated from the primary somatosensory cortex (Bauer et al., 2006). It has been suggested that γ-band oscillations in the somatosensory cortex reflect early stages of processing functionally relevant sensory information and that it is crucial in

communicating with other somatosensory areas for higher level processing.

The profile of the NTV-cortical cross-covariance was oscillatory, and the initial trough lagged the NTV by ~50 ms. This short delay is generally in alignment with the latency of early event related potentials recorded over the somatosensory cortex in response to mechanical stimuli (Braun et al., 2002; Simões et al., 2003; Davis et al., 2011). This NTV-cortical lag time specifically approximates the latencies of the Achilles tendon tap-evoked potentials observed in our experiment as well as in previous experiments (Davis et al., 2011).

2.5.5 Methodological considerations

There are some important considerations with regards to the assessment of reflexes using stimuli applied to the tendon. Tendon tap reflex responses (and likely NTV responses) might not reflect the strength of direct monosynaptic connections between triceps surae spindles and motoneurons for several reasons. First, in addition to targeting triceps surae spindles, tendon taps have been shown to evoke multiple spikes in Ia afferent fibers innervating extensor hallucis longus, tibialis posterior, and intrinsic muscles of the foot (Burke et al., 1983). Tendon taps have also been shown to alter the discharge of some type II spindle afferents as well as Golgi tendon organ and skin afferents (Burke et al., 1983). Despite this, however, it appears to be the input from type Ia spindle afferents that accounts for the motor response (Burke et al., 1983). Second, the rise time of composite excitatory postsynaptic potentials is broad enough to permit time for oligosynaptic pathways to contribute to the response; thus it should be considered that these methods might not strictly assess monosynaptic reflex strength (Burke et al., 1984).

It should also be noted that similar limitations regarding the purity of the afferent stimulus and spinal connections tested are present with direct nerve stimulation (H reflex; Burke et al.,1983, 1984). In addition, direct nerve stimulation bypasses natural mechanotransduction and generates very artificial, synchronized nerve impulses. Our noisy stimulation methodology has the advantage of mechanically stimulating receptors themselves within a physiological range and subsequently providing temporal and frequency information about somatosensory projections to muscle and to the cortex. Further exploration of tendon tap reflex responses of single motor units during standing using frequency and probability based measures (e.g., peristimulus time histograms and peri-stimulus frequencygrams), along with coherence between sensory and motor spike trains, is necessary to more fully understand the characteristics of the pathways that contribute to tendon tap and noisy vibration reflexes in humans while standing.

2.5.6 Conclusions

Our findings indicate that noisy vibration of the Achilles tendon is an effective novel approach to study somatosensory reflexes in lower limb muscles during standing. Additionally, NTV-muscular coherence can shed light on short latency communication between sensory receptors and the motoneuron pool across frequencies. Our findings also show promise for the use of NTV to concomitantly assess somatosensory related cortical activity, although this requires further investigation. These NTV methods could enhance researchers' and clinicians' ability to assess reflexes in posturally active muscles efficiently and with minimal interference with standing balance.

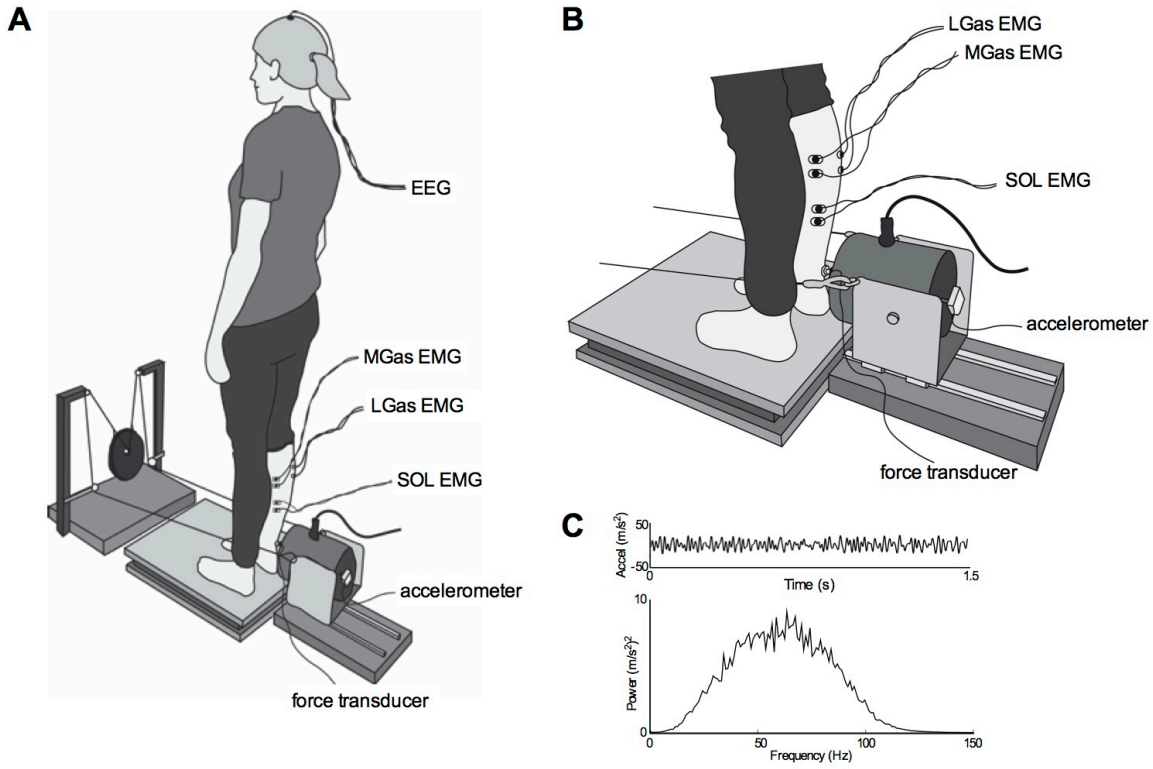

Figure 2-1 Experimental setup

Experimental setup showing the linear motor on frictionless slides pulled forward using a weighted pulley system (A), and a zoomed in view of the probe positioned against the Achilles tendon of a participant standing on a force plate (B). Sample profile of the noisy vibration acceleration over time and the acceleration power spectrum (C).

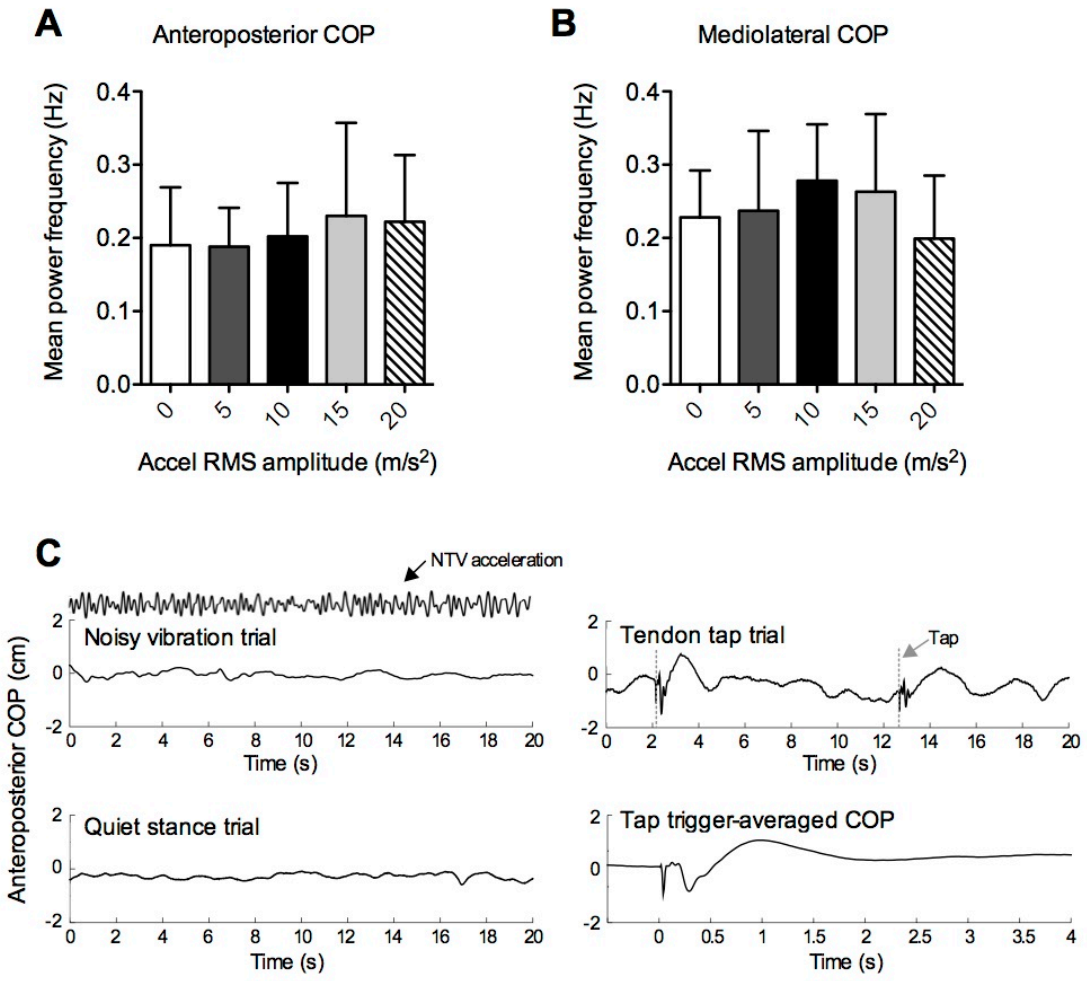

Figure 2-2 Postural sway during quiet standing, tendon vibration, and tendon taps

Mean power frequency of center of pressure (COP) in the anteroposterior (A) and mediolateral (B) directions across the four stimulus amplitudes and quiet stance (no stimulus) trials. Representative traces of anteroposterior (AP) COP during the noisy tendon vibration, quiet stance, and tendon tap trials, as well as a representative trace of AP COP trigger-averaged to the tap stimuli (C).

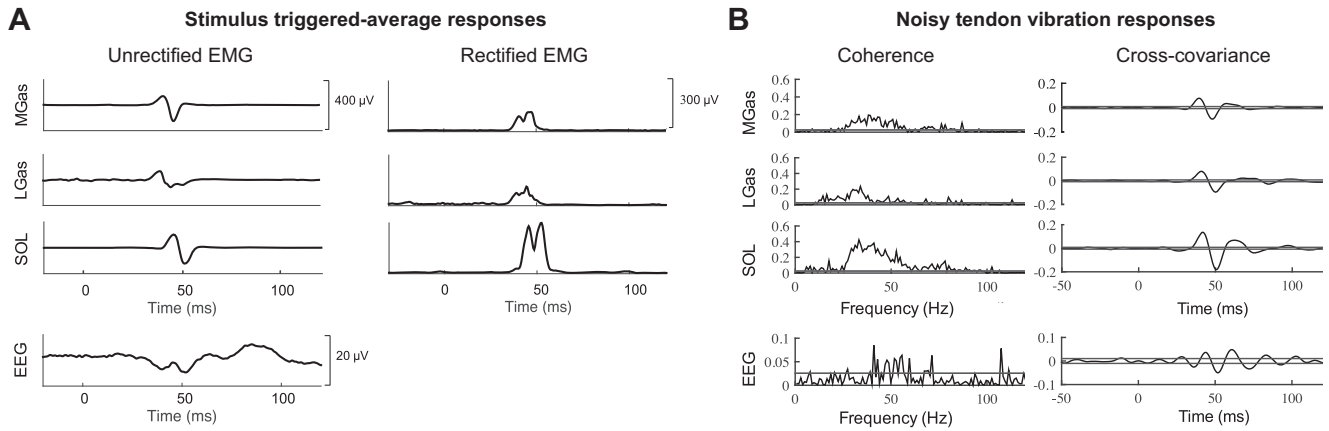

Figure 2-3 Representative responses to tendon taps and noisy tendon vibration

Representative traces of stimulus triggered-average muscular and cortical responses to tendon taps (A); data are shown for both un-rectified and rectified EMG. Representative traces of coherence and cross-covariance between the stimulus acceleration and triceps surae EMG and sensorimotor cortex EEG for the 10 m/s^2 (medium-low level) noisy stimulus (B). Horizontal lines indicate 95% confidence intervals.

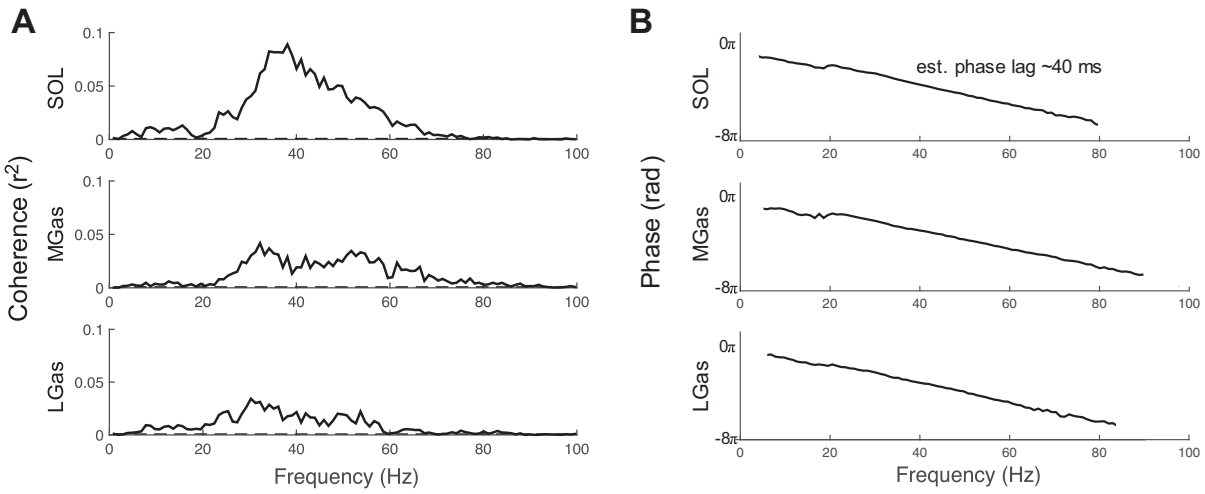

Figure 2-4 Pooled group responses to noisy tendon vibration

Coherence (A) and phase estimates (B) for each muscle for data pooled across participants and stimulus amplitudes.

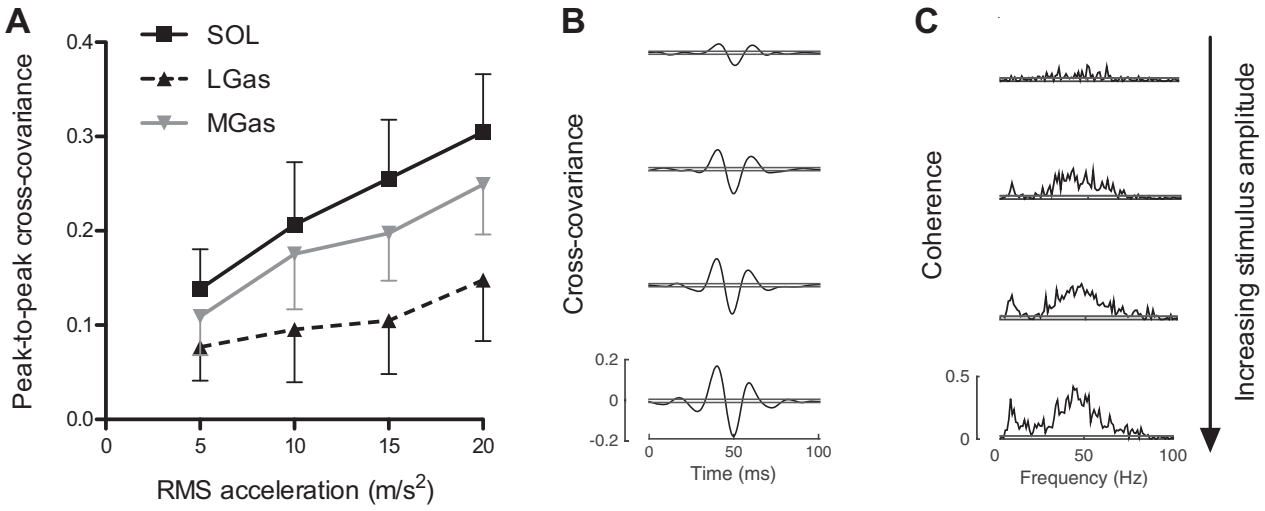

Figure 2-5 Scaling of responses to noisy tendon vibration

Noisy tendon stimulation results for the triceps surae muscles showing increases in mean peak-to-peak cross-covariance (A) in response to increases in tendon stimulation amplitude. Sample cross-covariance traces (B) and coherence traces (C) from the SOL muscle of one participant showing the increases with stimulus amplitude.

SOL = soleus; LGas = lateral gastrocnemius; MGas = medial gastrocnemius.

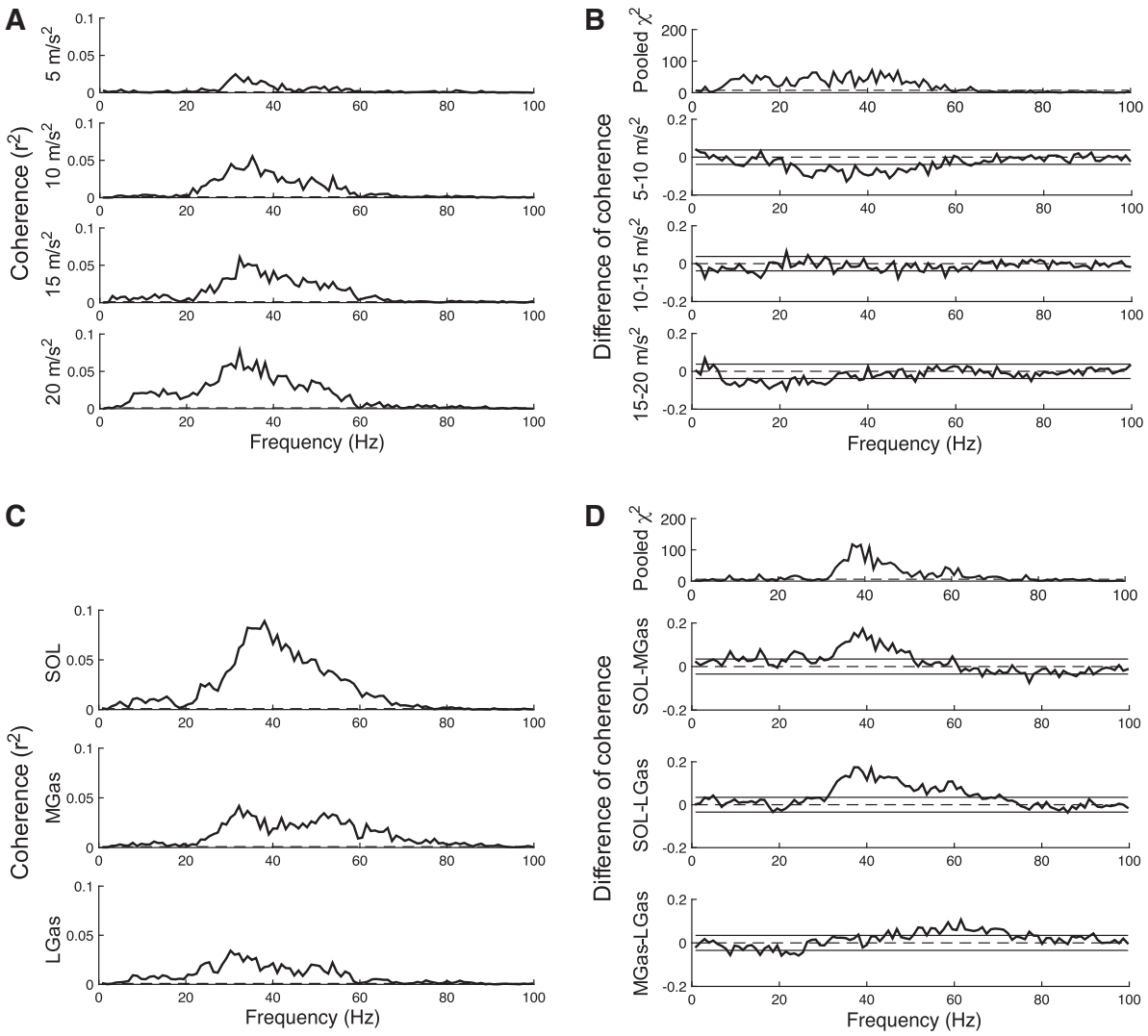

Figure 2-6 Differences in coherence between muscles and stimulus amplitudes

Results from data concatenated across participants and muscles to demonstrate overall coherence at each stimulus amplitude (A) as well as pooled difference of coherence (DOC) results across stimulus amplitudes, and pairwise DOC results between successive stimulus amplitudes (B). Results from data concatenated across stimulus amplitudes to demonstrate overall coherence for each muscle (C) as well as pooled DOC results across muscles, and pairwise DOC results between each muscle (D).

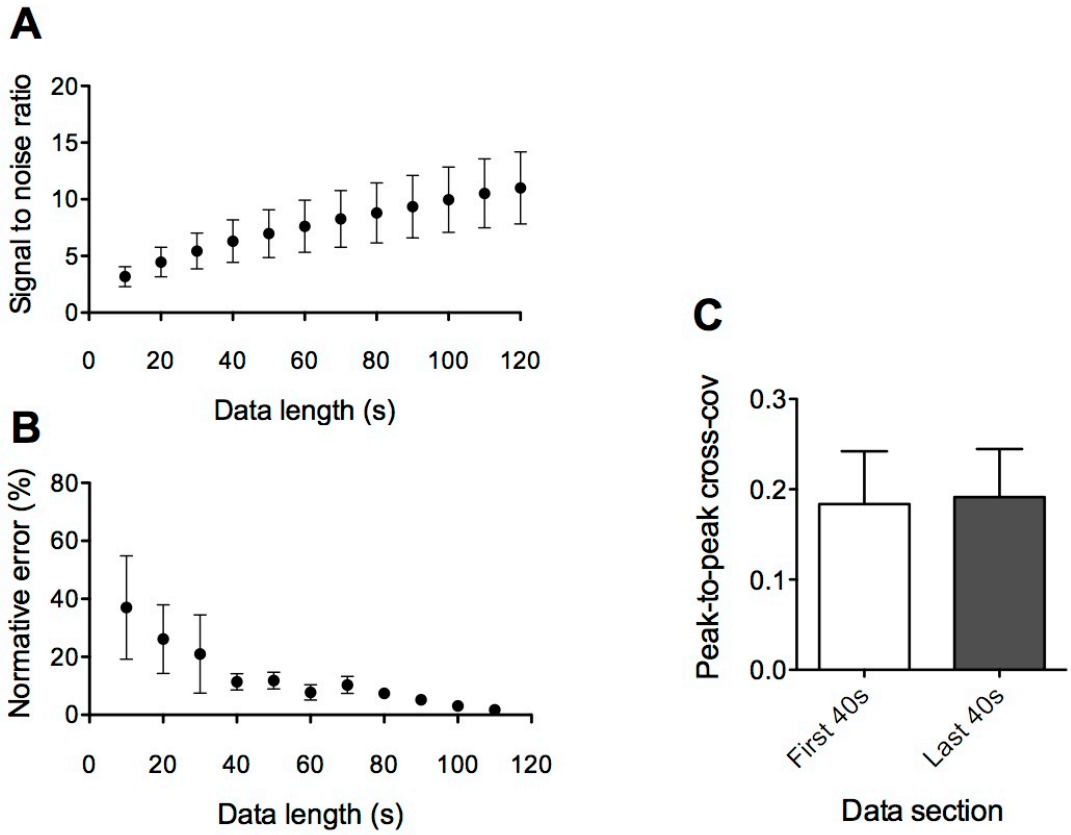

Figure 2-7 Trial durations and response habituation

Signal to noise ratios (A) and normative error in peak-to-peak cross-covariance between each data length and the full 120 s trial length (B). Mean peak-to-peak cross-covariance calculated from the first 40 s versus the last 40 s of the trial (C).

2.6 Bridging summary

In summary, this chapter tested a novel methodology to examine proprioceptive response characteristics in lower limb muscles during standing. Results from this study suggest there are stronger homonymous connections in the soleus muscle across a broader frequency bandwidth relative to the gastrocnemii. However, differences in surface EMG recordings and background motor unit activation patterns might also contribute to the differences observed between the soleus and gastrocnemii. Therefore, the following study (Chapter 3) was devised to dig deeper into potential differences in response characteristics between the soleus and medial gastrocnemius muscles by extracting the spike times of single motor units from each muscle using indwelling EMG. In addition, the following chapter addresses methodological considerations for the use of a linear systems analysis to examine input-output characteristics; we addressed whether single motor units exhibit non-linear phase locking to sinusoidal vibration. With sinusoidal vibration, we were also able to test whether motor units can respond to higher frequencies (80-100 Hz).

Chapter 3: Soleus single motor units show stronger coherence with Achilles tendon vibration across a broad bandwidth relative to medial gastrocnemius units while standing

3.1 Abstract

To probe the frequency characteristics of somatosensory responses in the triceps surae muscles, we previously applied suprathreshold noisy vibration to the Achilles tendon and correlated it with ongoing triceps surae muscle activity (recorded via surface EMG) during standing. Stronger responses to tendon stimuli were observed in soleus (SOL) relative to medial gastrocnemius (MGas) surface EMG; however, it is unknown whether differences in motor unit activity or limitations of surface EMG could have influenced this finding. Here, we inserted indwelling EMG into SOL and MGas to record the activity of single motor units while we applied noisy vibration (10-115 Hz) to the right Achilles tendon of standing participants. We analyzed the relationship between vibration acceleration and the spike activity of active single motor units through estimates of coherence, gain, phase, and cross-covariance. We also applied sinusoidal vibration at frequencies from 10-100 Hz (in 5 Hz increments) to examine whether motor units demonstrate non-linear synchronization or phase locking at higher frequencies. Relative to MGas single motor units, SOL units demonstrated stronger coherence and higher gain with noisy vibration across a bandwidth of 7-68 Hz, and larger peak-to-peak cross-covariance at all four stimulus amplitudes examined. SOL and MGas motor unit activity was modulated over the time course of the sinusoidal stimuli across all frequencies, but

their phase locking behaviour was minimal. These findings suggest SOL plays a prominent role in responding to disturbances transmitted through the Achilles tendon across a broad frequency band during standing.

3.2 Introduction

Somatosensory feedback can adjust motor output through connections to spinal cord circuitry as well as projections to supraspinal structures (reviewed in Proske and Gandevia, 2012; Proske, 2015). To probe these pathways, researchers and clinicians often deliver a brief sensory perturbation (e.g., discrete tendon or nerve stimulus, or brisk joint movement) and measure the evoked muscle or cortical response. Alternatively, we recently examined the use of suprathreshold noisy tendon vibration (NTV) applied to the Achilles to assess the frequency response characteristics of triceps surae muscles (measured using surface EMG) and cortical potentials (measured using EEG) (Mildren et al., 2017). A main benefit of this approach is that it induces minimal perturbations to standing balance. During standing, we observed that soleus (SOL) and medial gastrocnemius (MGas) surface EMG were linearly correlated with NTV across a broad frequency range (~10-80 Hz) with a phase-frequency relationship characteristic of a system governed by a fixed time delay (~40 ms) (Mildren et al., 2017). In addition, SOL surface EMG showed the strongest response to tendon vibration compared to MGas surface EMG across stimulus amplitudes, while weak or absent responses were observed in lateral gastrocnemius (LGas) surface EMG.

Differences in reflex coupling strength within the triceps surae group might reflect differences in the anatomy as well as the function of each muscle in the task of maintaining upright posture and balance. The anatomy of the SOL muscle, namely its monoarticular attachments and higher number and density of intramuscular receptors relative to the gastrocnemii (Banks et al., 2006), might reflect a prominent function of the SOL muscle in sensing and responding to disturbances at the ankle. In contrast, intramuscular receptors within MGas (a biarticular muscle) will be sensitive to disturbances at both the ankle and knee. Likewise, homonymous reflex connections in MGas will exert actions across the ankle and knee joints. In line with this, Peters et al., (2017) recently demonstrated that the activity of muscle spindle afferents innervating SOL, relative to the gastrocnemius muscles, exhibited more precise encoding of small ankle oscillations that mimicked the frequency content of standing sway.

During standing, MGas motor units typically display a bursting pattern of activation on top of the more tonic activation of SOL motor units, while LGas motor units remain relatively silent (Héroux et al., 2014). Evidence has been provided of differences in the sensory control over each muscle within the triceps surae group; for example, vestibular error signals elicit a stronger response in MGas relative to SOL motor units during standing (Dakin et al., 2016), and cutaneous afferent feedback was found to reflexively facilitate SOL and simultaneously inhibit MGas in the contralateral limb during gait (Duysens et al., 1991). Tibial nerve stimulation was found to evoke smaller H-reflex amplitudes in MGas relative to SOL (Simonsen et al., 2012), although it is unknown the extent the artificial antidromic volleys contributed to this finding due to

differences in efferent fibre makeup (since MGas contains a greater proportion of type II fibres; Alway et al., 1988). Specifically, the difference in efferent nerve fibres could influence the degree of H-reflex interference from antidromic volleys, which could confound the interpretation of differences in H-reflex amplitude between muscles. A schematic summarizing some of the differences between SOL and MGas that could lead to different response characteristics is provided in Fig. 3-1.

While stronger coherence has been observed between NTV and SOL relative to MGas surface EMG (Mildren et al., 2017), it is possible that differences in background muscle activation (type of motor units active and firing rate) between SOL and MGas or cross-talk could have contributed to this finding. Therefore, the primary aim of this experiment was to compare the frequency responses of SOL and MGas single motor units to noisy vibration of the Achilles tendon during standing. We investigated NTV-evoked muscle responses over a broad bandwidth (i.e. up to 100 Hz) because of the relevance of this frequency range in activities of daily living such as walking, running, jumping, and perturbations during standing. We hypothesized that the activity of single SOL, relative to MGas motor units, would exhibit stronger coherence and cross-covariance with NTV at all stimulus amplitudes across a broad frequency bandwidth during quiet standing. Similarly, we hypothesized that Achilles tendon taps would evoke a larger short latency response (increase in spike probability and frequency) in SOL relative to MGas motor units. Finally, using single motor unit recordings during sinusoidal vibration, we aimed to examine whether SOL or MGas motor units respond to high frequency stimuli (80-100 Hz) – frequencies often used to evoke kinaesthetic illusions and probe the involvement of

calf muscle spindles in standing balance (Ceyte et al., 2007; Proske and Gandevia, 2012; Barbieri et al., 2013). Sinusoidal stimuli also allowed us to examine whether motor unit responses to vibrations exhibit non-linear behaviour, such as phase locking with the stimulus, at higher frequencies. We hypothesized SOL and MGas motor units would demonstrate responses to high frequency (80-100 Hz) sinusoidal vibrations.

3.3 Materials and Methods

3.3.1 Participants

A total of 18 healthy young adults (age = 27.4 ± 6.3 yrs, 13 male) free of neurological and musculoskeletal disorders participated. Participants provided written informed consent and all procedures were approved by the University of British Columbia Research Ethics Board.

3.3.2 Electromyography recordings

Single motor unit activity was recorded through fine wire electrodes embedded into the SOL and MGas muscles. Fine wire electrodes were custom made; each electrode consisted of a pair (bipolar electrode configuration) of shielded stainless steel wires (California Fine Wire, USA), with a small portion (~1 mm) of the shielding removed at the tip of one wire. The two ends were folded to create small barbs to anchor the wire into the muscle. Wires were threaded into a 1.5 inch 25-gauge hypodermic needle (EXEL International Medical Products, USA) and then steam sterilized (PVdry2 Barnstead Harvey, USA) before insertion. Ultrasound imaging (SonoSite MicroMaxx, USA) was used to guide needle insertions (Héroux et al., 2014). One electrode was inserted into the

medial portion of SOL just below the distal edge of the MGas muscle, and one electrode was inserted approximately in the centre of MGas. Recent work suggests MGas motor units span a large portion of the muscle and are not localized based on recruitment threshold (in a distal-proximal gradient) or joint action (ankle vs. knee flexion) (Héroux et al., 2015). Therefore, recordings from a single location within MGas are likely representative of other areas of the muscle. In several participants, a second wire was inserted ~2 cm proximal or distal in either MGas or SOL to increase the chances of obtaining an identifiable motor unit. When single motor units could be identified on neighbouring wires, we ensured there was sufficient variability in their spike times to be confident that each wire was recording distinct motor units. A ground electrode was placed on the medial or lateral malleolus. Fine wire EMG was amplified (×2000), bandpass filtered (30-10000 Hz) (NeuroLog system, Digitimer Ltd, UK) and sampled at 20000Hz (Power 1401 DAQ, Cambridge Electronic Design, UK).

The most prominent single unit in either MGas or SOL was identified and discriminated online based on action potential size and shape using a template-matching algorithm in Spike2 software (Cambridge Electronic Design, UK). Participants were provided with auditory and/or visual feedback of the single motor unit spikes and instructed to maintain its firing rate ~7 Hz. Visual feedback of motor unit action potentials and mean firing rate was provided on a TV screen ~2 m in front of the participant. The target background rate (~7 Hz) was chosen to provide a controlled comparison between active low threshold (recruited during standing, which is typically <20% maximum force output) SOL and MGas single motor units since the amplitude of

the H-reflex response in single motor units has been found to be sensitive to background firing rate (when beyond ~4-10 Hz) (Miles et al., 1989). Although participants were required to maintain standing balance, it should be acknowledged that the feedback about motor unit firing rate could have the potential to interfere with the nature of the drive to the motoneurone pools during standing. After completion of the stimulation protocol while monitoring one unit (see *Noisy stimuli and tendon taps*), the protocol was repeated up to two additional times while monitoring the background firing rate of a different identifiable low threshold motor unit.

3.3.3 Noisy stimuli and tendon taps

To examine the frequency characteristics of single motor unit responses, we delivered suprathreshold noisy vibration to the Achilles tendon. For NTV trials, a white noise signal was generated and low-pass filtered at 100 Hz (LabVIEW 11 software, Labworks, USA) (Mildren et al., 2017); the recorded acceleration profile of the stimulus applied to the tendon contained power primarily between 10-115 Hz. For comparison with typical stimulus trigger-averaging approaches, we also applied tendon taps to examine evoked responses to transient stimuli. For tendon tap trials, 30 Hz raised cosine wave signals were generated. Signals were output at 5000 Hz from a PXI-6225 DAQ (running with a PXI-8106 real-time controller in a PXI-1031 chassis) to a motor amplifier (PA-141, Labworks, USA) controlling a linear motor (model MT-160, Labworks Inc, USA). The linear motor delivered stimuli to the right Achilles tendon through a 3 cm diameter custom probe; this apparatus was secured to frictionless linear slides and pulled onto the tendon using a weighted pulley system. A force transducer (Model 31,

Honeywell, USA) and accelerometer (Model 220-010, X Tronics, CA) were mounted on the motor. Force feedback was used to monitor tendon pre-load (maintained at ~1 N) and acceleration was used to analyze the relationship between tendon stimuli and muscle activity (see *Data analysis*). Both acceleration and force signals were differentially amplified (×1 and ×100, respectively) and low-pass analogue filtered (600 Hz cutoff; Brownlee model 440, NeuroPhase LLC, USA), then sampled at 2000 Hz.

NTV was continuously applied to the right Achilles tendon of standing participants (n = 11) for two minutes at four different amplitudes (vibration root-mean-square accelerations: 5, 10, 15, and 20 m/s^2). Amplitudes were delivered in a randomized order. Two trials of 20 tendon taps (root-mean-square acceleration = 25 m/s^2, 8-12 s inter-stimulus-interval) were also delivered in a block randomized order with NTV trials.

3.3.4 Sinusoidal vibration

In order to examine whether motor units respond to higher frequency stimuli (80-100 Hz) and exhibit phase-locking to vibration, we applied sinusoidal vibration to the Achilles tendon while we recorded SOL and MGas indwelling EMG. In 5 participants, sinusoidal vibration at frequencies between 10 and 100 Hz (in 5 Hz increments, 19 frequencies total) were applied to the right Achilles tendon for a duration of 35 s each. The velocity of vibration was calculated from the integrated acceleration, and we delivered the lower vibration frequencies (up to 25 Hz) at one velocity (peak-to-peak = 0.11 m/s), and the higher frequencies (30 Hz and above) at a higher velocity (peak-to-peak = 0.22 m/s).

3.3.5. Skin anesthetization

Vibration applied to the Achilles tendon will activate intramuscular receptors (muscle spindles and Golgi tendon organs) as well as cutaneous afferents. While the short latency EMG responses are characteristic of excitatory input to motoneurones from muscle spindles, it is possible cutaneous afferents could mediate the EMG responses (Clair et al., 2009). Therefore, in 2 participants, we examined SOL motor unit responses to NTV before and after we anesthetized skin across the back of the ankle. We inserted two fine wire electrode pairs into SOL and applied two 2-min trials of NTV at 15 m/s^2 (root-mean-square acceleration) before and after we anesthetized skin across the back of the ankle. To anesthetize the skin, we applied a topical anesthetic (EMLA, 2.5% prilocain and 2.5% lidocaine) to a large rectangular area of skin that spanned the posterior surface of the lower leg from just above the foot sole to below the distal border of the gastrocnemii, and between the medial and lateral malleoli. Monofilament perceptual thresholds (MPTs) were examined at 3 locations (proximal aspect, mid ankle, and lateral malleolus; see Mildren et al., 2017) before and after the anesthetic. The aim of the cutaneous block was to reduce cutaneous feedback from the mechanoreceptors beneath the vibrating probe, as well as mechanoreceptors in adjacent regions that could be activated by stretch of the skin.

3.3.6 Data analysis

Motor unit action potentials were discriminated again offline using the template-matching algorithm in Spike2 software. Identified motor units were exported as spike times for further processing in MATLAB (Mathworks, USA). To be included in the amplitude scaling comparison and comparison between muscles (SOL vs. MGas), we

required motor units to be identifiable across all four trials with an average firing rate between 4-11 Hz.

Acceleration data were digitally low-pass filtered at 600 Hz (5th order dual-pass Butterworth filter). We estimated time and frequency domain parameters that describe the relationship between hybrid data (vibration acceleration and motor unit spike times) (Rosenberg et al., 1989; Halliday et al., 1995). These measures include coherence, gain, and phase in the frequency domain and cross-covariance in the time domain. Coherence (R_{xl}^2) at each frequency (λ) was calculated as:

$$|R_{xl}(\lambda)|^2 = \frac{|f_{xl}(\lambda)|^2}{f_{xx}(\lambda)f_{ll}(\lambda)}$$

where f_{xl} is the cross-spectrum and f_{xx} and f_{ll} are the autospectra of the input (acceleration) and output (EMG) signals (Halliday et al., 1995). Gain at each frequency was estimated as the cross-spectrum divided by the power spectrum of the acceleration signal, and phase was estimated from the angle of the cross-spectrum. Gain and phase data were extracted and displayed only at frequencies that exhibited significant coherence. Finally, cross-covariance was obtained from the inverse Fourier transform of the cross-spectrum and normalized by the product of the vector norms of the input and output signals (Dakin et al., 2010). For analysis of single motor unit data, acceleration data were first up-sampled to 20000 Hz (equivalent to the fine wire EMG sample rate) and two-minute trials were examined using a frequency resolution of 2.44 Hz (0.409 seconds/segment; 292 segments per trial).

For the tendon tap trials, peri-stimulus time histograms (PSTH; 2 ms bin width) and frequencygrams (PSF) were constructed for individual motor units to determine changes in motor unit firing probability and frequency following tendon taps (Turker et al., 1997). These analyses were primarily conducted to examine the timing of short latency motor unit responses (increase in firing probability and frequency) to transient tendon stimuli. Motor unit firing frequency is almost linearly related to current input, thus potentially reflecting the net synaptic drive to the motoneurons (Turker et al., 1997). In response to tendon taps, Turker et al., (1997) previously observed a single excitatory response in SOL motoneurones (increase in spike frequency).

For sinusoidal vibration trials, we divided the data into individual sine wave cycles by identifying where the (mean-subtracted) acceleration crossed zero while heading in a positive direction (acceleration into the tendon). These zero crossing times were used for further analyses to construct histograms (1 ms bins) of spike probability over the sine wave cycle and raster plots. In these analyses, we removed sine wave cycles that did not contain spikes, and we randomly sampled 100 sine waves from the 35 s trial that contained spikes. Next, we calculated a metric of non-linear phase locking behaviour using an entropy based approach described by Kajikawa and Hackett (2005). Briefly, from the histogram of spike probability over the sine wave cycles, we calculated entropy (E) of the probability distribution using the equation:

$$E = -\sum_{t=0}^{T} Prlog_2(Pr)$$

Where Pr is the probability of firing at a given stimulus phase. The maximum entropy possible (Emax) (which would occur if spike times were uniformly distributed) was calculated as:

$$Emax = log_2(N)$$

Finally, phase locking index (PLI) was calculated as:

$$PLI = 1 - E/Emax$$

This measure (PLI) increases with greater synchronization of spike times (where a value of 1 would reflect perfect synchronization of spikes at one phase of the stimulus) and can be used to evaluate unimodal and multimodal distributions. We repeated this calculation of PLI by randomly resampling (with replacement) 100 sine waves with spikes 100 times to create a distribution of PLI values. The median value from the distribution was extracted as the final measure of PLI for each motor unit at each frequency. In addition, we calculated coherence and gain between the sinusoidal vibration acceleration and motor unit spike times (described above for noisy stimuli).

3.3.7. Statistics

Background firing rates were compared between SOL and MGas units using a Mann-Whitney U test. In individual trials and group data, responses in the frequency (coherence) and time (cross-covariance) domains were considered significant when they exceeded 95% confidence intervals constructed based on the number of disjoint segments and the assumption of independence between the two signals (Halliday et al., 1995). Gain and phase data were extracted at frequencies where coherence was significant. Motor unit data were concatenated across stimulus amplitudes and a pooled difference of coherence

(DoC; Amjad et al., 1997) test was used to compare coherence strength across frequencies between SOL and MGas motor units following a Fisher z-transformation. For SOL and MGas motor units, peak-to-peak cross-covariance was compared across stimulus amplitudes using a Kruskal-Wallis test, and peak-to-peak cross-covariance was compared between SOL and MGas units at each of the four stimulus amplitudes using Mann-Whitney U tests with a Bonferroni adjustment applied to an α-level of 0.05 (comparisons were therefore considered significant at $p < 0.0125$). To test the significance of PLI values calculated from each sinusoidal vibration trial for each motor unit, we created 1000 null hypothetical values of PLI from shuffled spike train data. Specifically, we shuffled the inter-spike-intervals of the original spike train to generate new spike trains that preserved the distribution of inter-spike-intervals (but had no relationship with the stimulus). These spike trains were used to calculate 1000 null hypothetical values of PLI for comparison with the value calculated from the original spike train (Kajikawa and Hackett, 2005).

3.4 Results

A total of 27 motor units were identified and successfully discriminated from the 11 participants during noisy vibration and tendon tap trials. Twelve single units (8 SOL and 4 MGas) from 10 participants were maintained throughout all four noisy vibration trials with a sustained background firing rate between 4.2 and 10.5 Hz (mean rate ± SD: 6.5 ± 1.2 Hz for SOL; 7.2 ± 1.0 Hz for MGas; $p = 0.639$) and were included in analyses to examine the frequency characteristics of motor unit responses and to make

comparisons between muscles. All 12 units showed significant (exceeding 95% confidence intervals) coherence and cross-covariance with the noisy vibration during each two-minute standing trial with the exception of one MGas unit during one low amplitude vibration trial (5 m/s^2). The main finding from this experiment is lower responses in MGas relative to SOL motor units across a broad frequency range; representative data from one SOL and one MGas motor unit are shown in Fig. 3-2. In the pooled motor unit data, SOL units demonstrated significant coherence generally spanning a bandwidth of ~7-75 Hz, with a small decrease in coherence at ~18-25 Hz, while MGas motor units responded to the stimulus over a smaller bandwidth (~15-40 Hz) and showed a similar decrease in coherence around 18-25 Hz (Fig. 3-3A). SOL motor units had significantly stronger coherence with NTV relative to MGas units across a bandwidth of 7-68 Hz (Fig. 3-3B). On average, gain was 25% (± 9.6%) larger for SOL relative to MGas motor units across the bandwidth of 7-68 Hz. Gain was highest ~10 Hz and decreased with frequency, and phase decreased approximately linearly with frequency for both SOL and MGas motor units (Fig. 3-3A). The time domain representation (cross-covariance) exhibited an early significant positive peak for SOL motor units (34.0 ± 3.1 ms lag) and MGas motor units (35.6 ± 4.9 ms lag) (Fig. 3-3A). These lag times (~35 ms) were expected based on the neural transmission delay for the short latency stretch response. The peak-to-peak cross-covariance scaled with stimulus amplitude for both SOL ($p < 0.001$) and MGas ($p = 0.009$) motor units, and SOL exhibited larger peak-to-peak cross-covariance than MGas at each of the four stimulus amplitudes (*p-values* < 0.01) (Fig. 3-3B).

Nine motor units (6 SOL and 3 MGas) from five participants were identifiable over the two tendon tap trials. As expected, the latency of the response to tendon taps was similar to the cross-covariance lag times (~35 ms). For SOL motor units, the PSTH demonstrated a short latency increase in spike events and frequency (35.6 ± 5.7 ms latency) followed by a silent period (Fig. 3-4). Following the silent period, the firing frequency of 4 SOL motor units re-emerged at a lower frequency relative to their background firing rate. The three MGas motor units showed a subtle short latency increase in spike events (local peak at 36.3 ± 2.3 ms) and no prominent change in firing frequency.

Sinusoidal vibration was applied to the tendon to investigate whether motor units respond to higher frequency stimuli (>80 Hz) and exhibit non-linear behaviour (synchronizing at a particular phase of the stimulus). Six SOL and four MGas motor units (from five participants) were examined during sinusoidal vibration across 19 frequencies from 10-100 Hz. Histograms and raster plots demonstrated that SOL and MGas motor units modulated their spike activity over the time course of the sinusoidal vibration (Fig. 3-5); however, non-linear phase locking behaviour was minimal across frequencies. In other words, spike times were typically observed across all or nearly all phases of the stimulus cycle without a strong tendency to synchronize at one particular phase. PLI values were ~0.05-0.3 across frequencies for both SOL and MGas motor units (Fig. 3-6A). At frequencies between 35-55 Hz, PLI values were significant in most (66%) SOL motor units, which indicates a stronger tendency for SOL spike times to cluster around certain phases of the stimulus at these frequencies. The pattern of motor unit responses to

sinusoidal vibration at discrete frequencies was similar to that observed during noisy vibration at each frequency component, including strongest coherence ~30-50 Hz and highest gain at ~10 Hz which then decreased with frequency (Fig. 3-6B). Motor units also showed significant responses to higher frequency stimuli (up to 100 Hz; Fig 3-6B).

Reducing cutaneous feedback from the ankle was used to determine whether cutaneous afferents contribute to the muscle responses evoked by the noisy tendon stimuli. The anesthetic increased MPT (reduced sensitivity) on average by 29 times (18 ± 17 mN to 586 ± 703 mN). Four SOL single motor units were examined over two NTV trials before and four SOL motor units were examined after the skin block. There was no substantial change in response amplitude after nearly complete removal of cutaneous feedback (Fig. 3-7).

3.5 Discussion

The primary aim of this experiment was to compare SOL and MGas single motor unit responses to Achilles tendon stimuli during standing. We observed stronger coherence and gain with NTV in SOL single motor units, relative to MGas, across a bandwidth of 7-68 Hz, and larger peak-to-peak cross-covariance at all four stimulus amplitudes applied. In addition, during sinusoidal vibration, single motor units also demonstrated responses to high frequency stimuli (~80-100 Hz) typically used to probe kinesthesia and balance control mechanisms (Ceyte et al., 2007; Proske and Gandevia, 2012; Barbieri et al., 2013), and SOL and MGas motor units demonstrated minimal phase locking behaviour. These findings indicate that the SOL muscle, in particular, can encode

mechanical vibrations mostly linearly across a broad range of frequencies (up to 100 Hz) during standing. Meanwhile, MGas motor units show poorer encoding of vibrations across a smaller bandwidth (up to ~60 Hz). A schematic of the main findings of this experiment (the transfer functions between the tendon vibration acceleration and motor unit activity for SOL and MGas) is provided in Fig. 3-8.

Our finding of stronger responses to tendon stimuli for SOL motor units likely reflects the density of muscle spindles and strength of connections to homonymous motoneurones. Within the triceps surae group, the SOL muscle contains the highest density and number of spindles (Banks, 2006), and their Ia afferent fibres project to the majority of homonymous motoneurones (Jankowska, 2015). Thus, SOL motoneurones integrate information from a large number of spindles (~400; Banks, 2006) that function to sense disturbances primarily at the ankle. (Knee movement will have a minor effect on SOL fascicle lengths through myofascial force transmission; Tian et al., 2012.) Although we cannot conclusively determine the sensory source driving the motor unit responses from these data, it is well known that tendon vibration is a powerful stimulus to Ia spindle afferent fibres. Tendon vibration can activate silent Ia afferents and modulate the activity of active Ia afferents across a broad frequency range (>100 Hz; Burke et al., 1976b; Fallon and Macefield, 2007). However, tendon vibration can also modulate feedback from cutaneous afferents, secondary spindle afferents, as well as Golgi tendon organs particularly during a background contraction (Burke et al., 1976a; Fallon and Macefield, 2007). The significant cross-covariance at a short time lag is similar to the short latency excitatory tendon tap response that is thought to be mediated primarily by Ia spindle

afferents. In response to tendon taps, we found the short latency excitatory response (increase in spike probability and frequency) was followed by a reduction in firing frequency for some SOL motor units, which could be attributed to a reduction in net synaptic current from inhibitory Ib feedback or withdrawal of facilatory input from spindle unloading. Blocking cutaneous feedback around the ankle did not result in a noticeable reduction in vibration-evoked EMG responses, which strongly suggests that cutaneous afferents do not drive the responses observed in our study. This indicates that vibration of the Achilles tendon allows us to examine the proprioceptive input from muscle spindles to motor units of the SOL and MGas muscles during standing, where proprioceptive feedback from the ankle joint is known to be critical for postural control.

The finding of stronger SOL single motor unit responses to tendon stimuli across a broad frequency range is in agreement with previous observations using surface EMG recordings (Mildren et al., 2017). The difference in coherence between SOL and MGas was larger and spanned a broader bandwidth with single motor unit recordings relative to surface EMG (~10-70 Hz with single units vs. ~30-50 Hz with surface EMG) (Mildren et al., 2017); this could be due to cross-talk from SOL to MGas using surface EMG, or differences in the task. In the present experiment, participants were provided with audio or visual feedback of motor unit activity while they were standing and it is possible that this feedback affected the nature of descending control over triceps surae motoneurons and/or interneurons. Another limitation of this study is our sample contained fewer MGas motor units; however, peak-to-peak cross-covariance was larger in nearly all SOL relative to MGas motor units at each stimulus amplitude; this provides support for stronger

modulation of SOL motor units despite the difference in sample size. The sample size of motor units in our study is comparable to other studies that have examined sensory evoked responses in triceps surae motor units during standing (Dakin et al., 2016).

During sinusoidal vibration, we observed significant coherence and modulation of spike activity at the highest frequency examined (100 Hz), which is beyond the bandwidth that we observed significant coherence during noisy vibration. Motor unit responses to high frequency (>80 Hz) sinusoidal vibrations are likely due to greater power at these individual frequencies during sinusoidal relative to noisy stimuli. Importantly, these high vibration frequencies (~80-100 Hz) are typically used to manipulate spindle feedback to evoke kinaesthetic illusions (Proske and Gandevia, 2012), and to probe the involvement of calf muscle spindles in the control of balance (Barbieri et al., 2013; Ceyte et al., 2007). Therefore, it is important to consider that high frequency stimuli (despite exceeding the upper limit of motoneuron firing rates) do have an influence on motoneuron pool output.

We observed minimal phase locking of motor unit activity with sinusoidal vibration, which could be due to the use of small amplitude vibrations that may be within the linear range of muscle spindles (Matthews and Stein, 1969). In addition, while standing upright, motor units receive input from multiple supra-spinal structures as well as other sensory afferent channels (e.g., cutaneous afferents, Ib afferents) in addition to the spindle afferent input generated by vibration. The multiple inputs to the motoneurons (which could be viewed as noise on top of the vibration induced spindle input) could be another mechanism that minimizes non-linear phase locking of motor unit spikes with

sinusoidal vibration by allowing some firing variability across all phases of the stimulus cycle. Similarly, in a model of the vestibular system, the addition of sufficient noise was found to nearly eliminate phase locking of the spike activity of neurons in the vestibular nuclei with sinusoidal current injections (Schneider et al., 2011). Other mechanisms may also contribute to minimizing non-linearities, including the circuitry in the spinal cord, the influence of fusimotor drive (Matthews and Stein, 1969), along with the pooling of input from a population of spindles. Importantly, minimal motor unit phase locking behaviour enables the use of linear systems analysis to characterize the input-output relationship. Using a noisy stimulus approach has several benefits relative to transient tendon stimuli; for example, tendon taps and H-reflex can perturb standing balance, whereas noisy vibration allows reflex circuitry to be probed more subtly (Mildren et al., 2017). In addition, the short trial duration (40 s; Mildren et al., 2017) needed to characterize muscle responses to mechanical vibrations may provide methodological benefits for examining sensorimotor function in populations with balance deficits.

The bandwidth of coherence between tendon stimuli and motor unit spike times encompassed spindle afferent firing frequencies that could be generated by both slower movements (e.g., sway, small stance perturbations) and more dynamic activities (e.g., walking, running, jumping). For example, heel contact during gait generates frequency components from 10 to 75 Hz (Simon et al., 1981). Previous studies support a role of short latency responses in regulating both slow deliberate movements as well as dynamic activities. During dynamic activities such as running and hopping, somatosensory feedback from ground contact generates short latency stretch reflexes that function to

assist muscle activation bursts (Zuur et al., 2010) and prevent yielding at the ankle joint (Cronin et al., 2011). During voluntary movement, small irregularities in speed caused by external perturbations or motor errors are compensated by short latency responses (Marsden et al., 1976; Burke et al., 1978). Human triceps surae muscle spindles also modulate their feedback during small, low frequency ankle oscillations characteristic of standing sway, both in passive and active muscle states (Peters et al., 2017), with SOL spindles exhibiting more precise coding of ankle angle. Although afferent firing behaviour during an active balancing task remains to be investigated, Peters et al., (2017) argued that spindles are sensitive enough to form part of the sensory feedback loops involved in the control of standing. Proprioceptive feedback from muscle spindles forms an important component of feedback models of standing balance, e.g., the spinal-like controller proposed by Elias et al., 2014. Since the SOL and MGas muscles have critical roles in upright standing and locomotion, an understanding of the frequency response dynamics to proprioceptive perturbations has implications for the design of neuroprosthetics, robotics, as well as approaches to modulate sensory feedback and/or motor output with ageing and neurological disorders (e.g., spinal cord injury, stroke).

In summary, we found the activity of SOL single motor units was linearly correlated with noisy Achilles tendon vibration across a broad bandwidth (7-75 Hz) during standing. In contrast, MGas motor units demonstrated lower correlations across a smaller bandwidth; this finding likely reflects differences in the anatomy and function of different muscles within the triceps surae group. Our results suggest that the SOL muscle plays a prominent role in short latency responses to mechanical stimuli transmitted

through the Achilles tendon during standing. Furthermore, our results suggest muscle spindles primarily drive the response to tendon vibration, since removing cutaneous feedback did not noticeably influence the response. Finally, with sinusoidal vibration, we observed motor unit responses to frequencies as high as 100 Hz, and motor units demonstrated minimal phase locking behaviour, which allows for the input-output relationship to be characterized using linear systems analysis.

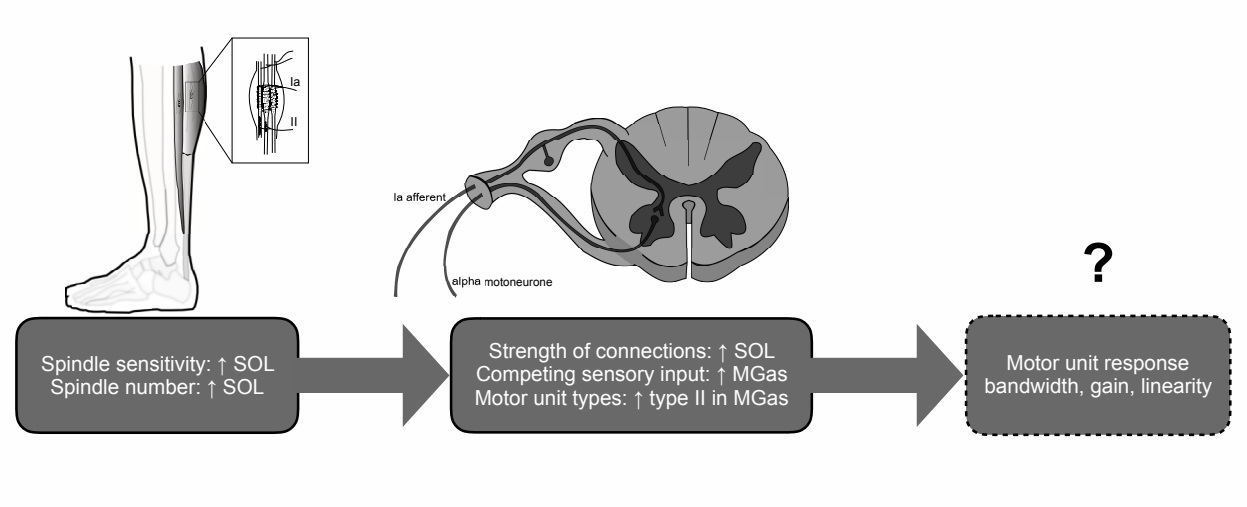

Figure 3-1 Schematic outlining differences between soleus and medial gastrocnemius

Schematic of the peripheral and central stages involved in generating the response to tendon stimuli. There is evidence of differences between soleus (SOL) and medial gastrocnemius (MGas) at the peripheral level (number and density of spindles) and central level (strength of monosynaptic connections, competing input, motor unit types). Processing at the peripheral and central level should determine the overall motor unit response bandwidth, gain, and linearity.

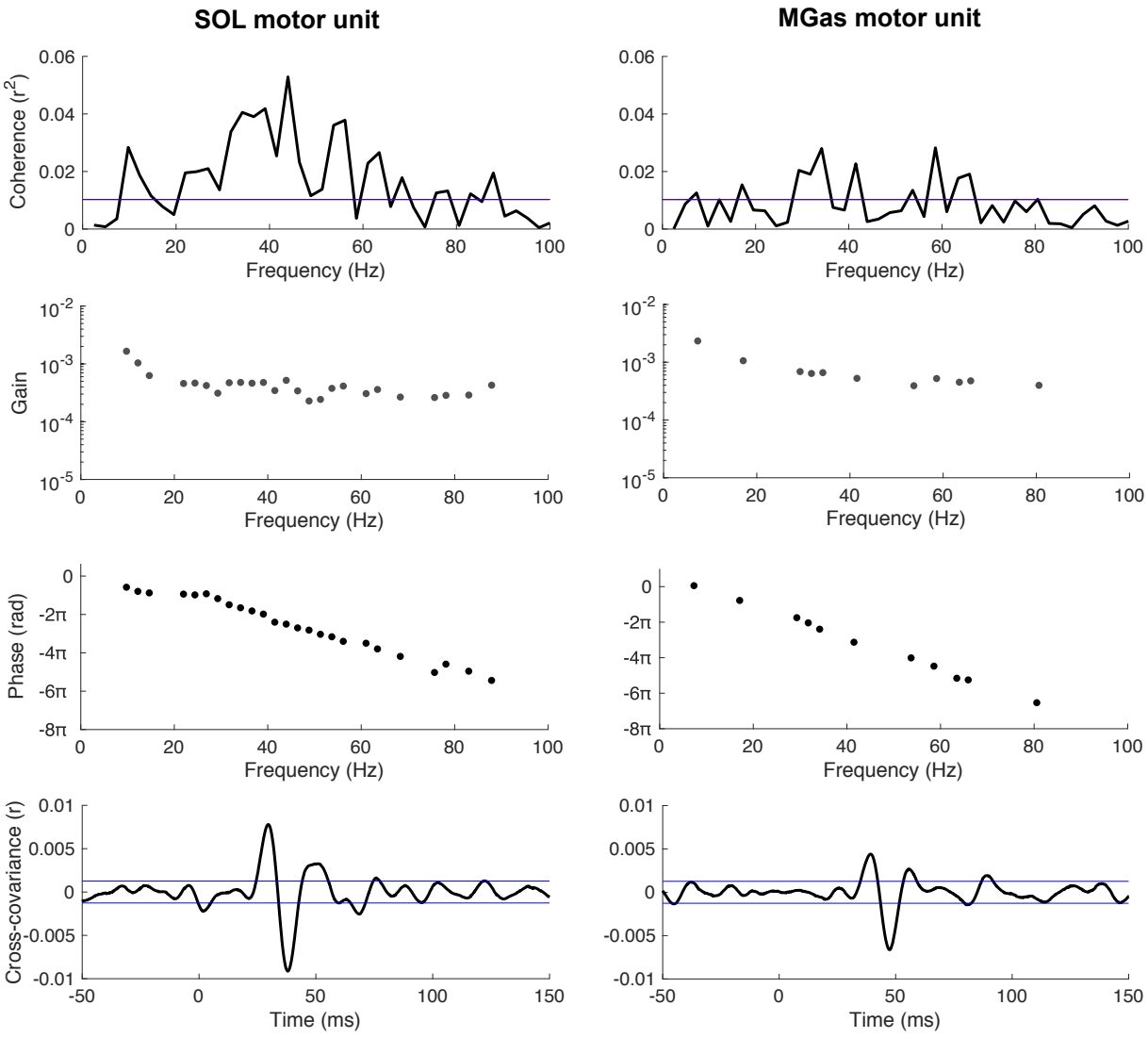

Figure 3-2 Single motor unit responses

Relationship between noisy tendon vibration acceleration and the spike activity of a single motor unit in the soleus (SOL) and medial gastrocnemius (MGas) muscle described in terms of coherence (r^2), gain (spikes/m/s^2), phase (rad), and cross-covariance (r).

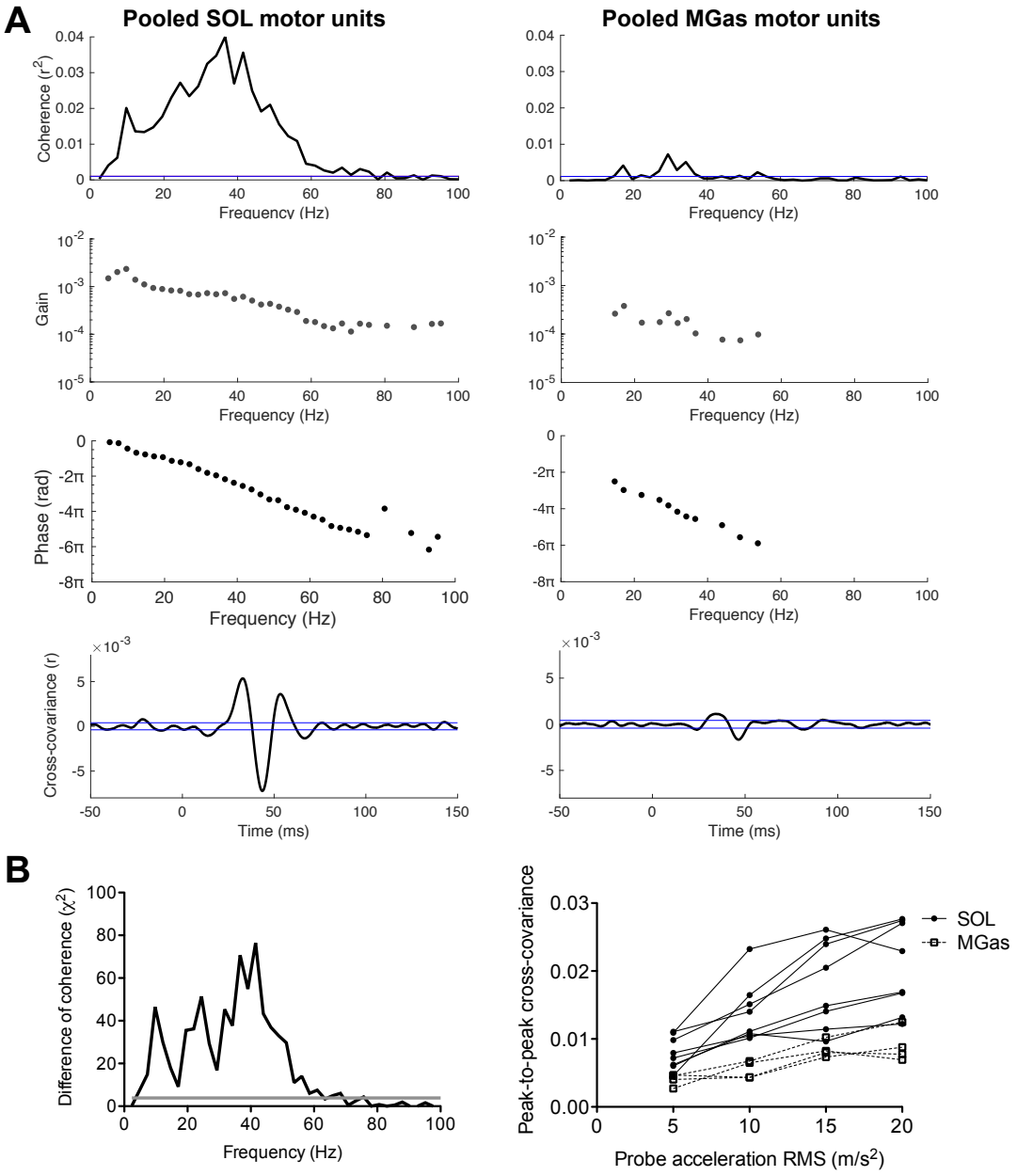

Figure 3-3 Pooled motor unit responses

Coherence (r^2), gain (spikes/m/s^2), phase (rad), and cross-covariance (r) for data concatenated across soleus (SOL; n = 8) and medial gastrocnemius (MGas; n = 4) single motor units (A). Difference of coherence between the SOL and MGas motor units (SOL >

MGas), the horizontal line indicates the significance level ($p < 0.05$) for the χ^2 distribution (B). Scaling of peak-to-peak cross-covariance for individual SOL and MGas motor units with increases in the stimulus amplitude; SOL motor unit responses were significantly larger at all four stimulus amplitudes.

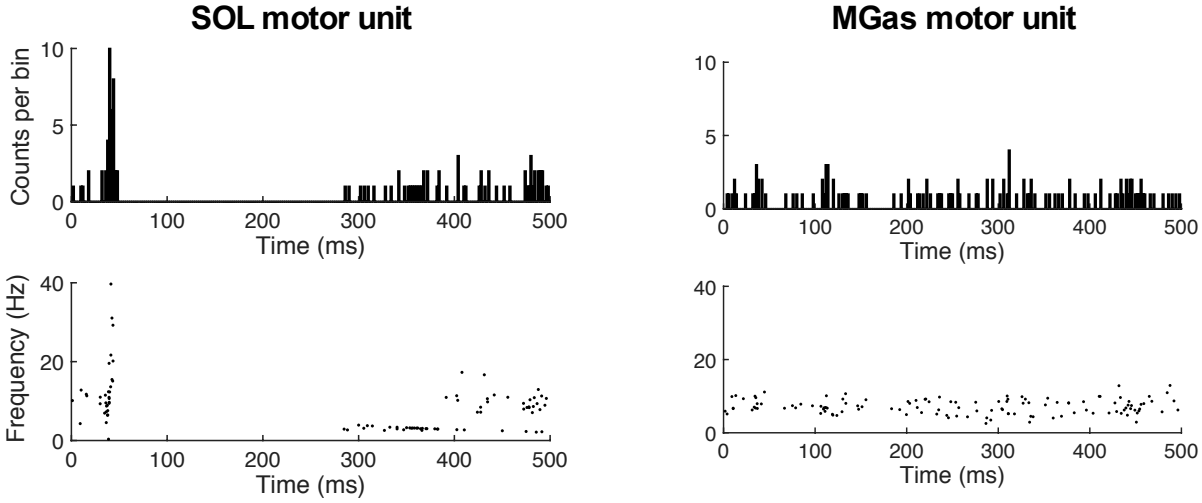

Figure 3-4 Peri-stimulus time histograms and frequencygrams

Peri-stimulus time histograms and frequencygrams for single soleus (SOL) and medial gastrocnemius (MGas) motor units in response to Achilles tendon taps. Note the latency of the response to tendon taps was similar to the cross-covariance lag times (~35 ms).

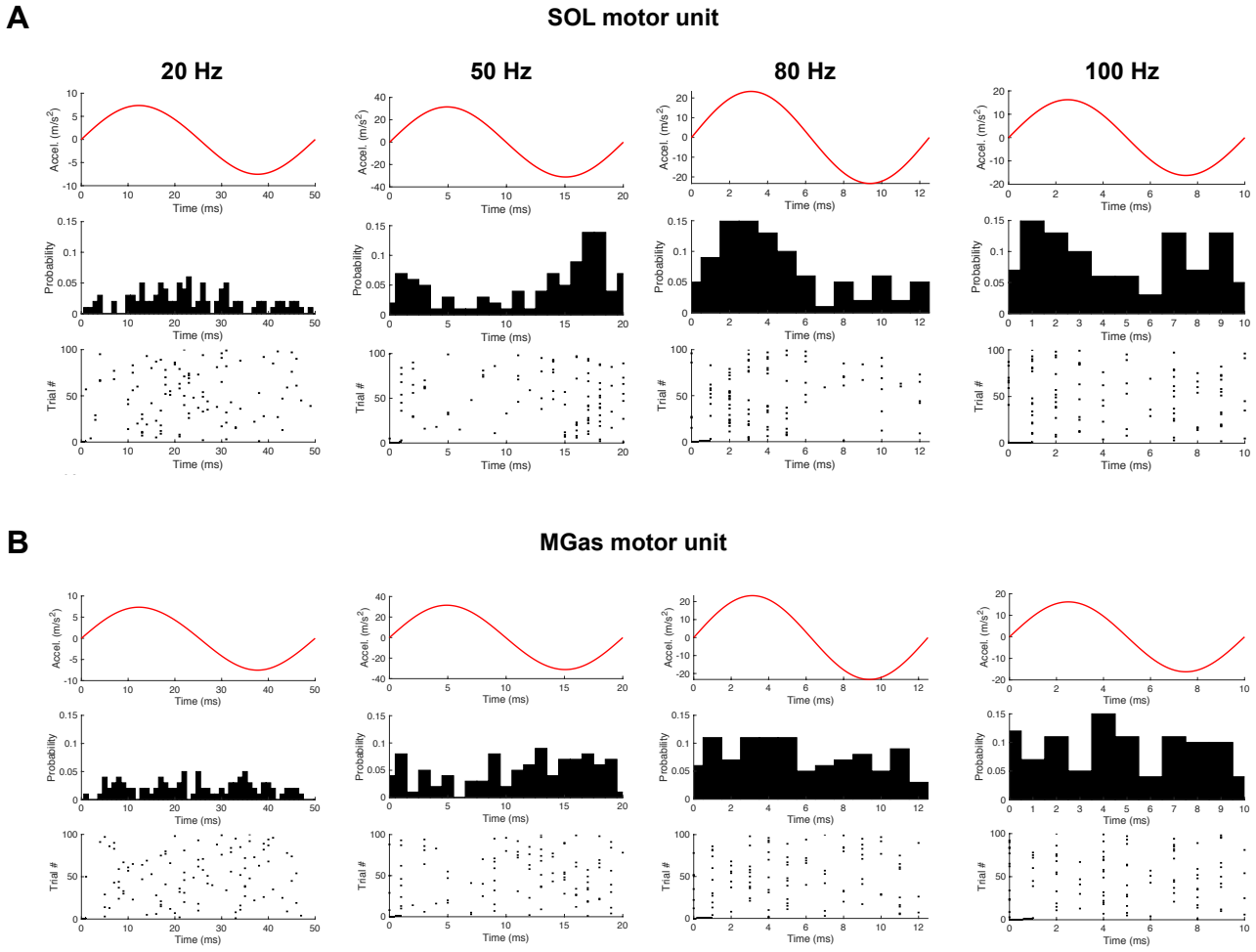

Figure 3-5 Responses to sinusoidal vibration

Example histograms and raster plots of the firing of a single soleus (SOL) motor unit (A), and a single medial gastrocnemius (MGas) motor unit (B) during 20, 50, 80, and 100 Hz sinusoidal vibration.

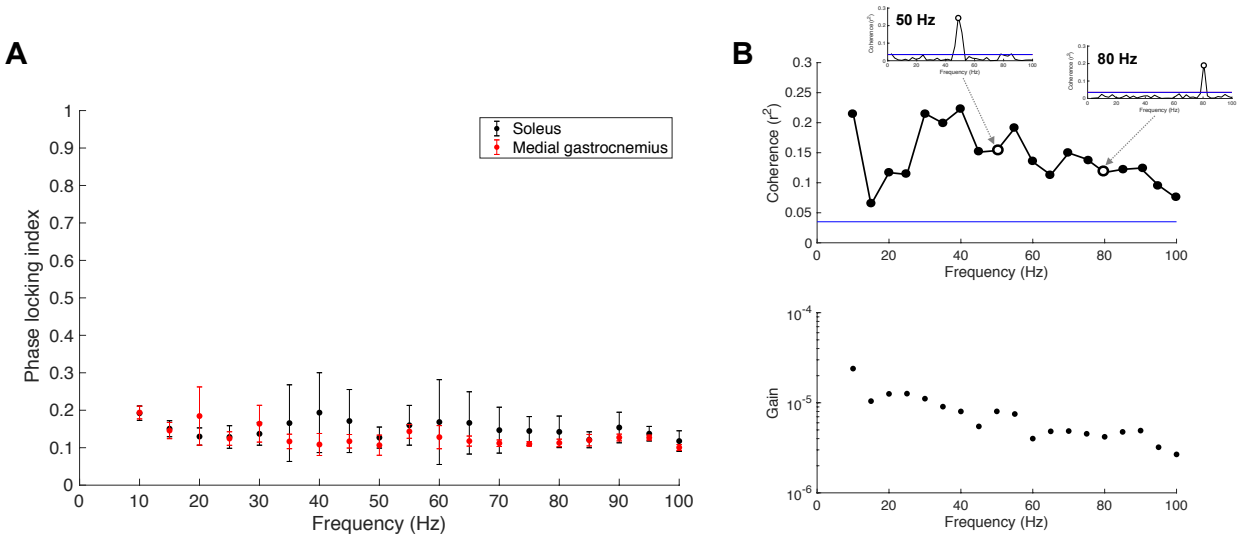

Figure 3-6 Motor unit phase locking

Phase locking index values for soleus (SOL; n = 6) and medial gastrocnemius (MGas; n = 4) motor units during sinusoidal vibration at frequencies from 10-100 Hz (A). Mean coherence (r^2) and gain (spikes/m/s^2) for SOL motor units at each sinusoidal vibration frequency (B). Insets show representative coherence data from one SOL motor unit during 50 and 80 Hz sinusoidal vibration.

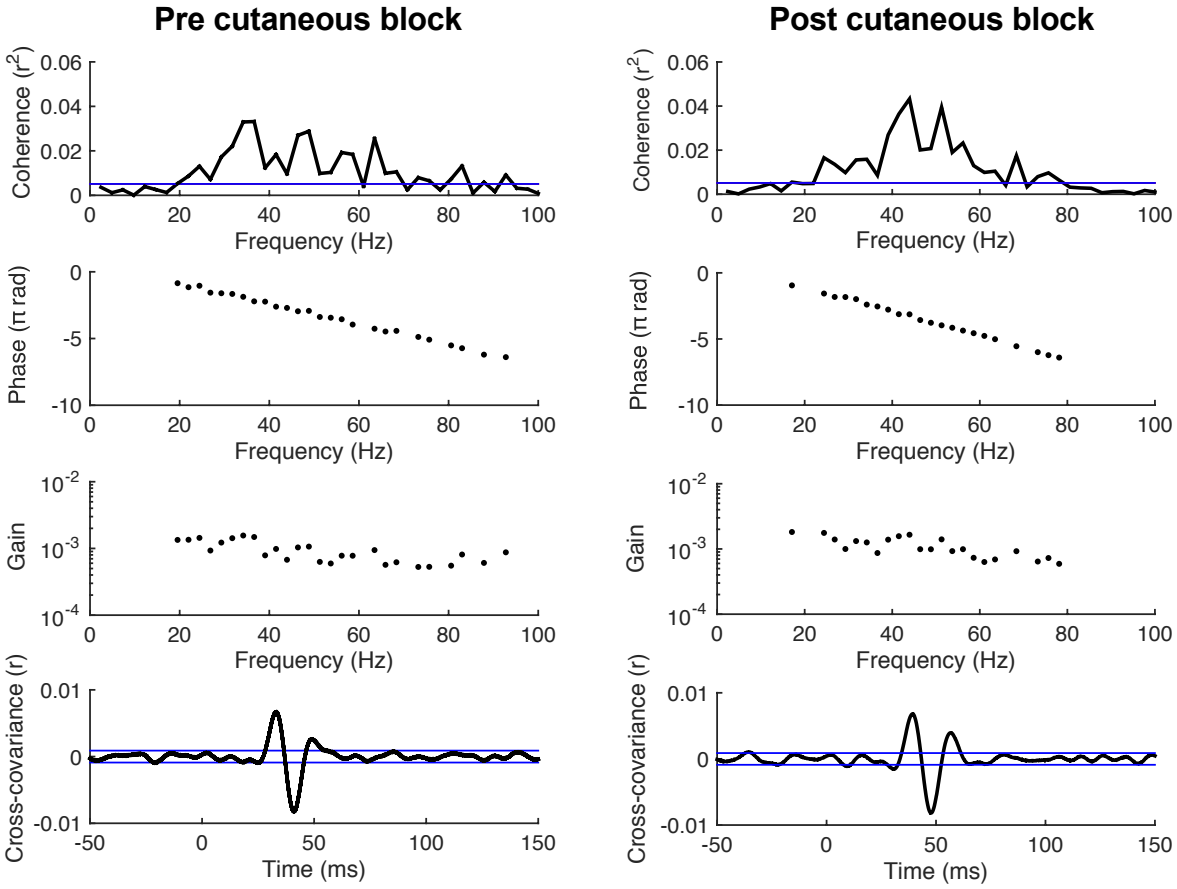

Figure 3-7 Responses after skin anaesthetization

Coherence (r^2), phase (rad), gain (spikes/m/s^2), and cross-covariance (r) for a soleus motor unit before and after skin on the posterior ankle was anesthetized.

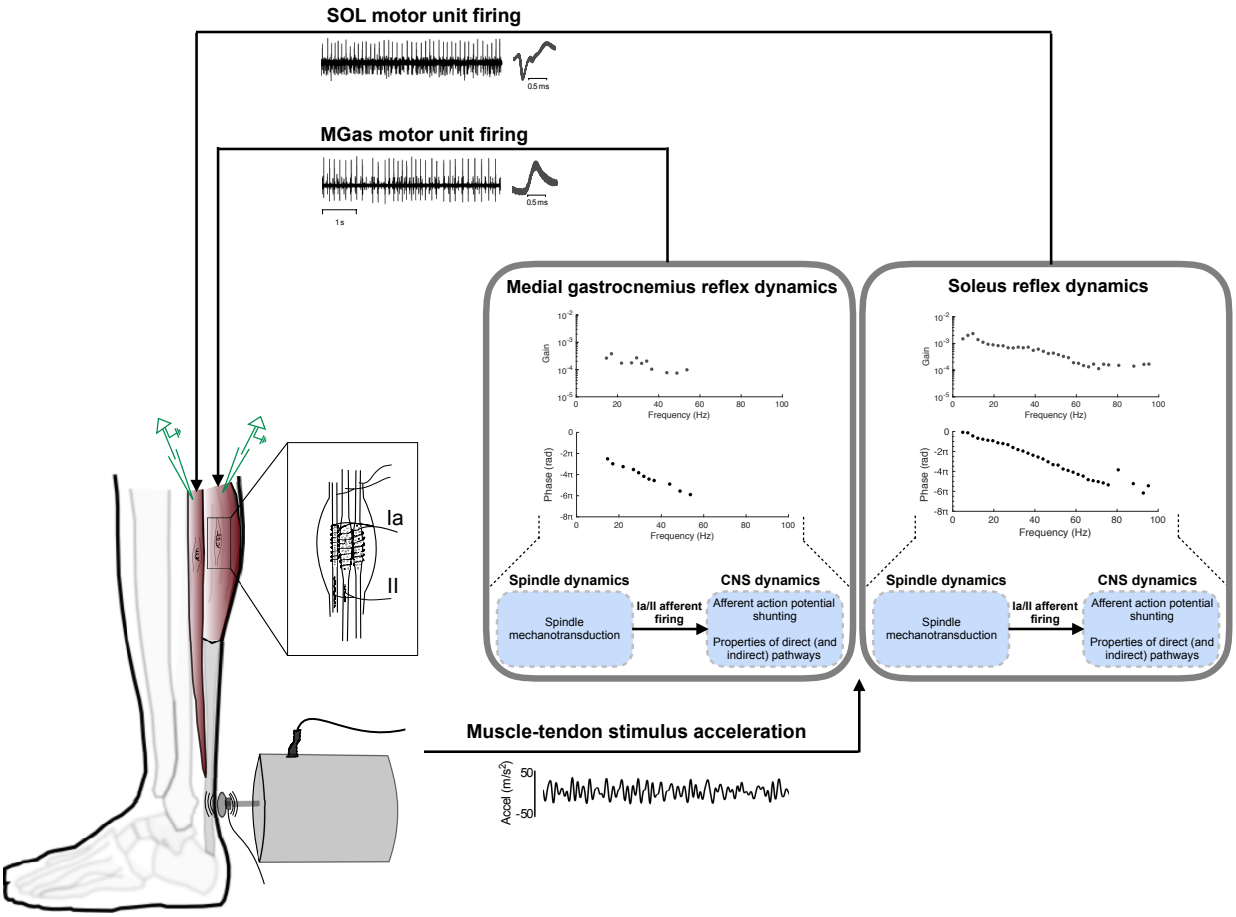

Figure 3-8 Transfer functions between proprioceptive stimuli and motor unit activity

Schematic showing the transfer functions (gain and phase) between mechanical stimuli applied to the Achilles tendon (vibration acceleration) and the firing of soleus and medial gastrocnemius motor units. The transfer functions obtained from our experiment are dictated by both the spindle dynamics (which influence the transformation of mechanical stimuli to afferent action potentials) and spinal cord dynamics (which influence the transformation of afferent action potentials to motor unit activity). CNS dynamics encompasses afferent action potential shunting (e.g., conduction block, presynaptic

inhibition), and the properties of direct (monosynaptic) and potentially indirect (polysnaptic or heteronymous) pathways. These direct and indirect pathways are under the influence of descending drive to spinal cord circuitry as well as peripheral feedback from other somatosensory channels. Gain and phase data are shown only where coherence values are significant; note that soleus motor units demonstrated higher gain across a broader bandwidth relative to medial gastrocnemius motor units. Templates beside raw EMG recordings demonstrate 100 overlaid spikes.

3.6 Bridging summary

Results from this experiment provide evidence of stronger vibration responses in single soleus relative to medial gastrocnemius motor units during standing. These data corroborate previous findings with surface EMG in Chapter 2, and extend our ability to characterize responses using this approach to the single motor unit level in humans. Furthermore, data from this study suggest muscle spindles primarily mediate the response to tendon vibration, since the reduction of cutaneous feedback did not noticeably influence the response. So far in this thesis, we have examined responses evoked by the stimulation of a single somatosensory channel alone – proprioceptive. Other somatosensory channels also provide input to α-motoneurons and interneurons in the spinal cord and play a role in the control of movement and balance. The following chapter expands our understanding of integration within the somatosensory system by probing how foot sole cutaneous feedback interacts with responses evoked by proprioceptive stimuli. During standing, afferent feedback from both the foot sole and triceps surae muscles provides relevant information for the control of balance, data gathered on how these sensory signals interact adds our knowledge of the processing in the spinal cord that contributes to the control of postural muscle activity.

Chapter 4: Soleus responses to Achilles tendon vibration are suppressed by heel and enhanced by metatarsal cutaneous stimuli during standing

4.1 Abstract

Cutaneous afferents from the foot sole provide sensory information that is relevant to balance control, and have the potential to interact with elements of the stretch reflex pathway. In this study, we examined the influence of cutaneous feedback from different regions of the foot sole (heel and metatarsals) on the soleus responses to proprioceptive perturbations generated by tendon vibration during standing. We delivered noisy (10-115 Hz) vibration to the right Achilles tendon while we applied electrical pulse trains (five 1 ms pulses at 200 Hz) intermittently (every 0.8-1.0 s) to the heel or metatarsals of the ipsilateral foot sole. We analyzed time-dependent (aligned to the cutaneous stimuli) coherence and cross-correlations between the vibration acceleration and rectified soleus EMG. Vibration-EMG coherence was observed across a bandwidth of ~10-80 Hz, and coherence was suppressed by heel and enhanced by metatarsal stimuli. Cross-correlations were similarly suppressed by heel (from 104-155 ms) and enhanced by metatarsal (from 75-128 ms) stimuli. We then probed potential mechanisms that might be involved in this interaction. We conducted two follow-up experiments to examine *1)* presynaptic inhibition, and *2)* modulations at the α- and γ-motoneuron pools. Results from these experiments suggest the effects of cutaneous stimuli required a modulation at the α-motoneuron pool and were likely not mediated by presynaptic inhibition. These

findings demonstrate that cutaneous information from different regions of the foot sole functionally tunes the soleus response to proprioceptive perturbations for the control of balance.

4.2 Introduction

Information from cutaneous afferents that innervate the foot sole can contribute to the control of standing balance (Kavounoudias 1998, 1999; Maki et al., 1999; Roll et al., 2002; Meyer et al., 2004; Wang et al., 2016). Stimulation of cutaneous afferents evokes muscle responses that are spatially and temporally organized and task dependent (Aniss et al., 1992; Zehr et al., 1997, 2012, 2014; Nakajima et al., 2006; Haridas et al., 2008; Zaback et al., 2018). For example, stimulation of skin under the heel facilitates ankle plantar flexor muscle activity and simultaneously inhibits dorsiflexor muscle activity; meanwhile, responses of opposite polarity are evoked by stimulation under the metatarsals (Aniss et al., 1992; Nakajima et al., 2006). In addition, cutaneous reflex gain is lower during standing relative to sitting (Aniss et al., 1992), and reflex polarity can flip between different phases of the gait cycle (Zehr et al., 1997, 2012, 2014). The spatial organization and task-dependent nature of cutaneous reflexes is thought to reflect a functional contribution to the control of movement and balance (van Wezel et al., 1997, 2000; Zehr et al., 1997, 2012, 2014).

Low threshold (tactile) cutaneous afferents provide dispersed input to the spinal cord. For example, cutaneous afferents have been shown to interact with Ia and Ib inhibitory interneurons that mediate reciprocal and autogenic inhibition, respectively

(Lundberg et al., 1977; Bergego et al., 1981; Pierrot-Deseilligny et al., 1981; Rossi and Mazzocchio, 1988), primary afferent depolarization (PAD) interneurons that mediate presynaptic inhibition (Iles, 1996), as well as γ-motoneurons that influence muscle spindle sensitivity (Hunt et al., 1951; Alnaes et al., 1965; Appelberg et al., 1977; Aniss et al., 1988, 1990). While the net cutaneous reflex is known to be spatially organized according to the skin region stimulated (Aniss et al., 1992; Nakajima et al., 2006), less is known about the spatial organization of cutaneous interactions with other spinal reflex pathways during standing.

An experimental approach often used to assess the interaction between sensory inputs is the condition-test stimulus paradigm. Specifically, a conditioning stimulus (e.g., cutaneous electrical pulses) is delivered at a pre-defined interval relative to a test stimulus (e.g., mixed nerve stimulation to evoke the H-reflex). This sensory collision approach has been used to gather snapshots of the influence of cutaneous input on transmission through the H-reflex pathway at discrete condition-test intervals while individuals are seated or prone (Sayenko et al., 2007, 2009; Knikou, 2007, 2010; Lowrey and Bent, 2009). Previous research has shown that electrical stimulation of skin under the metatarsals *inhibits* the soleus H-reflex at short condition-test intervals (6-60 ms, Knikou et al., 2007; 25-40 ms, Sayenko et al., 2009; 45 ms, Lowrey and Bent, 2009). Sayenko et al. (2009) also observed stimulation under the heel conversely *facilitates* the soleus H-reflex at a 50 ms condition-test interval. It has been speculated that these modulations are mediated through presynaptic inhibition via PAD interneurons, although this cannot be confirmed from these studies.

There are some properties of presynaptic inhibition that could be used to infer whether the changes evoked by cutaneous input are mediated by presynaptic inhibition; these include a change in reflex amplitude that is dissociated from α-motoneuron pool excitability over time, an early onset and long duration of modulation (due to slow dynamics of the GABA receptors that generate presynaptic inhibition), and a preferential modulation of low frequency responses (Eccles et al., 1962; Morita et al., 1998, 2001; Rudomin and Schmidt, 1999; Enríquez-Denton et al., 2002; Pierrot-Deseilligny and Burke, 2012). Previously, these temporal and frequency characteristics have been difficult to assess using the condition-test stimulus approach, since this approach constrains the ability to characterize interactions to a limited number of pre-defined intervals, and does not provide information about the frequency characteristics. In addition, mixed nerve stimulation (to evoke the H-reflex) evokes brief and synchronized afferent input to the spinal cord (Burke et al., 1983), which may not be processed in the same manner as the trains of afferent input generated through mechanotransduction (Morita et al., 1998; Enríquez-Denton et al., 2002). Electrical nerve stimulation also generates a perturbation to balance, and since the characteristics of cutaneous reflexes are task-dependent, it is important to be able to examine their integration in reflex pathways during standing.

To overcome some limitations associated with the condition-test stimulus approach, in this study we used a time-dependent linear correlation analysis. Specifically, we delivered a continuous proprioceptive stimulus (noisy Achilles tendon vibration; Mildren et al. 2017, 2019) along with intermittent cutaneous stimuli (electrical pulse trains) and examined time-dependent vibration-EMG coherence and cross-correlations

aligned to the onset of the cutaneous pulse trains. The primary aim of this study was to characterize the interaction between cutaneous input from the heel and metatarsals of the foot sole and the soleus response to Achilles tendon vibration during standing. We hypothesized that heel and metatarsal cutaneous stimuli would evoke distinct changes in the soleus responses to vibration, reflecting a functional integration of cutaneous feedback into the stretch reflex pathway during standing. Our results demonstrated that heel stimuli suppressed, and conversely metatarsal stimuli enhanced, the soleus vibration responses (vibration-EMG coherence and cross-correlations).

Next, we explored potential mechanisms that might mediate the observed cutaneous interaction with the soleus vibration responses. We specifically probed potential contributions from presynaptic inhibition as well as modulations at the α- and γ-motoneuron pools. To characterize the influence of presynaptic inhibition on vibration-EMG coherence and cross-correlations, we stimulated the deep branch of the common fibular (CF) nerve, since group I afferents in the CF nerve are known to activate PAD interneurons that mediate presynaptic inhibition (Eccles et al., 1962; Hultborn et al., 1987; Rudomin and Schmidt, 1999). To examine the potential contribution from γ-motoneurons, we reduced the current of the electrical stimulus to the skin to below motor threshold since γ-motoneurons have been shown to have a lower threshold to cutaneous input relative to α-motoneurons (Hunt, 1951; Eldred and Hagbarth, 1954; Alnaes et al., 1965; Appelberg et al., 1977). Collectively, results from these experiments suggest that the modulations of the vibration responses required a strong enough cutaneous stimulus

to alter the excitability the α-motoneuron pool, and were likely not mediated by presynaptic inhibition or changes in γ-motoneuron activity.

4.3 Methods

4.3.1 Participants

A total of 24 healthy young adults (age = 24.0 ± 3.0 yrs; 15 male, 9 female), free of musculoskeletal and neurological disorders, participated in this study. Written informed consent was obtained and the University of British Columbia Research Ethics Board approved all procedures.

4.3.2 Experimental setup

Participants stood on a force plate (OR6-7; AMTI, USA; forces and moments amplified ×1000-4000 and sampled at 100 Hz) with their stance width normalized to foot length. Participants first completed a 2-min quiet standing trial and ± 2 standard deviation (SD) bandwidths were calculated around mean centre of pressure (COP) position in the anteroposterior and mediolateral directions. We monitored COP position in subsequent trials and provided auditory feedback if COP drifted outside of a bandwidth. Noisy vibration was continuously applied to the right Achilles tendon for 2 mins while electrical stimuli were delivered intermittently (every 0.8-1.0 s) to the heel or metatarsals (*see 4.3.3 Experiment 1: Heel and metatarsal stimuli*), the CF nerve (*see 4.3.4 Experiment 2: Involvement of presynaptic inhibition*), or the metatarsals at a lower current (*see 4.3.5*

Experiment 3: Involvement of α- and γ-motoneuron pools). Six 2-min trials of noisy tendon vibration combined with electrical stimuli were delivered for each condition.

Surface electromyography (EMG) was recorded unilaterally from the right soleus and tibialis anterior muscles through surface electrodes placed in bipolar configuration ~2 cm apart over the muscle bellies with the ground placed on either the medial or lateral malleolus. EMG data were amplified ×2000, bandpass filtered 10-1000 Hz (NeuroLog NL824 preamplifier and NL820 Isolator; Digitimer, UK), and sampled at 2000 Hz.

Mechanical stimuli were applied to the right Achilles tendon through a 3 cm diameter probe controlled by a linear motor (model MG-160; Labworks, USA). The probe of the linear motor was pulled into the tendon using a weighted pulley system to maintain a preload force of ~1 N. The pre-load force of the probe on the Achilles tendon was sensed using a force transducer (model 31; Honeywell, USA); force signals were differentially amplified ×100, low-pass analogue filtered at 600 Hz (Brownlee model 440; NeuroPhase LLC, USA), and sampled at 2000 Hz (Power 1401 A/D board and Spike2 software; Cambridge Electronic Design, UK). Vibration acceleration was sensed using an accelerometer (model 220-010; X Tronics, CA); acceleration signals were differentially amplified ×1, low-pass analogue filtered at 600 Hz (Brownlee model 440; NeuroPhase LLC, USA), and sampled at 2000 Hz. A white noise signal was generated and low-pass filtered at 100 Hz using LabVIEW 11 software and sent to a motor amplifier (PA-141; Labworks, USA) to control noisy tendon vibration. In the recorded probe acceleration data, power at frequencies beyond a bandwidth 10-115 Hz was ≤ -13

dB (ref. peak plateau of power spectrum) (Mildren et al., 2017), and the root-mean-square amplitude of the vibration acceleration was 15 m/s^2.

4.3.3 Experiment 1: Heel and metatarsal stimuli

Twelve healthy adults (7 male, 5 female) participated in experiment 1. To investigate the influence of foot sole cutaneous feedback on the soleus responses to tendon vibration, we applied electrical stimuli to the heel or metatarsal regions of the right foot sole along with tendon vibration. Cutaneous stimuli were applied through 5 cm diameter adhesive electrodes (Dermatrode type 00200-340; Delsys, USA) (Fig. 4-1). For heel stimuli the anode was placed under the proximal aspect of the heel and for metatarsal stimuli the anode was placed under the first metatarsal. Using a constant current stimulator (DS7A, Digitimer, UK) controlled through Spike2 software, a train of five 1 ms square-wave pulses at 200 Hz was delivered at 2× perceptual threshold with 0.8-1.0 s inter-stimulus-intervals (ISI); this variability in ISI was programmed to minimize prediction of the cutaneous stimuli. Six 2-min trials of heel stimuli along with noisy tendon vibration and six 2-min trials of metatarsal stimuli along with vibration were conducted in block-randomized order.

4.3.4 Experiment 2: Involvement of presynaptic inhibition

Six adults participated in experiment 2 (4 male, 2 female), one had also participated in experiment 1. Experiment 2 was conducted to characterize the effects of presynaptic inhibition from PAD interneurons on the soleus vibration responses. Group I (Ia and Ib) afferents in the CF nerve that innervate receptors in ankle dorsiflexor muscles are known to provide strong input to PAD interneurons that regulate transmission through

primary afferent terminals of ankle plantar flexor muscles (Eccles et al., 1962; Hultborn et al., 1987; Rudomin and Schmidt, 1999). Therefore, we electrically stimulated the deep branch of the CF nerve to provide excitatory input to PAD interneurons that mediate presynaptic inhibition while we applied noisy Achilles tendon vibration. It was expected that if presynaptic inhibition can have a role in controlling the vibration responses, then it would manifest as an early and long lasting inhibition of vibration-EMG coherence and cross-correlations following CF nerve stimuli. A 4.5 × 9.5 cm carbon rubber electrode was placed just above the patella as the reference, and a custom metal ballpoint electrode was used to search for the deep branch of the CF nerve around the fibular head using single electrical pulses. Specifically, we searched for the stimulus location that produced activity in muscles innervated by the deep branch of the CF nerve (e.g., tibialis anterior, toe extensors, fibularis tertius) along with paresthesia between the hallux and second digit, in the absence of activity in muscles innervated by the superficial branch of the CF nerve (e.g., fibularis longus and brevis). The custom electrode was then replaced with an adhesive 1 × 1 cm EMG electrode and the current threshold needed to evoke a just noticeable M-wave in tibialis anterior from individual stimuli was identified by viewing stimulus-triggered surface EMG in Spike2 software. The CF nerve stimulus intensity was maintained at 1.3 × M-wave threshold for tibialis anterior (Pierrot-Deseilligny and Burke, 2012); M-wave threshold was retested if the M-wave amplitude changed during a trial or if the participant took a seated break between trials. We applied single electrical pulses to the deep branch of the CF nerve intermittently (every 0.8-1.0 s) while we applied noisy Achilles tendon vibration over six 2-min standing trials.

4.3.5 Experiment 3: Involvement of α- and γ-motoneuron pools

Ten adults participated in experiment 3 (6 male, 4 female); two had participated in experiment 1, and one had participated in both experiments one and two. This experiment was conducted to examine the roles of the α- and γ-motoneuron pools in the interaction between cutaneous feedback and the vibration responses. There is evidence that γ-motoneurons have a lower threshold to cutaneous input relative to α-motoneurons (Hunt, 1951; Eldred and Hagbarth, 1954; Alnaes et al., 1965; Appelberg et al., 1977). Therefore, a modulation in vibration-EMG coherence and cross-correlations in the absence of a cutaneous reflex could support involvement of cutaneous input to γ-motoneurons. Conversely, the presence of a modulation in vibration-EMG coherence and cross-correlations only in the presence of a cutaneous reflex would suggest a change in the excitability of the α-motoneuron pool might be necessary to observe a cutaneous interaction with the vibration responses. We found the highest stimulus intensity that could be applied to the metatarsals without evoking a cutaneous reflex in soleus rectified trigger-averaged surface EMG based on a minimum of 50 stimulus pulse trains (5 pulses at 200 Hz, 0.4-0.6 s ISI). This cutaneous stimulus intensity was typically just above perceptual threshold. We then applied this stimulus level to the metatarsals (5 pulses at 200 Hz, every 0.8-1.0 s) along with noisy tendon vibration over six 2-min standing trials.

4.3.6 Data analyses and statistics

EMG and acceleration data were digitally low-pass filtered at 600 Hz (4th order dual pass Butterworth filter) and EMG data were full-wave rectified. Stimulus artifacts in the EMG from the electrical pulses were replaced with mean EMG (therefore, the stimulus artifact location will appear in figures as a band of coherence and correlation strength equal to zero). For the time-dependent coherence and cross-correlation analyses, epochs of data were extracted from 250 ms before to 750 ms after the onset of each stimulus train; this provided ~780 epochs of data for each participant over the six 2-min trials of each condition (heel and metatarsal stimuli in experiment 1, CF nerve stimuli in experiment 2, and below threshold metatarsal stimuli in experiment 3). Since we were interested in the ~500 ms window following the cutaneous stimuli, these epochs provided ~250 ms of padding on either side of the window of interest. The last stimulus at the end of a trial was removed if there was an incomplete (<750 ms) epoch of data following it. Due to the nonstationarity of the EMG data, a Morlet wavelet decomposition method (Zhan et al., 2006; Blouin et al., 2011) was used to calculate time-dependent coherence (aligned to the onset of the cutaneous stimuli). This analysis was performed for individual participant data as well as data pooled across participants for each condition. Coherence [C(*t*,*f*)] was estimated using the following equation:

$$C(t,f) = \frac{|P_{xy}(t,f)|^2}{P_{xx}(t,f)P_{yy}(t,f)}$$

Where t is time following the onset of the cutaneous pulse train, f is frequency, $P_{xy}(t,f)$ is the cross-spectrum of the probe acceleration and EMG signals, and P_{xx} and P_{yy} are the auto-spectra of the acceleration and EMG signals, respectively. The time-dependent EMG spectrum was also examined on an individual participant bases for experiment 3 to determine if any changes in coherence were associated with changes in EMG power. Time-dependent coherence values were considered significant when they exceeded 99% confidence limits, since a 99% limit was shown to better represent an α-level of 0.05 due to the bidirectional nature of the data (Blouin et al., 2011). For illustrative purposes, all non-significant coherence values were set to 0.

Time-dependent cross-correlations (aligned to the onset of the electrical pulse trains) were calculated using a custom-written algorithm in Matlab (Blouin et al., 2011) using the convention that a positive correlation reflected acceleration into the tendon was associated with an increase in rectified EMG.

To illustrate the amount of variation in coherence and cross-correlations that could be expected to occur due to chance using our analysis approach, we randomly generated trigger times with an ISI of 0.8-1.0 s and used these as references for the time-dependent coherence and cross-correlation analyses. This analysis (random trigger time generation and time-dependent coherence and cross-correlations) was only run once for data pooled across participants for one condition (the heel condition). These data were used for comparison purposes with data properly aligned to the onset of the cutaneous stimuli, and to provide baseline variability to construct ± 2 standard deviation (SD) thresholds for statistical analysis of the cross-correlations (see below).

Time-dependent cross-correlations were examined on an individual participant bases to obtain information about the latencies and durations of the modulations in vibration responses following cutaneous stimuli. We examined the change in peak-to-peak (P2P) amplitude of the cross-correlations following electrical pulses. Specifically, on an individual participant basis, we extracted the P2P amplitude of the cross-correlations over time following the cutaneous stimuli (i.e., the maximum minus the minimum correlation amplitude was extracted along the correlation lag time axis, and then examined along the time axis following cutaneous stimuli; see example for one participant in Fig. 4-2B and C). The change in P2P amplitude over time following cutaneous stimuli (P2P amplitude minus the mean) was then averaged across participants. The onset of a significant change in P2P cross-correlations was identified as the latency when peak-to-peak cross-correlation values crossed a positive or negative 2-SD threshold and remained outside of this threshold for a minimum of 20 consecutive data points (10 ms); this SD was calculated based on the cross-correlations generated from random trigger times. Similarly, the offset of the modulation was identified as the time when the P2P cross-correlations returned and remained within the ± 2 SD bandwidth for a minimum of 20 consecutive data points. To determine whether the average P2P cross-correlation across participants differed between the heel and metatarsal conditions, the mean P2P cross-correlation was compared between heel and metatarsal conditions using a paired samples *t*-test. For each participant, the latency of the maximum change in P2P cross-correlations following the cutaneous stimuli was extracted, and the mean latency was compared between heel and metatarsal conditions using a paired samples *t*-test.

To examine the changes in soleus EMG evoked by heel, metatarsal, and CF nerve stimuli, EMG data were trigger-averaged to the onset of the electrical pulses. The resulting waveform average for each participant was then debiased and averaged across participants. To align the stimulus artifact in the EMG with the artifact in the cross-correlations, the EMG was shifted in time by 42 ms in the negative direction to correspond to the lag time where the vibration and EMG were correlated (since the EMG was correlated with stimulus acceleration when shifted ~42 ms backward in time due to the neural transmission delay).

4.4 Results

4.4.1 Experiment 1: Effects of heel and metatarsal stimuli

We observed significant baseline coherence across a frequency bandwidth of ~10-80 Hz, and coherence was suppressed following heel stimuli and enhanced following metatarsal stimuli at latencies of ~100 ms (representative data are presented in Fig. 4-2A, and group data are presented in Fig. 4-3A). Noisy Achilles tendon vibration was significantly correlated with soleus EMG at a lag of ~40 ms (peak correlation at 39.4 ± 1.9 ms), and on average the P2P amplitude of the cross-correlations (r) was 0.278 ± 0.08. The average P2P cross-correlation amplitude was lower during the heel (r = 0.266 ± 0.084) relative to the metatarsal (r = 0.290 ± 0.078) stimulus condition; however, this difference was not significant (p = 0.201). Cross-correlations were similarly suppressed and enhanced by heel and metatarsal stimuli, respectively, at ~100 ms latencies (representative cross-correlation data are presented in Fig. 4-2B). To further assess the

time course of this suppression and enhancement, the P2P cross-correlations were examined over time following the cutaneous stimuli (Fig. 4-2C). The change in P2P cross-correlations over time averaged across participants demonstrated that cross-correlations were significantly suppressed at 104 ms and returned to baseline at 155 ms following heel stimuli (Fig. 4-3B). Following metatarsal stimuli, the cross-correlations were significantly enhanced at 75 ms and returned to baseline at 128 ms (Fig. 4-3B). The maximum change in P2P cross-correlations occurred significantly earlier for metatarsal stimuli (peak increase at 96 ± 14 ms) compared to heel stimuli (peak decrease at 118 ± 23 ms) ($p = 0.008$). Heel cutaneous stimuli evoked an increased followed by a decrease in rectified surface EMG, while metatarsal stimuli evoked a decrease followed by an increase in EMG (Fig. 4-3B). The latencies of these cutaneous reflexes were similar to the latencies of the changes in P2P cross-correlations (Fig. 4-3B). The suppression of P2P cross-correlations following heel stimuli corresponded to the decrease in trigger-averaged EMG, while the enhancement in P2P cross-correlations following metatarsal stimuli corresponded to the increase in trigger-averaged EMG.

To illustrate the variation in coherence and cross-correlations that might occur by chance using this analysis approach, we replaced the skin stimulus times with randomly generated trigger times and aligned the time-dependent coherence and cross-correlation analyses to the random trigger times. The coherence and cross-correlations aligned to random trigger times did not demonstrate any noticeable changes over time (Fig. 4-4); and there were no changes in P2P cross-correlations that met our criteria of a significant modulation.

4.4.2 Experiment 2: Involvement of presynaptic inhibition

To examine the influence that presynaptic inhibition from PAD can exert on the vibration responses, and whether this influence is comparable to the effects of foot sole stimuli, we examined time-dependent coherence and cross-correlations aligned to CF nerve stimuli. Unexpectedly, we observed no evidence of presynaptic inhibition in vibration-EMG coherence; instead, CF nerve stimuli evoked an early and prolonged *facilitation* in coherence (Fig. 4-5A). The timing of the peak modulation in coherence also occurred earlier with CF nerve stimuli relative to heel and metatarsal stimuli, where the peak modulation was observed at a 30 ms latency after CF nerve stimuli (Fig. 4-5A), in comparison to 110 and 88 ms latencies after heel and metatarsal stimuli, respectively (Fig. 4-3A). The change in P2P cross-correlations following CF nerve stimuli also demonstrated an early and prolonged facilitation (Fig. 4-5B). In soleus surface EMG, CF nerve stimuli evoked an early and short inhibition that resembled disynaptic reciprocal inhibition, followed by a prolonged slight increase in EMG (Fig. 4-5B).

4.4.3 Experiment 3: Involvement of α- and γ-motoneuron pools

To examine whether the modulation from foot sole stimuli could be evoked in the absence of a change in α-motoneuron pool excitability, we reduced the metatarsal cutaneous stimulus current to below the threshold to evoke a cutaneous reflex in soleus surface EMG. Since γ-motoneurons have been shown to have a lower threshold to cutaneous input relative to α-motoneurons, a change in vibration-EMG coherence in the absence of a cutaneous reflex (i.e., change in α-motoneuron pool excitability) could point

toward involvement of γ-motoneurons in the modulation of the vibration responses by cutaneous input. Surprisingly, despite the absence of a cutaneous reflex (averaged over a minimum of 50 stimuli) during quiet standing, when we added tendon vibration, a cutaneous reflex emerged in four out of 10 participants (representative data are shown in Fig. 4-6A and B). This indicates tendon vibration may have facilitated the (previously sub-threshold) cutaneous reflex. Across participants, there was no evidence that a modulation in vibration-EMG coherence was evoked in the absence of a cutaneous reflex (i.e., change in trigger-averaged surface EMG or time-dependent EMG power) (a representative participant is demonstrated in Fig. 4-6C). Overall, these data indicate a modulation in vibration-EMG coherence via cutaneous input was only observed when there was a change in α-motoneuron pool excitability.

4.5 Discussion

The central nervous system continuously receives afferent feedback from multiple somatosensory channels, and these different channels likely interact functionally in the spinal cord. During standing, somatosensory receptors in both the foot sole skin and triceps surae muscles provide information that can be used for the control of balance (Fitzpatrick et al., 1994; Kavounoudias et al., 1998, 1999, 2001; Maki et al., 1999; Roll et al., 2002; Meyer et al., 2004; Wang et al., 2016). To characterize how foot sole cutaneous afferents interact with the pathway that mediates the soleus vibration responses, we examined changes in the correlations between tendon stimuli and soleus EMG over time

following foot sole electrical stimuli (heel and metatarsals). Our results showed that heel stimuli suppressed vibration responses in soleus, demonstrated by a suppression of vibration-EMG coherence and cross-correlations. Conversely, metatarsal stimuli enhanced soleus responses (enhancement of vibration-EMG coherence and cross-correlations). We further explored potential mechanisms that might mediate the observed interactions between cutaneous input and the soleus vibration responses (experiments 2 and 3). Results from those experiments suggest that the interactions were only present when there were changes in α-motoneuron excitability, and were likely not mediated by presynaptic inhibition or selective input to γ-motoneurons.

The modulations in the vibration responses that we observed were spatially organized (heel stimuli suppressed while metatarsal stimuli enhanced vibration-EMG coherence and cross-correlations). The suppression following stimulation of the heel occurred at a longer latency (104-155 ms; peak decrease at 118 ± 23 ms) relative to the enhancement following stimulation of the metatarsals (75-128 ms; peak increase at 96 ± 14 ms). The difference in latencies suggests there may be additional interneurons interposed in the pathway mediating the suppression evoked by heel stimuli, or involvement of a transcortical loop.

Our finding of relatively late (~100 ms) modulations in the soleus vibration responses contrasts with previous studies that observed earlier modulations (~40 ms latencies) in soleus H-reflex amplitude evoked by foot sole conditioning stimuli (Sayenko et al., 2007, 2009; Knikou, 2007, 2010; Lowrey and Bent, 2009). In addition to occurring

earlier, the cutaneous modulations of the H-reflex were also in the opposite direction (heel facilatory, metatarsals inhibitory) relative to the modulations in the correlations observed in our experiment (heel suppression, metatarsals enhancement). The difference between our findings and those of previous studies (Sayenko et al., 2007, 2009; Knikou, 2007, 2010; Lowrey and Bent, 2009) could be attributed to differences in the posture of the participants (standing vs. seated or prone) or the methodological approach.

Since cutaneous reflexes are modulated in a task-dependent manner, their interaction with the stretch reflex pathway may vary according to the posture and whether the muscles are engaged in the control of balance. Methodologically, H-reflex is very sensitive to α-motoneuron pool excitability and presynaptic inhibition, whereas the stretch and tendon tap responses are less sensitive to presynaptic inhibition (Morita et al., 1998). The lower sensitivity of mechanically generated trains of spindle input to presynaptic inhibition may contribute to the lack of suppression in coherence and cross-correlations in response to CF nerve stimuli (experiment 2). Another difference between H-reflex vs. tendon vibration methodologies is that the responses evoked by tendon vibration involve mechanotransduction and are therefore sensitive to changes in spindle sensitivity via γ-motoneuron drive to intrafusal fibres of muscle spindles. However, results from experiment 3 do not suggest that the cutaneous interactions were mediated by changes in γ-motoneuron drive. Therefore, it is possible that cutaneous input influences the transmission through the stretch reflex pathway either through a modulation at the α-motoneuron pool or interneurons of a polysynaptic pathway that may

contribute to later portions of the stretch reflex (Burke et al. 1983; Matthews 1975). An influence on a polysynaptic pathway seems unlikely, however, since the cross-correlations were sometimes strongly suppressed by heel stimuli, including the earliest portion of the response (Fig. 4-2B**)**; this indicates there was some cutaneous influence on the monosynaptic input to α-motoneurons.

The modulations in vibration-EMG coherence and cross-correlations following foot sole stimuli aligned with the latencies of the cutaneous reflexes evoked in soleus EMG. The characteristics of the cutaneous reflexes were similar to those described previously (Aniss et al., 1992; Nakajima et al., 2006). Altogether, these findings suggest the modulations in vibration responses from cutaneous input might rely on changes in the excitability of the α-motoneuron pool.

4.5.1 Enhancement of vibration responses following CF nerve stimuli

PAD interneurons can control the transmission through Ia afferents by affecting the axon depolarization level, where depolarization of afferent terminals is responsible for presynaptic inhibition (Eccles et al., 1962). Cutaneous afferents have been shown to provide inhibitory input to PAD interneurons in both cats (ten Bruggencate et al., 1974; Jiménez et al., 1984) and humans (Iles et al., 1996). In humans, the effect of cutaneous stimuli (sural nerve and distal foot) on presynaptic inhibition was found to begin early and reach a maximum strength at a 15 ms latency (Iles, 1996; Rudomin and Schmidt, 1999). In contrast, the modulations in reflex transmission we observed following foot sole stimuli occurred later (~100 ms). In addition, we did not observe other

characteristics of presynaptic inhibition, such as a modulation of low frequency responses (<30-50 Hz; Rudomin and Schmidt 1999).

To characterize how PAD could influence vibration-EMG coherence, we stimulated the deep branch of the CF nerve, which is known to provide strong excitatory input to PAD interneurons (Eccles et al., 1962; Hultborn et al., 1987; Rudomin and Schmidt, 1999). Interestingly, we did not observe any evidence of presynaptic inhibition, which may be due to a limited influence of PAD on gating trains of action potentials such as those generated by mechanical stimuli (Rudomin and Schmidt, 1999). Surprisingly, we observed an early and prolonged *enhancement* in vibration-EMG coherence. While an enhancement could be evoked by input from antagonist Ib afferents in the CF nerve (reciprocal facilitation), the duration of this facilitation was longer than would be expected from Ib input (Pierrot-Deseilligny and Burke, 2012), which suggest that another mechanism may also contribute to this enhancement, such as presynaptic facilitation.

Since the initial description of presynaptic inhibition by Frank and Fuortes (1957), and experiments conducted by Eccles and colleagues (1962), there have been recent findings that suggest PAD may have more complex functions in the regulation of afferent transmission (Li et al., 2017; Lucas-Osma et al., 2018). Activation of GABA receptors generates afferent depolarization, which causes presynaptic *inhibition* through action potential shunting at afferent terminals (Cattaert and Manira, 1999; Willis, 2006). However, it has been proposed that afferent depolarization by GABA receptors at branch points could facilitate transmission by preventing conduction block (Li et al., 2017; Lucas-Osma et al., 2018). Conduction block is a common feature of long and highly

branched nerve fibres (such as muscle spindle afferents). The change in time-dependent coherence and cross-correlations we observed following CF nerve stimuli could reflect facilitation of afferent transmission; however, more experiments are necessary to explore this possibility.

4.5.2 Role of α- and γ-motoneuron pools

Distinct interneuron pathways to α- vs. γ-motoneurons have been identified in decerebrate cats (Connell et al., 1986); these distinct pathways could result in dissociation between intra- and extrafusal fibre contraction. Sensory input to the spinal cord (particularly from cutaneous afferents) was found to support dynamic γ-motoneuron activity in cats (Hunt, 1951). Dynamic γ-motoneuron stimulation has been shown to increase the gain of Ia afferent responses to sinusoidal muscle stretching (Hulliger et al., 1977) and cause a 50% increase in the number of spikes evoked by tendon taps (Morgan et al., 1985). While cutaneous input to γ-motoneurons has been demonstrated in animal experiments (Hunt, 1951; Eldred and Hagbarth, 1954; Alnaes et al., 1965; Appelberg et al., 1977), cutaneous input to γ-motoneurons has been more difficult to observe in humans. Aniss et al. (1990) found indirect evidence in humans of a cutaneous modulation of γ activity (modulation of spindle afferent firing not explained by muscle stretch) in a small sample of spindle afferents of dorsiflexor muscles while participants were standing.

Given the potential for a role of γ-motoneurons, we conducted experiment 3 to determine if a modulation in the soleus vibration response could be evoked with stimuli

that were sub-threshold for activating the α-motoneuron pool. Since γ-motoneurons were found to have a relatively lower threshold to cutaneous input (Hunt, 1951; Eldred and Hagbarth, 1954; Alnaes et al., 1965; Appelberg et al., 1977), a modulation in coherence in the absence of a cutaneous reflex could provide evidence for involvement of γ-motoneurons. However, we did not observe any modulation in vibration-EMG coherence in the absence of a cutaneous reflex, which does not support select involvement of γ-motoneurons in generating the cutaneous interactions with the vibration responses.

Interestingly, in some participants, when we added noisy tendon vibration, the previously subthreshold metatarsal stimuli became suprathreshold (i.e., cutaneous stimuli evoked responses in soleus EMG). This indicates that proprioceptive input to the spinal cord might be able to facilitate interneurons involved in the cutaneous reflex pathway.

4.5.3 Functional implications

During standing, available information should be integrated into the stretch reflex pathway so responses are adapted to the current situation. In a backward leaning posture, it would be advantageous for cutaneous feedback from the heels to suppress the soleus stretch response, since the risk of falling backward is greater. Conversely, metatarsal cutaneous feedback during a forward lean could help support the reflex activation of soleus and the generation of plantar flexion torque toward a neutral posture. Similarly, a forward perturbation (such as a push from behind) during standing would cause an anterior shift in pressure under the feet as well as stretch of the triceps surae muscles; in this situation, cutaneous and proprioceptive information may be combined to enhance the

plantar flexor muscle response. Overall, our results suggest that different regions of the foot sole have a functional role in tuning proprioceptive responses for the control of standing posture and balance.

4.5.4 Conclusions

In summary, our findings demonstrate spatially organized interactions between foot sole cutaneous and triceps surae proprioceptive feedback in humans during standing. Specifically, heel stimuli suppressed, while metatarsal stimuli enhanced, the soleus muscle responses to proprioceptive perturbations generated by Achilles tendon vibration. Results from our experiments also suggest these interactions required a strong enough cutaneous stimulus to modulate the α-motoneuron pool, and were likely not mediated by presynaptic inhibition. These findings indicate that cutaneous feedback from the foot sole is integrated into the stretch reflex pathway to functionally modulate (suppress or enhance) responses to proprioceptive perturbations during standing.

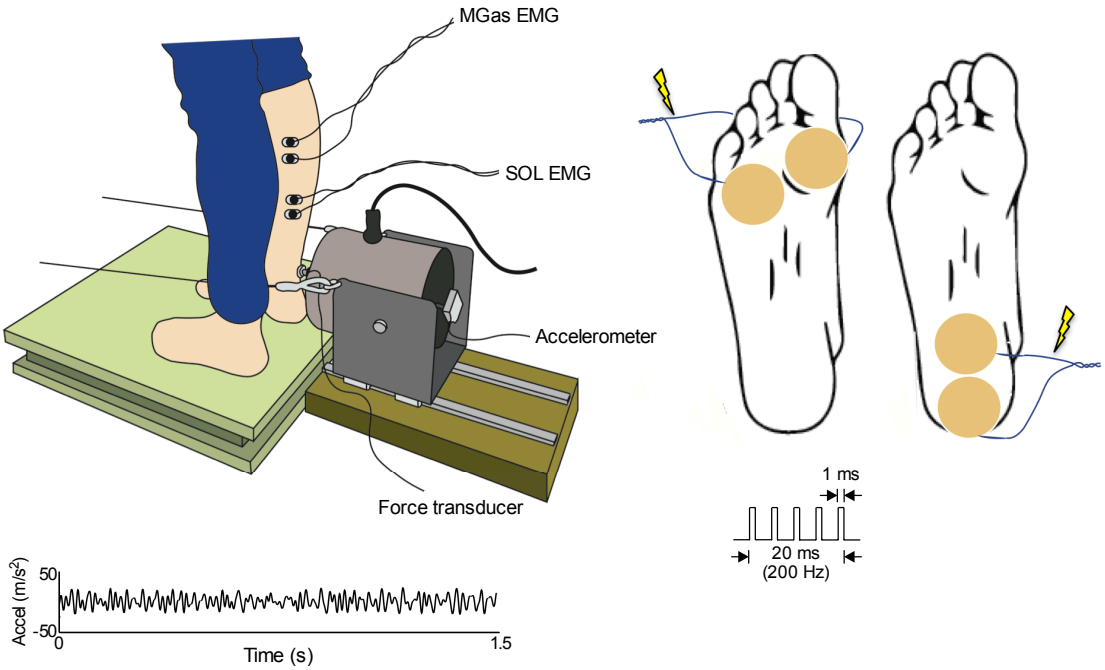

Figure 4-1 Experimental setup and stimulus parameters

Illustration of the experimental setup used to apply noisy Achilles tendon vibration along with electrical pulse trains to the heel or metatarsals of the foot sole during standing. A sample of the vibration acceleration profile, as well as the parameters of the cutaneous stimuli, are also demonstrated.

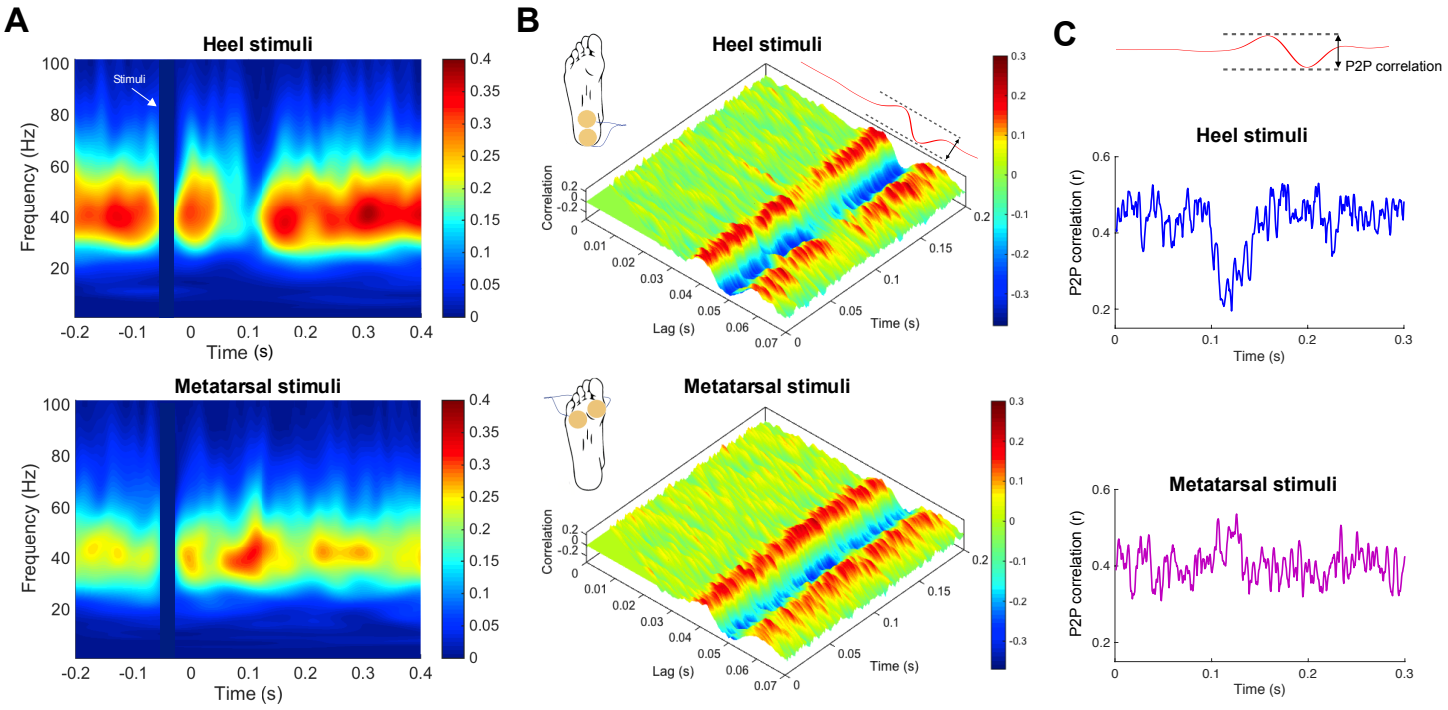

Figure 4-2 Representative participant data for heel and metatarsal stimuli

Representative data from one participant of time-dependent vibration-EMG coherence (A) and cross-correlations (B) following cutaneous pulse trains applied to the heel and metatarsals. The peak-to-peak (P2P) amplitude of the cross-correlations was extracted over time following the cutaneous stimuli and plotted in panel C. Note the suppression in coherence and cross-correlations following heel stimuli and the enhancement following metatarsal stimuli.

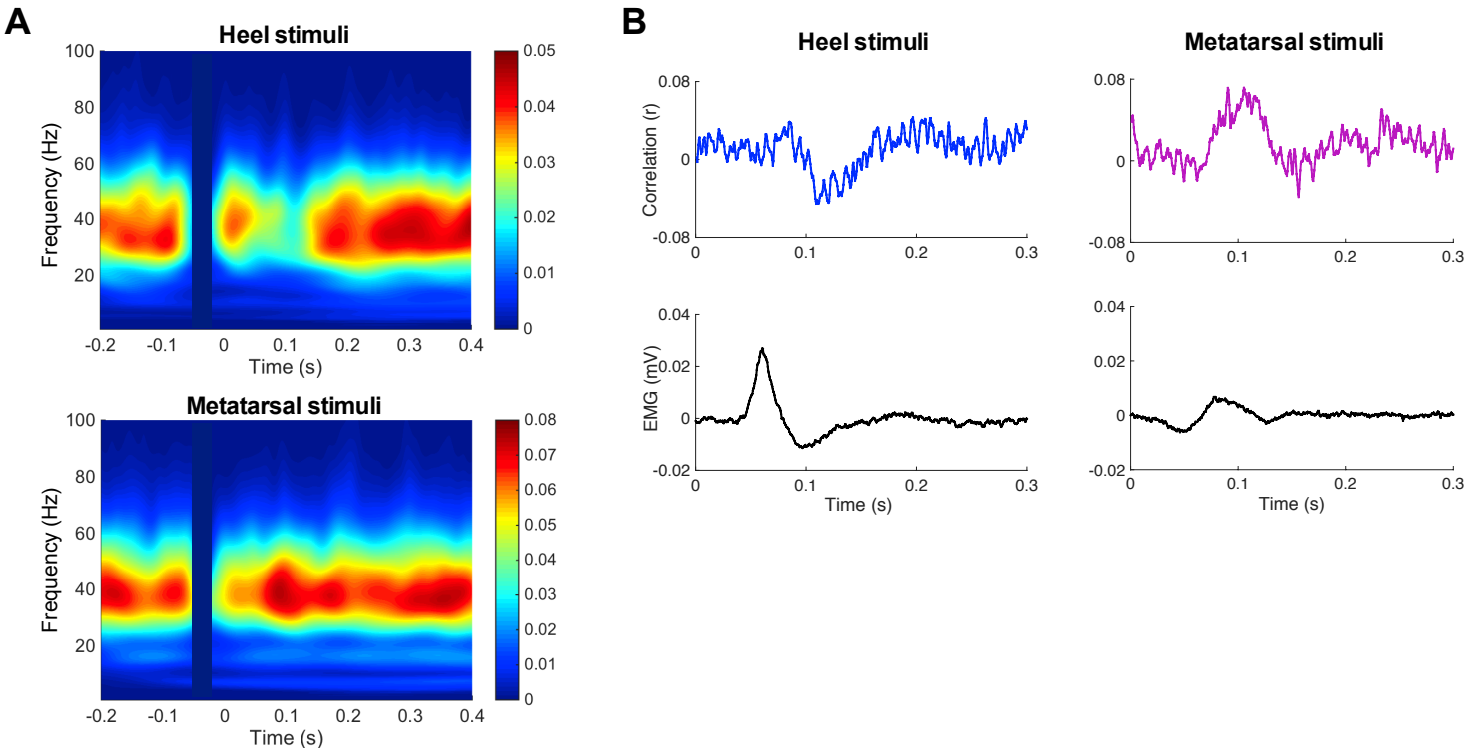

Figure 4-3 Group responses to heel and metatarsal stimuli

Group results for time-dependent coherence following heel and metatarsal stimuli (A) along with the average change in peak-to-peak (P2P) cross-correlations following cutaneous stimuli and the cutaneous reflexes in surface EMG (B) (n = 12). Note the depression and enhancement in coherence and cross-correlations following heel and metatarsal stimuli, respectively. Also note the modulations in P2P cross-correlations occur at similar latencies as the cutaneous reflexes.

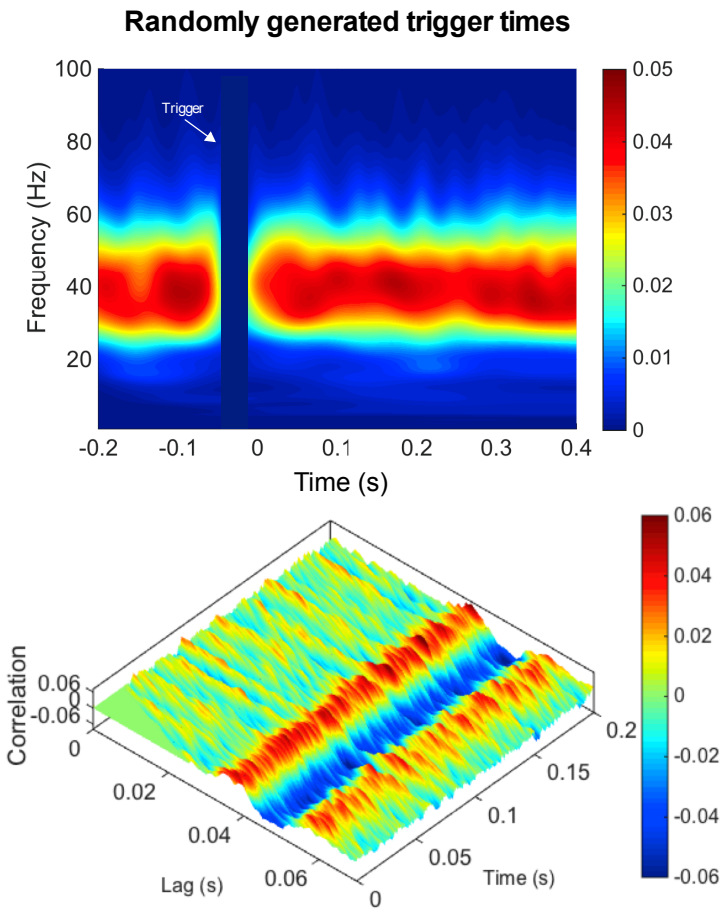

Figure 4-4 Time dependent coherence and cross-correlations aligned to randomly generated trigger times

Time-dependent coherence and cross-correlations aligned to randomly generated trigger times (i.e., not aligned to cutaneous stimuli) (n = 12). For comparison purposes, these data illustrate the amount of variation in coherence and cross-correlations over time that might be expected to occur due to chance.

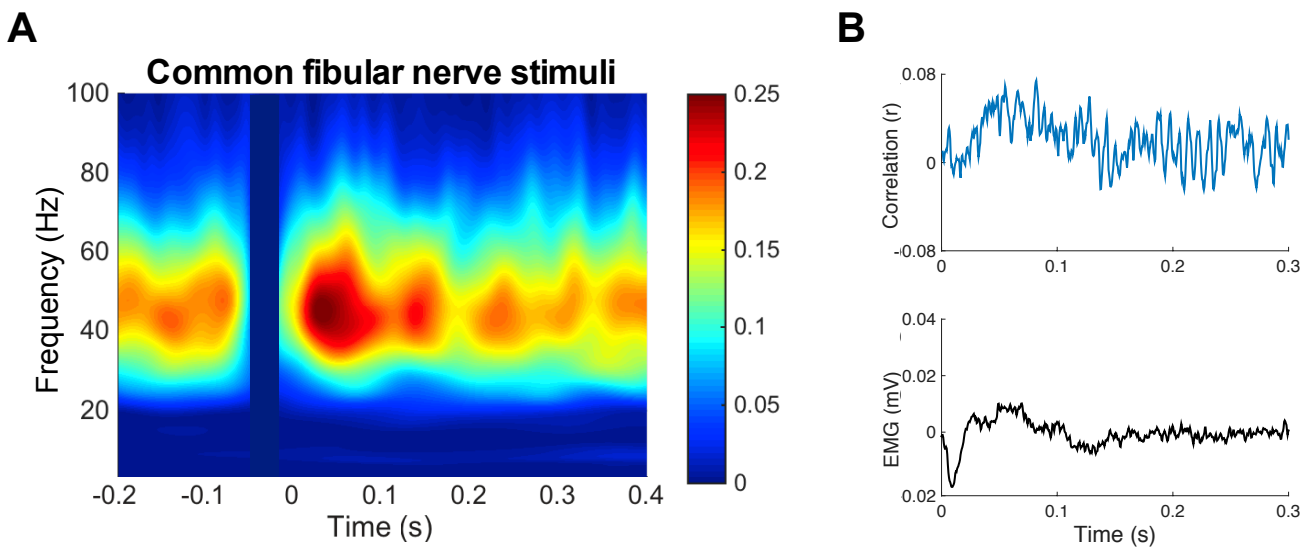

Figure 4-5 Group responses to common fibular nerve stimuli

Time-dependent vibration-EMG coherence following common fibular (CF) nerve stimuli (A) and the average change in peak-to-peak cross-correlations and soleus surface EMG following CF nerve stimuli (n = 6) (B). Note the early enhancement in coherence and cross-correlations following CF nerve stimuli.

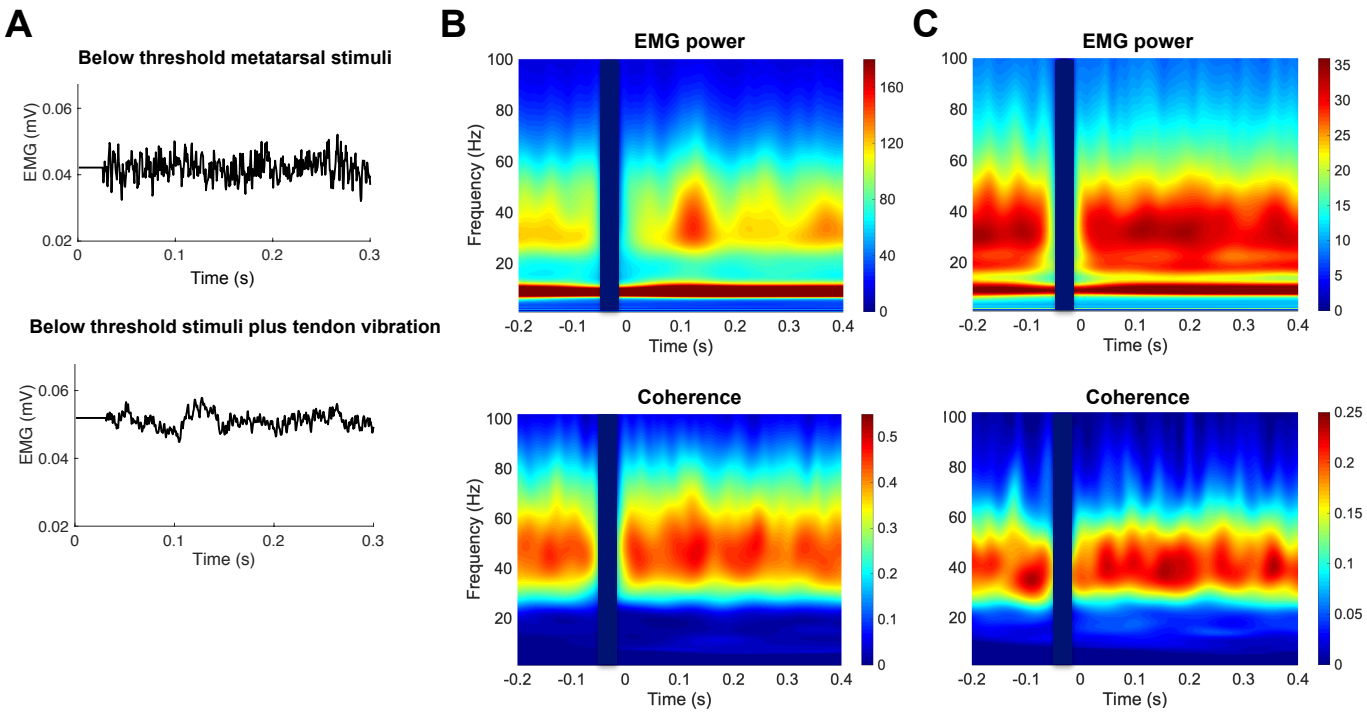

Figure 4-6 EMG and coherence during subthreshold metatarsal cutaneous stimuli

Example from one participant of trigger-averaged surface EMG when cutaneous stimuli were delivered below reflex threshold, and trigger-averaged surface EMG at the same stimulus level while vibration was applied (A). Time dependent EMG power and coherence in one participant that demonstrated a cutaneous reflex (change in EMG power) when vibration was added to previously sub-threshold cutaneous stimuli (B). Data from one participant that did not demonstrate a cutaneous reflex or modulation in vibration-EMG coherence (C).

4.6 Bridging Summary

The experiments described in Chapters 2 and 3 examined the characteristics of vibration responses in triceps surae muscles during standing in healthy young adults. This previous chapter (Chapter 4) added another layer by examining the integration of cutaneous feedback into the responses evoked by proprioceptive stimuli. Next, healthy ageing is known to alter multiple aspects of the sensorimotor system, which leads to impaired mobility and an increased risk of falls. The following chapter of this thesis addresses how the bandwidth, gain, amplitude, and scaling of soleus responses to tendon vibration during standing change over the adult lifespan.

Chapter 5: Influence of age on the frequency characteristics of the soleus muscle response to Achilles tendon vibration during standing

5.1 Abstract

Proprioceptive information from the ankle joint plays an important role in the control of posture and balance. Ageing influences many components of the sensorimotor system, which could contribute to poor mobility and falls. We examined the characteristics of the soleus muscle responses to proprioceptive error signals generated by noisy (10-115 Hz) Achilles tendon vibration during standing in 54 healthy adults across a broad age range (18-82 yrs). Relative to young adults, the bandwidth of the soleus response (vibration-EMG coherence) was narrower in middle aged and old adults, and gain was lower in the old adults ~28-54 Hz. Across the age range, the response amplitude (peak-to-peak cross-covariance), as well as the scaling of the response with stimulus amplitude, were both negatively correlated with age. Our findings suggest there is a progressive change in the frequency characteristics of the soleus response to proprioceptive error signals during standing with age, which could contribute to impaired responses to perturbation and an increased risk of falls.

5.2 Introduction

The sensorimotor control of ankle plantar flexion torque is critical for upright posture and balance, and sensory receptors in muscles that cross the ankle joint are known to provide crucial feedback for the control of balance (Fitzpatrick et al., 1994). At the

ankle joint, impaired proprioception has been associated with poorer objective as well as self-reported measures of balance and mobility in adults up to 97 yrs old (Deshpande et al., 2016). Proprioceptive feedback is provided by sensory receptors in the muscle and tendon. Muscle spindles sense muscle stretch and rate of stretch during movement and form sensorimotor feedback loops that help regulate muscle activity. The soleus muscle, in particular, has a high number and density of muscle spindles (Banks, 2006) which have strong connections to the α-motoneuron pool of the soleus muscle as well as the α-motoneuron pools of other muscles (Jankowska, 2015; Eschelmuller et al., 2019). In healthy young adults, soleus motor units respond to tendon vibration (which activates muscle spindles) up to 100 Hz during standing (Mildren et al., 2019); a bandwidth that encompasses frequencies generated in spindle afferents across a range of activities or perturbations (e.g., walking; Simon et al., 1981). These features suggest an important function of soleus muscle spindle feedback to postural muscles for the control of upright posture and standing balance.

Ageing is known to influence the structure and function of many aspects of the sensorimotor system, and these changes lead to impaired mobility and increased risk of falls (Henry and Baudry, 2019; Ferlinc et al., 2019). Many components of the stretch reflex pathway are affected by ageing, including muscle spindle mechanoreceptors and their afferent axons (Swash and Fox, 1972; Liu et al., 2005; Kim et al., 2007; Vaughan et al., 2017; Swallow, 1966), as well as α-motoneuron axons and cell bodies, neuromuscular junctions, and muscle fibres (Zhang et al., 1996; Lexell and Downham, 1991; Hepple and

Rice, 2016). Interestingly, some of the age-related remodelling of α-motoneurons, including the shrinkage of cell bodies (increase in input resistance; Zhang et al., 1996) and reinnervation of denervated muscle fibres (Lexell and Downham, 1991; Hepple and Rice, 2016) may help preserve the α-motoneuron responses to spindle afferent input. There is also evidence that the motor units of some muscles (including the soleus muscle; Dalton et al., 2008, 2009) are more resistant to age-related changes than others. In contrast, the changes in muscle spindle morphology that occur progressively with age likely reduce the capacity of spindles to transduce mechanical stimuli. These changes include an increase in the thickness of spindle capsules (Swash and Fox, 1972), unravelling and swelling of the annulospiral afferent nerve endings (Kim et al., 2007; Vaughan et al., 2017), a decrease in the number of intrafusal muscle fibres (Swash and Fox, 1972; Liu et al., 2005), and a decrease in the overall number of spindle afferent nerve fibres (Swallow, 1966; Vaughan et al., 2017). Overall, these morphological changes with age likely contribute to the decrease in muscle spindle dynamic responses to stretch that have been demonstrated in rats (Kim et al., 2007).

During standing, Baudry et al., (2015) observed lower spinal excitability (soleus maximal H-reflex amplitude normalized by M-max) along with higher corticospinal excitability (maximal motor evoked potential amplitude normalized by M-max) in old relative to young adults. These authors suggested old adults rely on a strategy of reducing reliance on peripheral afferent feedback and increasing reliance on descending pathways and co-activation of ankle muscles during standing (Baudry et al., 2015, 2016). In agreement with this suggestion, old adults have been shown to exhibit lower ankle plantar

flexion torque output in response to toes up support surface rotations (Keshner et al., 1993) and Achilles tendon taps (Chung et al., 2005). The amplitude of the soleus short latency response to toes up ankle rotations was also found to be smaller in old relative to young adults during a background contraction (Kawashima et al., 2004; Obata et al., 2010) and during standing (Allum et al., 2002). While previous studies indicate the soleus response to proprioceptive stimuli generated by mechanical perturbations is weaker in old adults, it is unknown how age influences the characteristics of responses during standing balance across frequencies encountered in daily activities.

The first aim of this study was to compare the frequency characteristics of the soleus response to noisy Achilles tendon vibration between young, middle aged, and old adults during standing – where proprioceptive error signals are relevant to the control of balance. We applied a broad frequency bandwidth (10-115 Hz) of suprathreshold noisy vibration to the Achilles tendon and examined vibration-EMG coherence, gain, phase, and cross-covariance. Due to the changes described in muscle spindle morphology and stretch responses with age, we hypothesized vibration-EMG coherence would be weaker in middle aged and old adults. The second aim of this study was to examine whether the soleus response amplitude (peak-to-peak cross-covariance) and scaling declines with age across a broad age range (18-82 yrs), and whether there are associations between age, response amplitude, and centre of pressure (COP) movement in the anteroposterior (AP) direction. We hypothesized soleus response amplitude would be negatively correlated with age, and AP COP frequency would be positively correlated with age and negatively correlated with soleus response amplitude.

5.3 Methods

5.3.1 Participants

A total of 54 adults (25 male, 29 female) between the ages of 19 and 82 yrs participated in the experiment. All participants self-reported they were free of musculoskeletal and neurological disorders. Written informed consent was obtained and all procedures were approved by the University of British Columbia Research Ethics Board.

5.3.2 Achilles tendon stimuli

To examine the characteristics of responses in the soleus muscle to tendon stimuli, we applied suprathreshold noisy vibration to the Achilles tendon while we recorded ongoing leg muscle activity. Some of the benefits of this approach (relative to transient tendon taps or electrical nerve stimuli) include that noisy vibration does not noticeably perturb standing balance, requires relatively short trial durations to elicit consistent responses, and provides information about the frequency characteristics of the evoked responses (Mildren et al., 2017). We applied the noisy (10-115 Hz) vibration through a 3 cm diameter probe using a linear motor (model MG-160; Labworks, USA). The noisy vibration signal (white noise low-pass filtered at 100 Hz) was generated in LabVIEW 11 software (National Instruments, USA) and sent from a multifunctional data acquisition card (PXI-6225, National Instruments, USA) controlled by a real-time computer (PXI-8106, National Instruments, USA) to a motor amplifier (PA-141; Labworks, USA). The probe was pushed against the Achilles tendon with a preload force of ~1 N

(monitored using a force transducer; model 31; Honeywell, USA). Force signals were differentially amplified ×100, low-pass analogue filtered at 600 Hz (Brownlee model 440; NeuroPhase LLC, USA), and sampled at 2000 Hz (Power 1401 A/D board and Spike2 software; Cambridge Electronic Design, UK). An accelerometer (model 220-010; X Tronics, CA) was mounted to the motor piston to record probe acceleration; acceleration signals were differentially amplified ×1, low-pass analogue filtered at 600 Hz (Brownlee model 440; NeuroPhase LLC, USA), and sampled at 2000 Hz. In the recorded probe acceleration data, power was primarily contained within the bandwidth of 10-115 Hz.

5.3.3 Experimental procedures

Participants stood with their stance width equal to their foot length and with each foot on a separate force plate (Bertec, USA; type 4060-08); forces and moments were amplified (×2-10; type AM6-4; Bertec, USA) and sampled at 100 Hz. Participants first completed one 2-min quiet standing trial, followed by three 2-min trials of vibration at different acceleration amplitudes (root-mean-square acceleration = 10, 15, and 20 m/s^2) applied to the left and right Achilles tendon, resulting in six vibration trials total. The three amplitudes were presented in randomized order on each Achilles tendon, and the order of sides (right and left Achilles) was randomized between participants. During the vibration trials, we monitored the vertical ground reaction forces as well as the AP moments on each force plate. When necessary, we verbally guided participants to maintain a similar posture (within ~2 standard deviations of AP moments) and symmetrical weight distribution on each force plate throughout the trials.

Surface electromyography (EMG) was recorded bilaterally from the soleus muscle; electrodes were placed in a bipolar configuration 2 cm apart over the muscle belly and the ground electrode was placed on the right lateral malleolus. EMG data were amplified ×2000, bandpass filtered 10-1000 Hz (NeuroLog NL824 preamplifier and NL820 Isolator; Digitimer, UK), and sampled at 2000 Hz.

5.3.4 Data analysis and statistics

EMG and acceleration signals were de-biased and digitally low-passed filtered at 600 Hz (4th order dual pass Butterworth filter), and EMG data were full-wave rectified. Force plate forces and moments were low-pass filtered at 10 Hz (4th order dual pass Butterworth filter) and COP position in the AP direction was calculated for both force plates merged. To examine postural control during the quiet stance trial, AP COP data were de-biased and mean power frequency (MPF) (frequency resolution 0.0244 Hz), and root-mean-square amplitude (RMS) were calculated.

To examine the characteristics of the soleus response to ipsilateral Achilles vibration, we estimated coherence, gain, phase, and cross-covariance between the vibration acceleration (input) and surface EMG (output) for each standing vibration trial (see section *5.3.3. Experimental procedures*). Analyses were performed using a frequency resolution of 0.9765 Hz (1.024 s/segment, 117 disjoint segments per trial). Coherence was calculated as the magnitude of the signal cross-spectrum squared divided by the product of the autospectra of the input and output signals. Coherence values provide information about the linear association between the input (vibration acceleration) and output (rectified EMG) signals across frequencies. Gain was estimated as the cross-spectrum

divided by the autospectrum of the input signal to provide information about the amplitude of the output relative to the input, and phase was estimated from the angle of the cross-spectrum to provide information about the delay between the input and output signals across frequencies. As a measure of the association between the input and output signals in the time domain, cross-covariance was obtained from the inverse Fourier transform of the cross-spectrum normalized by the product of the vector norms of the input and output signals (Dakin et al., 2010). We used the convention that acceleration into the tendon and increased rectified EMG were both in the positive direction. Therefore, a positive cross-covariance would indicate acceleration into the tendon was associated with increased EMG or acceleration away from the tendon was associated with decreased EMG.

To examine the change in frequency response characteristics with age, we pooled data within young (18-29 yrs, n = 14), middle aged (40-59 yrs, n = 11), and old (70-82 yrs, n = 14) adult groups during the largest stimulus amplitude on the right side and calculated coherence, gain, phase, and cross-covariance for each group. To determine where coherence was significantly different among the three age groups, we performed a χ^2 extended difference of coherence (DOC) test. This was followed up with pairwise χ^2 DOC tests between the young and middle aged, middle aged and old, and young and old groups to further examine how the frequency characteristics of the response differed between each age group.

To determine the significance of responses, 95% confidence intervals (CI) based on the number of segments were constructed around coherence (positive threshold) and

cross-covariance (positive and negative thresholds) estimates for individual data as well as data pooled across age groups. The bandwidth of significant coherence was identified as the number of frequencies that contained coherence values exceeding the 95% CI for individual data, and compared between the young, middle aged, and old adult groups using independent samples *t*-tests. Gain and phase data were extracted and illustrated only at frequencies associated with significant coherence. Lower gain would reflect less EMG output relative to the stimulus, and a steeper phase slope would indicate a longer time delay between the vibration stimulus and correlated EMG activity. To determine differences in gain between the young, middle aged, and old groups, we constructed 95% CIs by resampling (with replacement) the number of participants in each group (e.g., 14 participants' data from the old group) and calculating gain values across frequencies (with gain values removed where coherence was non-significant) from analysis of their pooled data. This was repeated 10000 times to construct point wise 95% CIs (positive and negative limits) at each frequency. Similarly, to examine phase slopes for each age group, we resampled the number of participants in each group (with replacement) and calculated phase frequency slopes using linear regression 10000 times. Phase values were only used in the slope calculation if they were obtained at frequencies with significant coherence and were within a bandwidth that contained a minimum of 8 of 10 adjacent points with significant coherence. In addition, phase-frequency slopes were not included if the R^2 of the linear regression was < 0.95. Slope values were divided by 2π to estimate the time delay and the mean and standard deviation were calculated.

To examine how the amplitude of the soleus vibration response in the time domain differed with stimulus amplitude and sides, we calculated the peak-to-peak (P2P) cross-covariance for each participant at each stimulus amplitude for the right and left soleus muscles. We examined whether there were differences between the stimulus amplitudes and sides using a two-way repeated measures ANOVA (amplitude by side), with a Greenhouse-Geisser correction applied with violations of Mauchly's test of Sphericity and a Bonferroni adjustment applied to an α-level of 0.05 for follow-up pairwise comparisons. Since there was no significant difference in response amplitude (P2P cross-covariance) between the right and left soleus muscles ($F_{(1,53)} = 0.642$, $p = 0.427$), or interaction between stimulus amplitude and side ($F_{(2,106)} = 0.030$, $p = 0.971$) we averaged data across the right and left sides for further analyses. To examine how the response amplitude varied with age, we examined the Pearson correlation between age and the P2P cross-covariance at the largest stimulus amplitude (RMS acceleration = 20 m/s^2). In addition, we extracted the slope of the P2P cross-covariance plotted against stimulus amplitude in each participant as a measure of the response scaling, and we examined the Pearson correlation between age and response scaling. To explore whether AP COP measures were influenced by age, and whether COP measures were related to response amplitude, we determined the Pearson correlations between age and AP COP MPF and RMS, as well as between P2P cross-covariance and COP MPF and RMS.

5.4 Results

To explore how the frequency characteristics of the soleus response to noisy Achilles tendon vibration were influenced by age, we examined vibration-EMG coherence, gain, phase, and cross-covariance within young, middle aged, and old adult groups. Our results showed that coherence between the vibration and ipsilateral soleus EMG became weaker with age, and the frequency bandwidth that contained significant coherence became compressed (Fig. 5-1). Specifically, in the young adult group, soleus vibration-EMG coherence was significant (above the 95% CI) over a larger bandwidth (64 ± 17 Hz), compared to the middle aged (46 ± 14 Hz) and old (24 ± 22 Hz) adult groups; these bandwidth differences were significant between the young and middle aged (p = 0.007), middle aged and old (p = 0.006), and young and old groups ($p < 0.001$) (Fig. 5-1). Coherence for all three age groups are overlaid for comparison in Fig. 5-2A. There was a significant difference in coherence within the three age groups across a frequency bandwidth of ~7-64 Hz (Fig. 5-2B). The pairwise DOC tests revealed stronger coherence between ~7-62 Hz in the young compared to the middle aged group with no difference, however, between ~12-27 Hz. The pairwise DOC tests also showed stronger coherence ~30-50 Hz in the middle aged compared to old adults, and ~7-64 Hz in the young compared to old adults (Fig. 5-2C).

Gain demonstrated low pass filtering characteristics in all three age groups, with the highest gain observed at low frequencies (Fig. 5-3). Gain was similar among the three age groups at low frequencies (up to ~10 Hz) and then began to separate, with higher gain in the young relative to the old group, and middle aged in between (Fig. 5-3). In

particular, gain was significantly different (95% CIs not overlapping) between the young and old groups across a bandwidth of ~28-54 Hz. The response time delays obtained from the phase slopes were 42 ± 1.4 ms for the young, 45 ± 3.2 ms for the middle aged, and 44 ± 4.8 ms for the old adult groups.

To examine how response amplitude was influenced by age within our sample of healthy adults across a broad age range (18-82 yrs), we calculated the correlation between age and P2P cross-covariance extracted in each subject. We found a significant negative correlation between age and P2P cross-covariance (R = -0.6520, P < 0.001; Fig. 5-4A), which suggests a progressive decline in response amplitude with age. We applied three stimulus amplitudes to examine the amplitude scaling of the response (P2P cross-covariance). Responses significantly differed among stimulus amplitudes ($F_{(1.6,86.9)}$ = 73.333, $p < 0.001$), and there were significant increases in the response amplitude as the stimulus amplitude increased from low, to medium, to high (*p-values* < 0.001). We then examined if response scaling was influenced by age across a broad age range (18-82 yrs), and found the response scaling was significantly negatively correlated with age (R = -0.5305, $p < 0.001$; Fig. 5-4B), which indicates a shallower increase in response amplitude with stimulus amplitude.

To examine changes in postural control with age, we extracted COP MPF and RMS amplitude in the AP direction for each participant during quiet standing. We found AP COP MPF was significantly positively correlated with age (R = 0.2785, $p = 0.0414$), which indicates a shift toward higher frequency AP COP movement. There was no significant correlation between AP COP RMS and age (R = 0.0306, $p = 0.8258$), and no

significant correlations between COP measures (MPF and RMS) and response amplitude (P2P cross-covariance) (MPF vs. response amplitude: R = -0.2013, p = 0.144; RMS vs. response amplitude: R = -0.0924, p = 0.5062).

5.5 Discussion

The primary aim of this study was to examine the influence of age on the characteristics of the soleus muscle response to noisy Achilles tendon vibration during standing. Our results showed the bandwidth of the frequency response (vibration-EMG coherence) became progressively narrower in middle aged and old adults relative to young adults, and coherence significantly differed across a broad bandwidth (7-62 Hz) among the three age groups. In addition, the response gain was lower in the old relative to young adult groups across a bandwidth of ~28-54 Hz. Within the sample of 54 adults, the amplitude of the response (P2P cross-covariance) as well as the scaling of the response with stimulus amplitude were negatively correlated with age from 18 to 82 yrs old. Altogether, our findings suggest ageing is associated with a narrowing of the frequency bandwidth as well as a decline in the gain, amplitude, and scaling of the soleus response to proprioceptive perturbations during standing.

Our finding of an age-related change in the amplitude of the response to a mechanical perturbation at the ankle is in agreement with previous literature (Keshner et al., 1993; Nardone et al., 1995; Allum et al., 2002; Kawashima et al., 2004; Chung et al., 2005; Obata et al., 2010). Our main novel findings are a narrowing of the frequency bandwidth and a shift toward primarily low frequency responses with age, with reduced

gain at higher frequencies. Similarly, a compressed and narrower frequency bandwidth of the soleus response to vestibular error signals during standing has been observed (Dalton et al., 2014). Therefore, the change in ability to encode or process higher frequency information with age may occur across multiple sensory systems. The age-related changes in soleus response characteristics that we found could be related to changes in tissue mechanical properties, altered spindle morphology, reduced efficacy of central connections, or remodelling of motor units. A schematic of some of the changes described in the nervous system with age that likely contribute to altered soleus response characteristics is provided in Fig. 5-5.

Remodelling of motor units encompasses cycles of denervation of muscle fibres, often followed by reinnervation of orphaned fibres by surviving α-motoneurons (Lexell and Downham, 1991). This process leads to fibre type grouping (i.e., clustering of fibres of the same type), which could subsequently result in grouped fibre atrophy with the loss of that α-motoneuron and failed reinnervation (for review, see Hepple et al., 2016). However, previous research would suggest that changes in the motor units are likely not the primary contributor to the age-related changes in vibration responses that we observed in the soleus muscle. Firstly, loss of α-motoneurons does not occur until beyond the age of ~60 yrs (Tomlinson and Irving, 1977); this timing does not align with the changes in response characteristics that we observed between the young and middle aged adults. Secondly, muscles that tend to be chronically used, e.g., the diaphragm (Nguyen et al., 2019), trapezius (Kirk et al., 2019), and soleus (Dalton et al., 2008, 2009), seem to be

more protected against age-related changes. Specifically, the soleus muscle does not exhibit substantial changes in physiological cross-sectional area (Morse et al., 2005), the estimated number of motor units (Dalton et al., 2008), or motor unit firing rates (Dalton et al., 2009) with age. These previous findings would suggest that the changes observed in our study could be primarily driven by altered connections in the spinal cord, morphological changes in muscle spindles, and changes in tissue mechanics.

In the spinal cord, an increase in presynaptic inhibition or a decrease in the strength of Ia afferent connections with α-motoneurons could contribute to the decrease in the amplitude of the soleus vibration response we observed with age. Maximal H-reflex amplitude has been shown to progressively decline with age (Baudry, 2016). However, the thresholds of afferent and efferent axons to electrical stimuli become more homogenous with age (Scaglioni et al., 2003), which causes a larger M-wave and associated antidromic action potentials that could artificially contribute to a smaller H-reflex evoked by an electrical nerve stimulus. There is evidence that old adults have higher tonic levels of presynaptic inhibition of Ia afferents (Koceja and Mynark, 2000), and this higher level of presynaptic inhibition is accentuated during standing (Baudry et al., 2015). However, presynaptic inhibition has been shown to have a relatively weak ability to gate trains of afferent input (Rudomin and Schmidt, 1999), such as those associated with tendon stimuli (Burke et al., 1983). Therefore, altered strength of Ia afferent synaptic connections to α-motoneurons or changes in muscle spindles may play a larger role in the altered vibration responses observed in this study.

Previous research has described progressive changes in muscle spindle mechanoreceptors and their afferent innervation with age, which likely contributes to the changes in the frequency characteristics of the soleus response observed in our study. For example, there is a linear increase in the amount of collagen in muscle spindles with age in humans, which causes an increase in spindle capsular thickness (Swash and Fox, 1972). In the soleus muscle, the innervation of spindles by Ia afferents is also altered in middle aged and old rats relative to young rats (Kim et al., 2007; Vaughan et al., 2017). These changes in innervation include shortening, unravelling, and swelling of Ia afferent annulospiral endings, along with a decrease in the diameter and overall number of spindle afferents (Kim et al., 2007; Vaughan et al., 2017). Altogether, these changes likely contribute to the lower spindle dynamic index observed in old rats, which was primarily driven by a decrease in the peak afferent firing rate generated by muscle stretch (Kim et al., 2007). These authors suggested that there may be a preferential impairment of Ia relative to type II afferents with age, or alternatively a shift in behaviour such that type Ia afferents resemble the characteristics of type II afferents (i.e., a shift from more dynamic to static coding) (Kim et al., 2007). In humans, however, Nardone et al., (1995) suggested that type II afferents are more impaired with ageing, based on the assumption that the medium latency stretch response, which they found to be decreased with age, is mediated by type II afferents. The shift toward lower frequency responses we observed in old adults is in line with the reduced ability of Ia afferents to generate higher firing rates in response to muscle stretch (Kim et al., 2007), although we cannot confirm this directly from our study.

Changes in tissue mechanical properties with age may also influence the transmission of mechanical stimuli to muscle spindles. Some studies have shown tendon stiffness is lower in old adults (Stenroth et al., 2012) while others have shown no age-related differences (Karamanidis and Arampatzis, 2005). Results from a meta-analysis suggest Achilles tendon stiffness is lower in old adults, although this conclusion was based on a limited number of studies and the inconsistencies in results across studies was high (Delabastita et al., 2018). Lower tendon stiffness may reduce the transfer of strain to spindles within the muscle and contribute to poorer Ia afferent coding of perturbations and therefore lower muscle responses evoked by vibration.

We observed a weak positive correlation between age and AP COP frequency (MPF), which aligns with age-related changes in postural stability (Warnica et al., 2014; Vette et al., 2016). However, we did not observe any significant correlations between soleus response amplitude (P2P cross-covariance) and AP COP MPF or RMS. The lack of correlations between soleus responses and COP parameters may be due to many other factors – descending commands and other sensory feedback signals – that contribute to balance control. In addition, triceps surae muscle spindles may be more involved in sensing external perturbations and less involved in feedback control of quiet stance due to the poorer coding of small ankle oscillations during a background contraction (Peters et al., 2017) and the paradoxical behaviour of triceps surae muscles during standing sway (Loram et al., 2004).

In conclusion, our findings suggest there is a decline in the frequency bandwidth, gain, amplitude, and scaling of the soleus response to proprioceptive error signals during

standing. These altered responses reflect the age-related changes described previously in spindle morphology (Swallow, 1966; Swash and Fox, 1972; Liu et al., 2005; Vaughan et al., 2017) and stretch sensitivity in rats (Miwa et al., 1995; Kim et al., 2007). Proprioceptive feedback from the lower limbs plays a critical role in responses to perturbations in the AP direction (Bloem et al., 2002). The altered soleus responses to proprioceptive stimuli in old adults across a broad frequency bandwidth likely contributes to an impaired ability to respond to balance perturbations (Keshner et al., 1993; Allum et al., 2002; Lin and Woollacott, 2002) and an increased risk of falls.

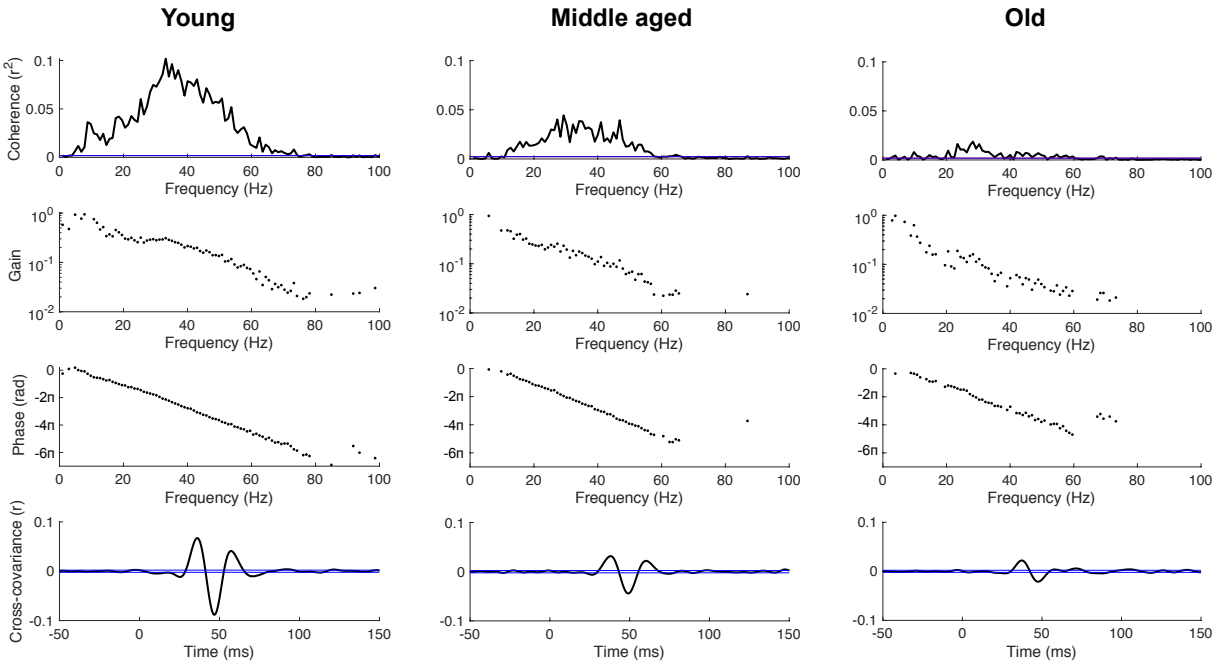

Figure 5-1 Pooled responses for the young, middle aged, and old adult groups

Coherence (r^2), gain ($mV/m/s^2$), phase (rad), and cross-covariance (r) between noisy Achilles tendon vibration and soleus muscle activity in a group of young (18-29 yrs; n = 14), middle aged (40-59 yrs; n = 11), and old (70-82 yrs; n = 14) adults. Thin blue lines represent 95% confidence intervals. Note the lower coherence, gain, and peak-to-peak cross-covariance in the middle aged and old adults relative to the young adults.

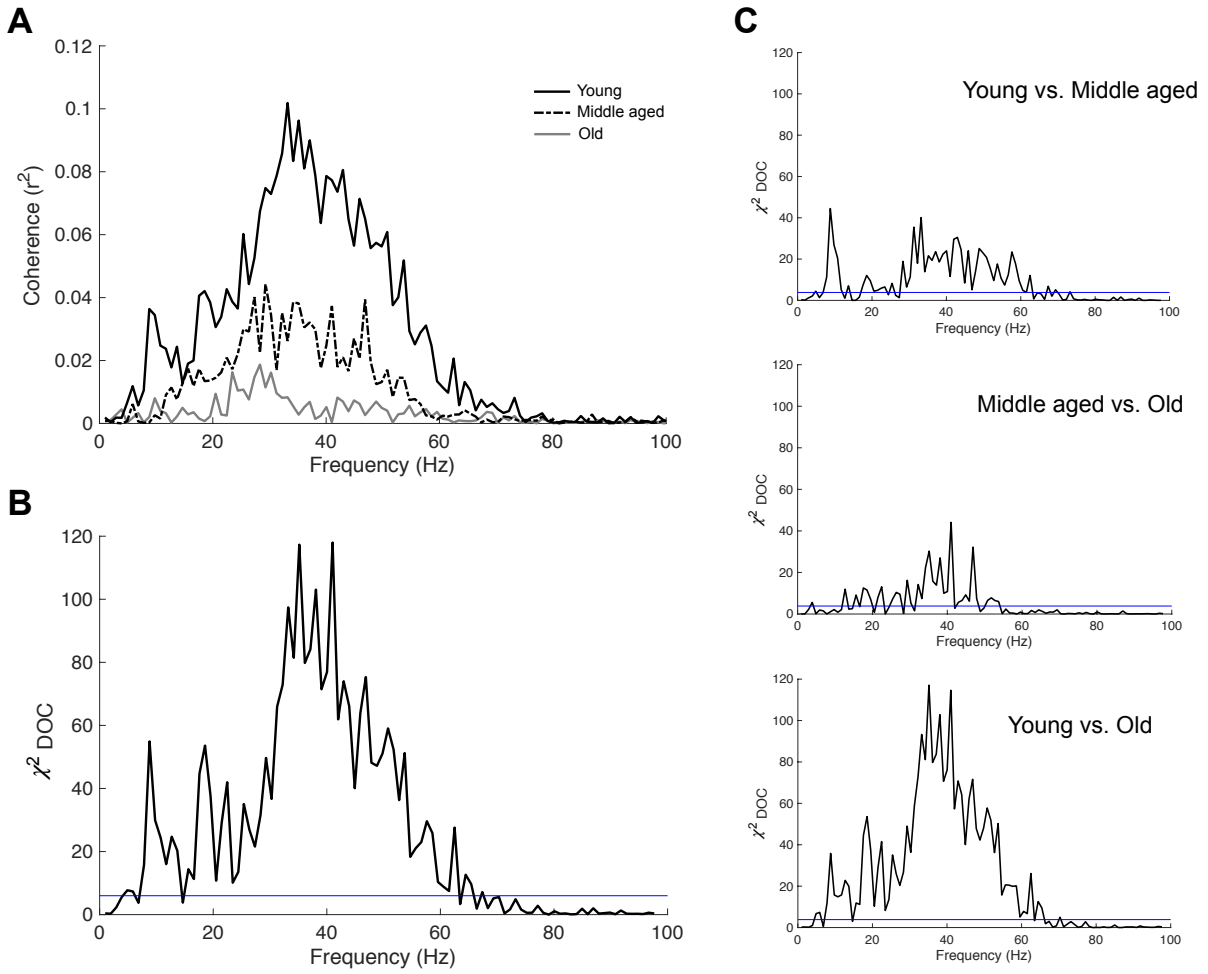

Figure 5-2 Difference in coherence between young, middle aged, and old adult groups

Coherence (r^2) across frequencies in the young, middle aged, and old adults (A), along with the difference of coherence among the three groups (B). Results of the pairwise difference of coherence tests between the young and middle aged adults, middle aged and old adults, and finally young and old adults (C). Values above the 95% confidence intervals (thin blue line) indicate a significant difference.

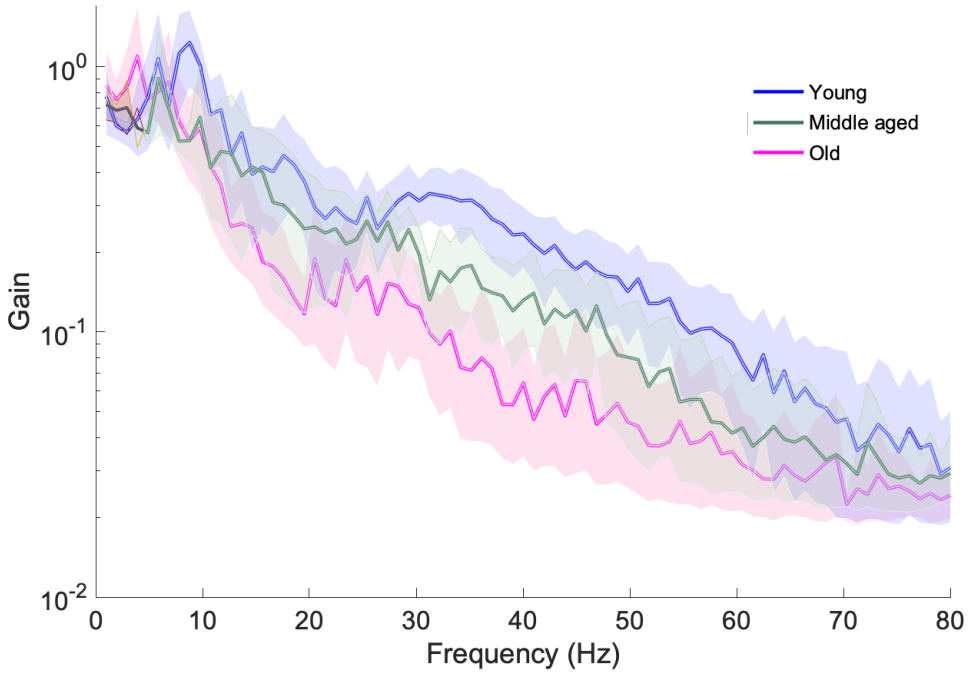

Figure 5-3 Comparison of gain between young, middle aged, and old adult groups

Gain (mV/m/s^2) of the soleus response to noisy Achilles tendon vibration in the young, middle aged, and old adult groups. Shaded areas represent 95% confidence intervals.

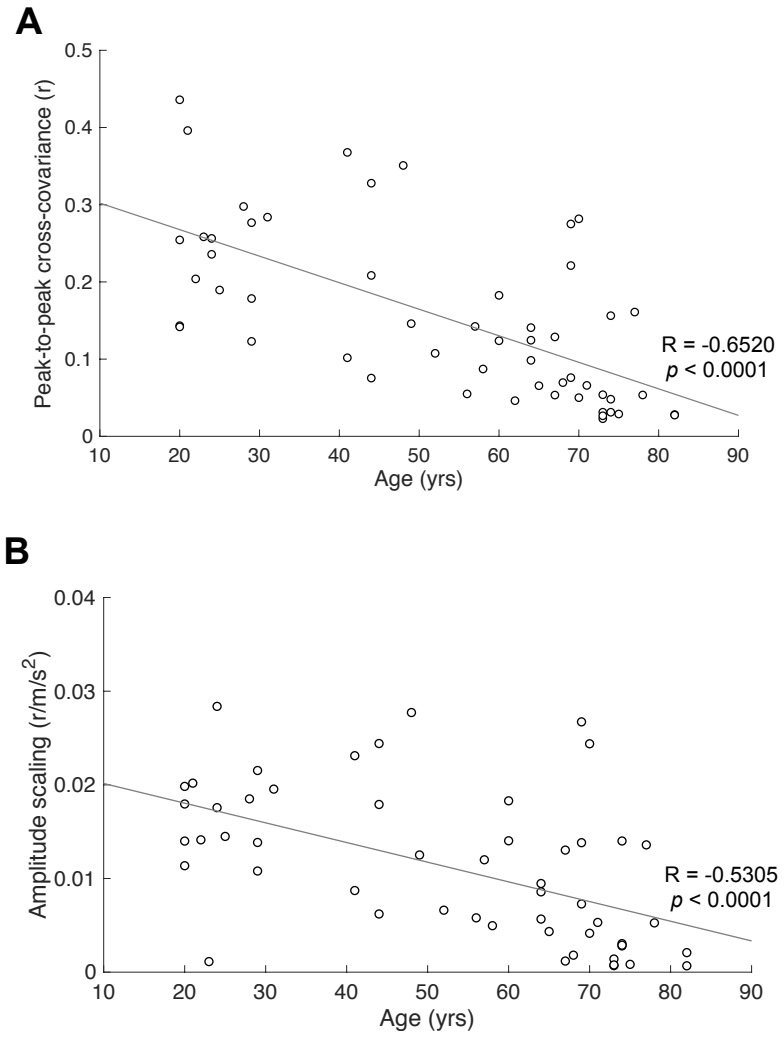

Figure 5-4 Correlations between age and response amplitude and scaling

Correlations (n = 54) between age and peak-to-peak (P2P) cross-covariance amplitude (A) and the scaling of the P2P cross-covariance with increases in vibration amplitude (B). Note both the P2P amplitude and scaling significantly declined with age.

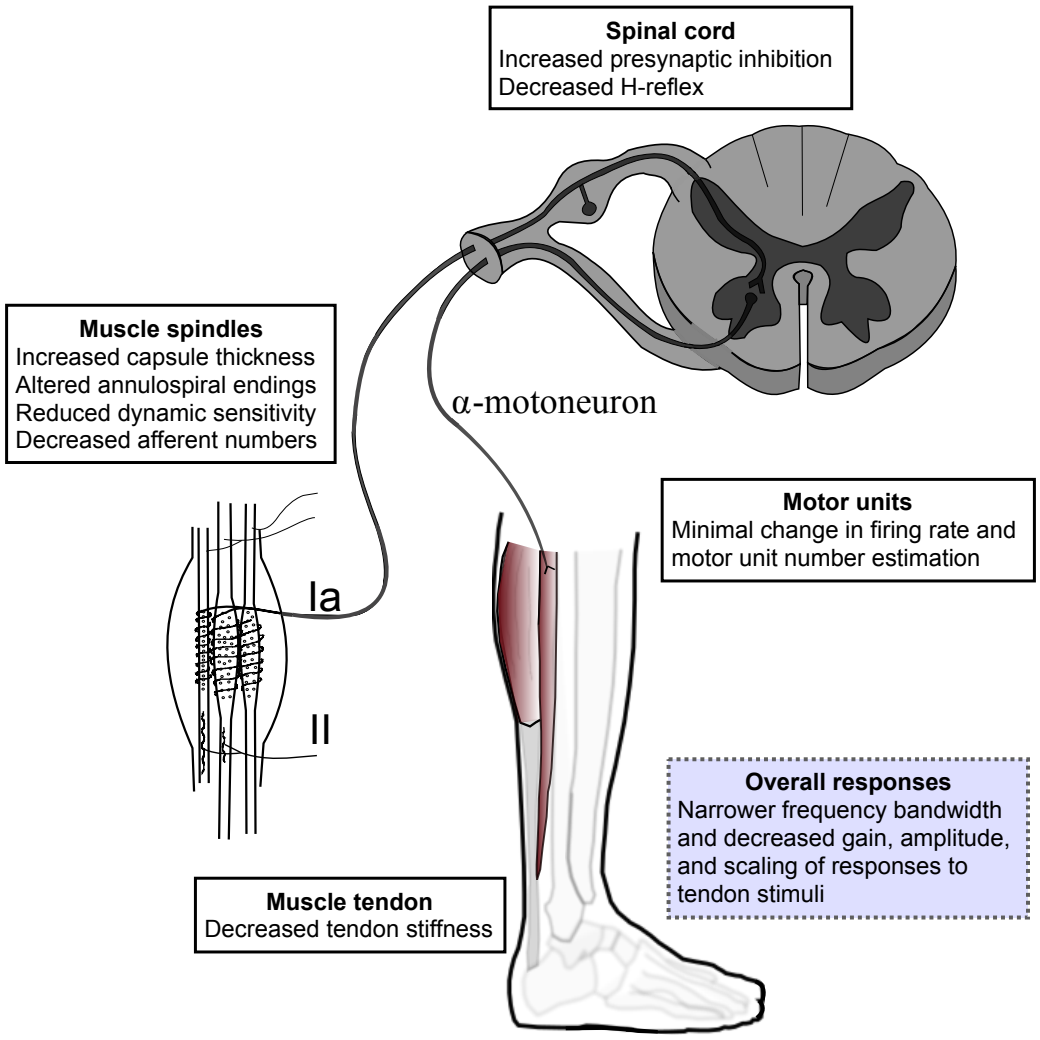

Figure 5-5 Summary diagram of age-related changes

Summary of age-related changes described in components of the stretch reflex pathway that likely lead to the overall difference in response characteristics that we observed in this study. Specifically, the findings of an age-related decrease in the bandwidth of significant coherence, gain, and cross-covariance amplitude and scaling with stimulus amplitude.

5.6 Bridging Summary

Data presented in Chapter 5 suggest there is an age-related narrowing of the bandwidth of vibration-EMG coherence, along with a decrease in gain, cross-covariance amplitude, and scaling with stimulus amplitude during standing. A stroke disrupts descending information from the brain to interneurons and motoneurons in the spinal cord, which causes impaired motor control and altered reflexes. The final chapter of this thesis examines how chronic stroke influences the characteristics of the soleus response to proprioceptive perturbations, along with postural control and tissue mechanical properties during standing.

Chapter 6: The influence of chronic stroke on the characteristics of the soleus muscle response to noisy Achilles tendon vibration during standing

6.1 Abstract

Damage to neural tissue caused by a stroke can influence information sent from the brain to the spinal cord. Altered responses to proprioceptive stimuli are often found on the affected side post-stroke; however, less is known about the characteristics of responses in muscles engaged in the control of posture and balance. We examined soleus responses to suprathreshold noisy (10-115 Hz) Achilles tendon vibration on the affected and less affected sides of chronic stroke participants, as well as both sides of healthy control participants. In addition, to examine changes in mechanical properties of the muscle-tendon unit, we examined mechanical admittance (the force-velocity relationship across frequencies) of the vibration against the tendon. Results showed a tendency for larger asymmetries between sides in the response amplitude (vibration-EMG peak-to-peak cross-covariance) in the chronic stroke group relative to the control group, and participants with poorer recovery (lower Fugl-Meyer scores) showed an asymmetry driven by larger responses on the affected side. The affected side had lower admittance across a bandwidth of ~20-90 Hz, and the peak admittance occurred at a higher frequency, relative to the less affected side and control group. Centre of pressure amplitude (root-mean-square) and frequency (mean power frequency) were lower under the affected limb, which suggests less reliance on the affected limb for balance control. These data suggest

changes in the frequency characteristics of both the soleus responses to proprioceptive perturbations and tissue mechanical properties may contribute to impaired balance and falls post-stroke.

6.2 Introduction

A cerebrovascular accident (stroke) compromises blood supply to part of the brain and can affect neural structures involved in sensorimotor control. Specifically, a stroke can influence the information sent from the brain to interneurons and motoneurons in the spinal cord, which can cause impaired motor control primarily on the side of the body opposite to the stroke location. The altered descending input to the spinal cord can influence both the voluntary control of muscles as well as the automatic responses evoked by sensory stimuli (e.g., muscle stretch responses). One motor symptom that often develops post-stroke is spasticity, which is commonly defined as a velocity dependent increase in tonic stretch responses, along with enhanced tendon tap responses (Lance, 1980). Altered stretch responses may result from a disruption of cortical input to the spinal cord and brainstem, leading to greater reliance on brainstem pathways (Jankelowitz and Colebatch, 2004; Li et al., 2014; Miller et al., 2014, 2016; Sohtaoğlu et al., 2016; Miller and Rymer, 2017).

In addition to the neural changes induced by a stroke, changes in tissue mechanical properties can also occur over time. In plantar flexor muscles, fascicles have been found to become shorter and stiffer on the affected side post-stroke (Gao et al., 2009; Zhao et al., 2015). In contrast, the Achilles tendon was found to become longer and more

compliant (lower Young's modulus) (Zhao et al., 2015). In the biceps brachii muscle, in addition to stiffening of the muscle-tendon unit, a change in the strain behaviour in response to tendon indentations was also observed across the proximal-distal axis (Chardon et al., 2020). The intrafusal fibres of muscle spindles lie in parallel with the extrafusal fibres that are responsible for muscle force production. Therefore, changes in the stiffness and strain behaviour across the tendon and muscle would influence how intrafusal fibres are stretched in response to mechanical perturbations. In line with this, the changes in mechanical properties induced by immobilization of the peroneus longus muscle at a shortened length were shown to alter the dynamic responses of muscle spindles to stretch in cats (Gioux and Petit, 1993). Therefore, it is important to consider the changes in mechanical properties alongside the changes in muscle responses evoked by proprioceptive stimuli.

In clinical assessments of spasticity, it is difficult to distinguish changes in muscle tone as a result of reflex mediated responses to stretch versus passive tissue mechanical properties. Furthermore, stretch and tendon tap responses are typically assessed in muscles at rest both clinically and experimentally, and response characteristics may differ when muscles are holding a background contraction or engaged in a sensorimotor task such as standing. For example, it was shown that stretch responses were not enhanced in plantar flexor muscles (Ada et al., 1998) and the biceps brachii (Burne et al., 2005) on the affected side post-stroke while holding a background contraction. Impaired modulation of lower limb muscle responses to balance perturbations has been observed on the affected side post-stroke (Marigold et al., 2004), and stroke survivors have a high risk of falls

(Maeda et al., 2009; Mansfield et al., 2018). Spasticity in the lower limb was found to be associated with increased falls in individuals with chronic stroke (Soyuer and Ozturk, 2007). Therefore, it is of interest to examine the characteristics of muscle responses to proprioceptive perturbations post-stroke while the neuromuscular system is engaged in the control of balance.

Short latency muscle stretch responses are primarily mediated by muscle spindle primary afferents that are sensitive to the velocity of stretch. Muscle spindles can respond to stimuli across a range of frequencies (up to 100 Hz; Fallon and Macefield, 2007), and a broad range of frequencies are generated by normal activities such as postural sway, external perturbations, and walking. It is unknown how a stroke influences the frequency characteristics of both the mechanical properties of the tissue and stretch responses. Noisy (containing a 10-115 Hz frequency bandwidth) Achilles tendon vibration has been used in healthy adults to examine the frequency characteristics of triceps surae muscle responses during standing (Mildren et al., 2017, 2019). Importantly, this methodological approach was shown to have a minimal influence on standing balance and provide consistent response measures with short trial durations (<60 s) (Mildren et al., 2017). Therefore, this noisy tendon vibration stimulus is an ideal way to probe response characteristics in clinical populations including stroke survivors. The first aim of this study was to examine the characteristics of the soleus responses to proprioceptive perturbations induced by noisy tendon vibration during standing. In this study, we delivered a continuous noisy (10-115 Hz) vibration to the Achilles tendon and analyzed electromyography (EMG) responses using a linear correlation analysis. Due to the enhanced responses to transient

stretches and tendon taps that are commonly observed post-stroke, we hypothesized vibration-EMG coherence and gain would be stronger on the affected side of the stroke group relative to both the less affected side and controls. In addition, we hypothesized there would be larger asymmetries in the amplitude of the soleus response (vibration-EMG cross-covariance) between sides in the stroke relative to control group.

The second aim of this study was to examine how chronic stroke influences the mechanical properties of the muscle-tendon unit across frequencies by examining the relationship between the velocity and force of the vibration stimulus applied to the Achilles tendon (mechanical admittance). We hypothesized mechanical admittance would be lower on the affected side to reflect less probe motion relative to the force applied (i.e., the tissue would provide higher impedance). We also hypothesized the frequency that contains the peak admittance would be higher on the affected side since resonant frequency increases with stiffness.

6.3 Methods

6.3.1 Participants

Eight adults (6 male, 2 female) ages 48-66 yrs (mean 59.5 yrs) who suffered a single cerebrovascular accident that predominantly affected one side of the body (hemiparesis) participated in the study. Eight (4 male, 4 female) healthy controls age-matched within two yrs of each participant in the stroke group (ages 48-66, mean 59.6 yrs) who self-reported they were free of neurological and musculoskeletal disorders also participated. Participants in the stroke group self-reported they were free of any other

neurological or musculoskeletal disorders. All participants were able to stand unassisted for 2 min periods and follow instructions. In the stroke group, ankle tone was evaluated using the Modified Ashworth Scale (MAS), and lower limb motor recovery was evaluated using the Fugl-Meyer Assessment (FMA) of the lower extremity (maximum score = 34) and Chedoke-McMaster Stroke Assessment (CMSA) stage of recovery of the foot and ankle (maximum score = 7). Clinical assessments were performed either before or after the experimental procedures. All participants provided written informed consent and all procedures were approved by the University of British Columbia Research Ethics Board.

6.3.2 Experimental procedures

Participants stood with each foot on a separate force plate (Bertec, USA; type 4060-08) and their vision directed onto a target ~3 m ahead at approximately eye-level. To examine postural control during standing, participants first performed one 2-min quiet standing trial. Moments and forces from both force plates were amplified (×2-10; type AM6-4; Bertec, USA) and sampled at 100 Hz (Power 1401 A/D board and Spike2 software; Cambridge Electronic Design, UK). Next, to examine response characteristics in the soleus muscle to proprioceptive stimuli, we applied six 2-min trials of noisy (10-115 Hz) Achilles tendon vibration at three different stimulus amplitudes (acceleration root-mean-square amplitude = 10, 15, and 20 m/s^2) unilaterally. The three different amplitudes were applied in randomized order, and all three trials were applied to one side and then the other. The order of sides was randomized between participants. Since individuals with chronic stroke tend to stand asymmetrically with more weight on the less affected limb (Marigold et al., 2004; Singer et al., 2013), we monitored vertical ground

reaction forces and coached participants to stand with their weight evenly distributed between both legs throughout the trials with Achilles tendon stimuli.

The vibration was applied to the Achilles tendon through a 3 cm diameter probe controlled by a linear motor (model MT-160; Labworks, USA). The vibration signal was white noise low-pass filtered at 100 Hz; this stimulus signal was generated in LabVIEW 11 software (National Instruments, USA) and sent from a real-time computer (PXI-8106, National Instruments, USA) to a multifunctional data acquisition card (PXI-6225, National Instruments, USA) to the motor amplifier (PA-141; Labworks, USA).

The motor probe was pushed into the Achilles tendon with a pre-load force of ~1 N (measured with a force transducer; model 31, Honeywell, USA). The force signal was differentially amplified ×100, low-pass analogue filtered at 600 Hz; Brownlee model 440; NeuroPhase LLC, USA), and digitized at 2000 Hz. Vibration acceleration signals were recorded using an accelerometer (model 220-010; X Tronics, CA); accelerations signals were differentially amplified ×1, low-pass analogue filtered at 600 Hz (Brownlee model 440; NeuroPhase LLC, USA), and digitized at 2000 Hz.

Surface EMG was recorded bilaterally from the soleus muscles using a bipolar surface electrode configuration positioned over the muscle bellies ~2 cm apart with the ground placed on the right lateral malleolus. EMG signals were bandpass analog filtered 10-1000 Hz (NeuroLog NL824 preamplifier and NL820 Isolator; Digitimer, UK) and sampled at 2000 Hz.

6.3.3 Data analyses

Forces and moments from each force plate were low-pass filtered at 10 Hz (4th order dual pass Butterworth filter) and centre of pressure (COP) positions in the anteroposterior (AP) direction were calculated and de-biased. To examine AP postural adjustments, we extracted measures of AP COP amplitude (root-mean-sqaure; RMS) and frequency (mean power frequency; MPF) (frequency resolution = 0.0244 Hz) for each force plate. To examine how postural control differed between the affected and less affected sides of the stroke group (as well as between the right and left sides of the control group), we compared AP RMS and MPF between sides using paired *t*-tests.

To examine differences in soleus response characteristics between the affected and less affected sides of the stroke group and either side of control group, we estimated coherence, gain, phase and cross-covariance between the acceleration of the vibration stimulus and soleus surface EMG. Acceleration and surface EMG signals were first de-biased and digitally low-pass filtered at 600 Hz with a 4th order dual pass Butterworth filter, and soleus EMG was full-wave rectified. A frequency resolution of 0.9765 Hz (1.024 s/segment, 117 disjoint segments per trial) was used for analyses of individual trials for each participant as well as for data concatenated across participants for the affected side, less affected side, right side of controls, and left side of controls during the trial with the largest stimulus amplitude (RMS = 20 m/s^2). Individual participant data were used to examine scaling of response amplitude (cross-covariance) with stimulus amplitude, and the asymmetry in response amplitude between the right and left sides. Pooled data were used to examine group differences in coherence, gain, and phase.

Coherence was calculated as the magnitude of the cross-spectrum of the acceleration and EMG signals squared divided by the product of the auto spectra of those signals. Coherence describes the linear relationship between the proprioceptive stimulus and muscle activity across frequencies. Gain was calculated as the cross-spectrum divided by the auto spectrum of the acceleration signal; thus, gain reflects the amplitude of the response relative to the stimulus. Phase was estimated from the angle of the cross-spectrum to reflect the delay between the stimulus and response. Finally, to examine the response in the time domain, cross-covariance was calculated from the inverse Fourier transform of the cross-spectrum normalized by the product of the vector norms of the acceleration and EMG signals (Dakin et al., 2010). We used the convention that acceleration into the tendon and increased rectified EMG were positive; therefore, a positive cross-covariance would reflect acceleration into the tendon is associated with increased muscle activity or acceleration away from the tendon is associated with decreased activity.

For both individual and group data, to determine where responses were significant, we constructed 95% confidence intervals (CIs) based on the number of segments for coherence values (positive threshold) and cross-covariance (positive and negative thresholds) (Halliday et al., 1995). Next, phase and gain data were extracted at frequencies that contained significant coherence values for both individual and pooled data. For each side of the control and stroke group, we constructed 95% CIs around gain estimates by resampling (with replacement) the eight participants in each group 10000 times and calculating gain values across frequencies (with gain values only included at

frequencies with significant coherence). To obtain phase slopes for each group, we resampled the eight participants in each group (with replacement) and calculated phase-frequency slopes using linear regression 10000 times. Phase values were only used in the slope calculations if they were 1) obtained at frequencies with significant coherence, and 2) were within a bandwidth that contained a minimum of 8 of 10 adjacent points with significant coherence. Third, if the fit of the linear regression was <0.95, the slope value was not included. The mean and standard deviation (SD) of the time delay was obtained from the phase slopes.

From individual participant data, we extracted the peak-to-peak (P2P) cross-covariance amplitude for each stimulus amplitude and side. At the largest stimulus amplitude (RMS = 20 m/s^2), we examined the response asymmetry index between the affected and less affected sides of the stroke participants as well as between the right and left sides of control participants using the equation:

$$[(\text{affected side} - \text{less affected side}) \div (\text{affected} + \text{less affected side})] \times 100$$

(Miller et al., 2014), where the affected and less affected sides were respectively the right and left sides for control participants. Therefore, positive asymmetry values would indicate larger responses on the affected side of stroke participants, or larger responses on the right side of control participants. We compared asymmetry index, as well as the absolute value of the asymmetry index, between stroke and control groups using independent samples *t*-tests. In addition, we calculated the scaling of the response with increases in stimulus amplitude (the average slope of the peak-to-peak cross-covariance across stimulus amplitudes) for both sides of the stroke and control participants. Scaling

was compared between sides for the stroke and control groups using paired samples *t*-tests, as well as between the affected side of the stroke group and control group (averaged across sides) using an independent samples *t*-test.

To examine differences in mechanical properties of the muscle-tendon unit, we looked at the relationship between the probe velocity and force against the tendon across frequencies (mechanical admittance). To calculate mechanical admittance, the probe acceleration signal was high-pass filtered at 1 Hz to minimize low frequency drift (4th order dual pass Butterworth filter) and then integrated to obtain velocity. Mechanical admittance was then calculated as the gain (force-velocity cross-spectrum divided by the auto spectrum of the velocity signal) of the force-velocity relationship across frequencies using a resolution of 1.95 Hz. Lower admittance indicates the tissue provides greater impedance to probe motion at that frequency. Plots of admittance across frequencies were used to identify the frequency that contained the peak admittance value, since a peak in admittance indicates a higher velocity of motion achieved by a given (or lesser) force applied to the tendon and can indicate a resonant frequency. A higher resonant frequency would indicate an increase in stiffness of the muscle-tendon unit.

Admittance was calculated for each participant during the highest vibration stimulus amplitude trial (RMS = 20 m/s^2) on both sides, and the frequency that contained the peak admittance was extracted. The frequency with the peak admittance value was compared between sides for the stroke and control groups using paired samples *t*-tests, as well as between the affected side of the stroke group and the control group (averaged across sides) using an independent samples *t*-test. To illustrate group results, we then

averaged admittance values across participants on the affected side, less affected side, left side of controls, and right side of controls. To help interpret whether changes may be due to differences in the resulting force or velocity of the probe, the RMS force and RMS velocity (de-biased) of the probe against the tendon were calculated and compared between the affected and less affected sides using paired samples *t*-tests (α set at 0.05).

6.4 Results

Five participants in the stroke group had a MAS of 1+ (slight increase in tone), two had a score of 0 (no increase in tone) and one had a score of 2 (more marked increase in tone). FMA scores ranged from 24-30 (out of 34, with higher scores indicating greater motor recovery), and CMSA scores ranged from 2-6 (out of 7, with higher scores indicating greater motor recovery). Five participants suffered an ischemic stroke and three suffered a hemorrhagic stroke, their strokes occurred between 3 and 19 years prior to the study. Demographic and stroke characteristic information is provided in Table 1.

To evaluate postural control, we examined AP COP movement under each leg during quiet standing. AP COP RMS amplitude was lower on the affected side (2.67 ± 1.05 mm) relative to the less affected side (6.15 ± 2.24 mm) ($p = 0.001$) of the stroke group; while RMS amplitude did not differ between the right and left sides of the control group (right: 3.95 ± 2.85 mm; left: 3.13 ± 1.24 mm) ($p = 0.466$). Similarly, AP COP MPF was lower on the affected side (0.038 ± 0.048 Hz) relative to the less affected side (0.214 ± 0.086 Hz) ($p < 0.001$) of the stroke group; while MPF was similar on the right and left sides of the control group (right: 0.147 ± 0.049 Hz; left: 0.109 ± 0.068 Hz) ($p = 0.233$).

The lower COP amplitude and frequency on the affected side of the stroke group indicates they primarily relied upon ground reaction forces generated by the less affected side to make postural adjustments. Representative COP traces from one participant are demonstrated in Fig. 6-1C.

We examined soleus responses to suprathreshold noisy (10-115 Hz) Achilles tendon vibration during standing to determine differences in response characteristics between the affected and less affected sides and either side of control participants. Results for one participant in the stroke group (participant 6) are shown in Fig. 6-1A; this participant demonstrated stronger coherence, higher gain, and a larger peak-to-peak cross-covariance on the affected side relative to the less affected side. In addition, we calculated mechanical admittance to examine changes in tissue properties that might influence the transmission of stimuli to muscle spindles. This participant also demonstrated a different pattern of admittance across frequencies on the affected relative to the less affected side; the less affected side showed a peak admittance located at a frequency of ~80 Hz, while the affected side showed a blunted increase in admittance from ~50-100 Hz with the peak admittance located at ~98 Hz (Fig. 6-1B). These findings suggest there are mechanical changes in the tissue along with differences in soleus response characteristics on the affected side in this participant. A similar pattern of admittance and soleus response asymmetry was observed in participants 2, 3, and 5; all of these participants had relatively lower scores on the FMA (poorer motor recovery) (Table 1). Participant 8 showed a similar altered pattern of admittance on the affected side; however, he demonstrated a soleus response asymmetry in the opposite direction (larger response on the less affected

side). This participant had the highest ankle tone in the group (MAS = 2). The remaining participants (participants 1, 4, and 7) showed minimal changes in admittance patterns and either a neutral or negative response asymmetry (larger response on the less affected side); these participants tended to have higher scores on the FMA (greater motor recovery).

Data pooled within groups demonstrated that coherence was similar on the left and right sides of the control group. Coherence tended to be higher on the affected side in the ~20-40 Hz bandwidth relative to the less affected side of the stroke group, but coherence on the affected side was similar to both sides of the control group (Fig. 6-2). There were minimal differences in gain across groups, although gain tended to be higher on the less affected side at low frequencies (<10 Hz) but higher on the affected side at higher frequencies (~20-40 Hz) (Fig. 6-3). The phase slope equated to a time delay that was 36.9 ± 7.6 ms on the affected side, 44.2 ± 7.1 ms on the less affected side, and respectively 46.1 ± 4.7 ms and 43.8 ± 7.9 ms on the right and left sides of the control group.

The scaling of the response (P2P cross-covariance) with stimulus amplitude was not significantly different between the affected (0.00516 ± 0.00712 r/m/s^2) and the less affected side (0.00344 ± 0.00354 r/m/s^2) of the stroke group ($p = 0.600$), or between the right and left sides of the control group (0.00529 ± 0.00579 r/m/s^2 and 0.00464 ± 0.00597 r/m/s^2 respectively; $p = 0.813$). There was also no significant difference between the affected side of the stroke group and the control group (averaged across the right and left side) ($p = 0.949$).

An asymmetry index was calculated to represent differences in response amplitude (P2P cross-covariance) between sides. The asymmetry as well as the absolute value of the

asymmetry tended to be higher in the stroke group (Fig. 6-4); however, these differences were not significant (*p-values* = 0.788 and 0.207, respectively). The average asymmetry index for the stroke group was 12.3 ± 51.4 (positive values indicate larger responses on the affected side). The average asymmetry index for the control group was 6.4 ± 33.1 (positive values indicate larger responses on the right side). The absolute value of the asymmetry was on average 26.2 ± 18.9 in the control group and 42.1 ± 28.2 in the stroke group.

Tendon admittance tended to increase with frequency to a peak at ~80 Hz and then decrease (Fig. 6-5). Overall, admittance was lower on the affected side of the stroke group across a bandwidth of ~20-90 Hz relative to the less affected side and either side of the control group. In addition, the frequency that contained the highest admittance value on average trended toward being higher on the affected side (89 ± 8 Hz) relative to the less affected side (79 ± 11 Hz) ($p = 0.056$). In the control group, there was no significant difference in the frequency that contained the highest admittance between the right and left sides (right: 80 ± 7 Hz, left: 83 ± 4 Hz; $p = 0.404$). The frequency with the highest admittance on the affected side of the stroke group was significantly higher than the control group (averaged across the right and left sides) ($p = 0.033$). The average RMS force of the probe against the tendon was higher on the affected side (0.15 ± 0.03 N) relative to the less affected side (0.12 ± 0.02 N) ($p = 0.023$), while the average RMS velocity was not significantly different between sides (affected: 0.032 ± 0.004 m/s, less affected: 0.033 ± 0.004 m/s; $p = 0.123$).

6.5 Discussion

This study examined soleus responses to noisy Achilles tendon vibration in individuals with chronic stroke during standing, along with mechanical admittance of the muscle-tendon unit. Our results showed a tendency for greater response asymmetries between sides in the stroke group relative to the control group, with larger amplitude responses on the affected side in participants with poorer motor recovery. The response time delays obtained from the slope of the phase estimate suggested an earlier response on the affected side relative to the less affected side and either side of the control group. Our data also showed the pattern of mechanical admittance across frequencies differed on the affected side, with lower admittance across a bandwidth of ~20-90 Hz and a higher frequency with peak admittance relative to the less affected side and either side of the control group. A schematic is provided in Fig. 6-6 to illustrate the stages along the pathway from tendon stimuli to the muscle response that can be influenced by chronic stroke.

Our finding of a shorter response time delay on the affected side is in agreement with previous literature that found shorter response latencies evoked by tendon taps in biceps brachii single motor units (Hu et al., 2015) and surface EMG (Afzal et al., 2019). Similarly, in the soleus muscle, shorter latency and larger amplitude H-reflex and stretch responses have been observed in stroke survivors (Levin and Hui-Chan, 1993; Bakheit et al., 2003). Shorter latency responses to proprioceptive perturbations could be due to motoneuron hyperexcitability as a result of altered descending drive to the spinal cord (Hu et al., 2015; Afzal et al., 2019; Son et al., 2019). Changes in Ia excitatory post-synaptic

potentials (EPSPs) may also contribute to enhanced responses to proprioceptive stimuli, such as a shorter EPSP rise time (Suresh et al., 2005) and prolonged EPSP time course (Son et al., 2019). Presynaptic inhibition was also shown to be reduced in stroke survivors with spasticity, which would release some gating of Ia input to motoneurons and enhance responses to proprioceptive stimuli (Lamy et al., 2009). The amount of post-activation depression was also found to be reduced, and this change was strongly correlated with the severity of spasticity (Yang et al., 2015). A more depolarized motoneuron resting membrane potential from altered descending drive from the brainstem (Miller et al., 2014; Li et al., 2015) may also contribute to altered proprioceptive evoked responses in chronic stroke survivors.

Our results showed an altered pattern of admittance on the affected side, with lower admittance ~20-90 Hz and a higher frequency with peak admittance. In plantar flexor muscles, the properties of the muscle and tendon have been shown to change in opposite directions post-stroke; the muscle was found to become shorter and stiffer (Gao et al., 2009; Zhao et al., 2015), whereas the Achilles tendon was found to become longer and more compliant (Zhao et al., 2015). The aggregate changes in the muscle-tendon unit of the biceps brachii following a stroke have been shown to result in increased stiffness, as well as altered strain behaviour such that the strain becomes more homogenous across the proximal-distal axis (Chardon et al., 2020). Our findings of lower mechanical admittance and higher RMS force of the probe against the tendon suggest higher stimulus forces were applied for a similar velocity at frequencies beyond ~20 Hz. In addition, we found the frequency with the peak admittance was higher on the affected side (~90 Hz)

relative to the less affected side and either side of the control group (~80 Hz). Peaks in admittance can indicate where there is mechanical resonance, and the resonant frequency increases with spring stiffness. Thus, the higher frequency with peak admittance on the affected side is in agreement with findings of a stiffer muscle-tendon unit (Gao et al., 2009; Zhao et al., 2015).

Changes in tissue mechanical properties can influence the transmission of stimuli to the intrafusal fibres of muscle spindles, and the force-velocity relationship of stimuli is important to examine because Ia spindle afferents, which mediate tendon tap responses, are sensitive to stretch velocity. The increase in stiffness induced by immobilization in cats was shown to increase spindle static and dynamic responses to stretch (Gioux and Petit, 1993), possibly as a result of more uniform strain across the muscle and therefore more transmission of length and velocity stimuli through intrafusal fibres (Chardon et al., 2020). However, while the increase in muscle stiffness post-stroke may enhance the transmission of stimuli through the muscle, the more compliant Achilles tendon may offset this in the human triceps surae muscles (Zhao et al., 2015). Further experiments using muscle imaging or direct afferent recordings would be required to understand how the changes in tissue mechanical properties influence the stretch of the muscle and activation of spindle afferents in response to perturbations post-stroke.

In this study, we contrasted responses between both the affected and less affected sides of the chronic stroke group as well as both sides of the healthy control group. This is important because the less affected side may not serve as an appropriate control since alterations in descending pathways likely influence both sides to a degree. For example,

the reticulospinal tract is known to project bilaterally to the spinal cord to coordinate activity of both ipsilateral and contralateral motoneurons (Jankowska, 2003; Schepens and Drew, 2006; Davidson and Buford, 2006; Sakai et al., 2009). In addition, both the reticulospinal and vestibulospinal tracts have been shown to provide input to commissural interneurons (inhibitory and excitatory) that influence motoneurons on the contralateral side (Krutki et al., 2003). Therefore, the altered connections between the cortex, brainstem, and spinal cord that are thought to contribute to spasticity on the affected side would likely influence the contralateral side to an extent as well. Evidence has been provided of enhanced motoneuron excitability on the less affected side of stroke survivors relative to healthy controls (Afzal et al., 2019). Our results showed the time delay was similar on the less affected side compared to controls, although gain at low frequencies tended to be higher on the less affected side, which suggests there might be some changes in proprioceptive response characteristics on the less affected side.

We observed changes in the control of balance through ground reaction forces on the affected versus the less affected side of the stroke group. COP RMS amplitude and MPF in the AP direction were both lower on the affected side, which suggests chronic stroke survivors primarily relied upon postural adjustments made by the less affected side. Pollock et al. (2019) previously showed muscle activity on the less affected side post-stroke was more strongly correlated with COP movement relative to the affected side during standing; this also suggests the less affected limb is more involved in the control of postural adjustments. In addition, the introduction of greater challenges to standing balance resulted in less of an asymmetry in COP between sides (Pollock et al., 2019),

which indicates challenging balance may be one way to encourage the use of the affected side to contribute to balance control.

Using a single force plate, previous research has shown higher COP velocity and path length in the AP direction in chronic stroke survivors (Margold et al., 2006; Sawacha et al., 2013). These changes in single force plate COP measures observed previously are likely driven by the high amplitude and frequency adjustments made by the less affected side to compensate for limited contribution from the affected side. Similar to our findings, in patients with acute stroke, a larger RMS amplitude on the less affected side was found (Mansfield and Inness, 2015).

In conclusion, our results indicate there are mechanical changes in the muscle-tendon unit on the affected side post-stroke (lower admittance and a higher resonant frequency) that would influence the transmission of proprioceptive stimuli to muscle spindles during standing. On the affected side, we also found changes in ground reaction forces (lower amplitude and frequency adjustments) during standing. Participants in the stroke group with relatively poorer motor recovery showed an asymmetry in the amplitude of the soleus response to tendon vibration between sides with a larger response on the affected side. Due to the low sample size of stroke participants, further research is needed to clarify how differences in the muscle response characteristics to proprioceptive stimuli relate to motor impairment, as well as how changes in tissue mechanical properties influence spindle encoding of proprioceptive perturbations.

Table 1: Profile of participants in the chronic stroke group.

Participant #	Age	Gender	Yrs post-stroke	MAS	FMA	CMSA	Stroke side	Type of stroke
1	62	M	3	1+	28	3	R	Ischemic
2	52	M	15	1+	24	2	R	Hemorrhagic
3	59	M	4	0	26	3	R	Ischemic
4	66	M	5	1+	29	6	R	Hemorrhagic
5	65	M	13	1+	25	3	R	Hemorrhagic
6	62	F	19	1+	25	4	L	Ischemic
7	48	F	5	0	30	4	R	Ischemic
8	63	M	4	2	29	3	R	Ischemic

Note: *MAS: Modified Ashworth Scale at the ankle; FMA: Fugl-Meyer Assessment of the lower extremity; CMSA: Chedoke-McMaster Stroke Assessment for the foot and ankle*

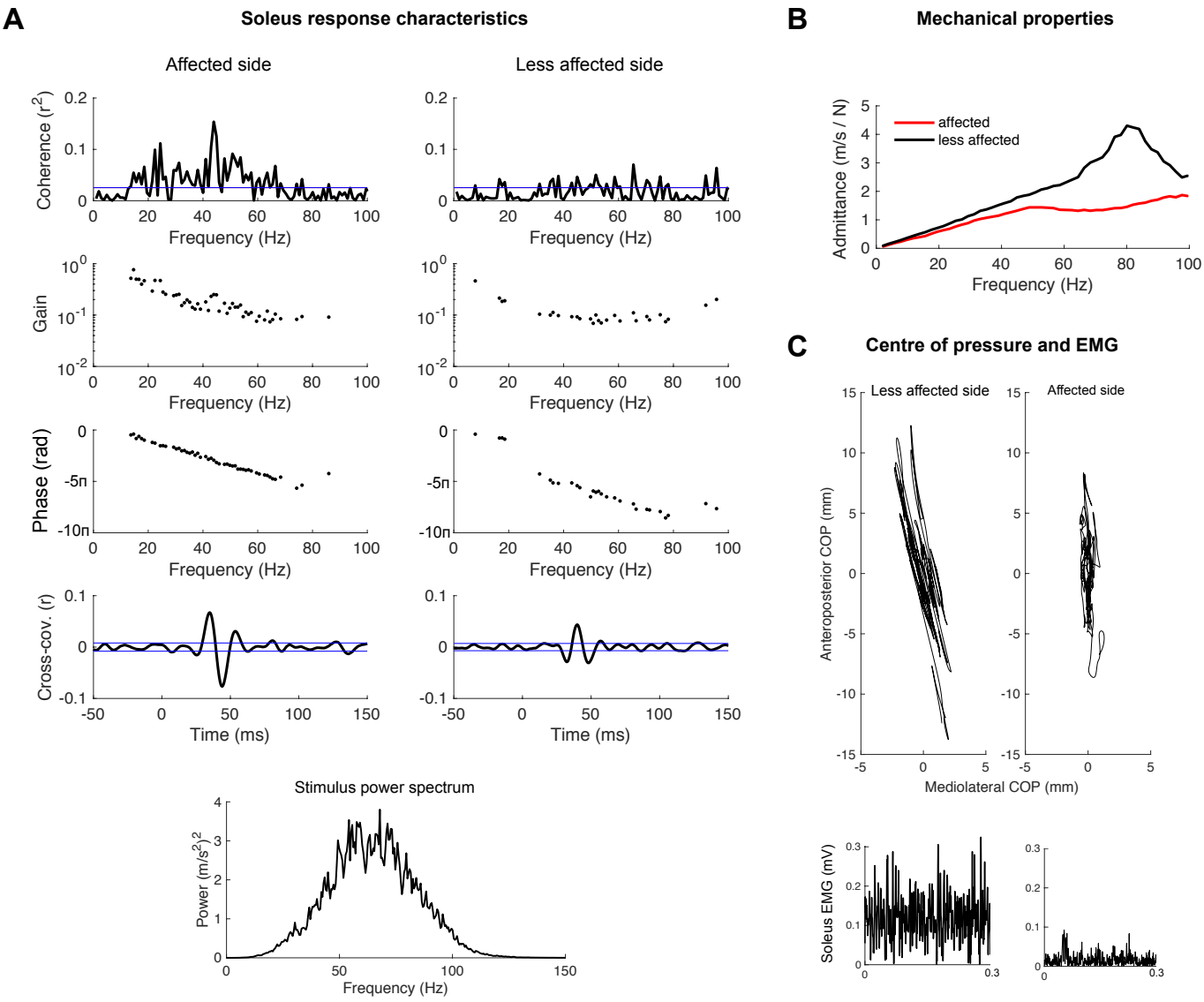

Figure 6-1 Representative stroke participant data

Representative data for one participant (participant 6) with chronic stroke demonstrating coherence (r^2), gain ($mV/m/s^2$), phase (rad), and cross-covariance (r) on the affected and less affected side, along with the power spectrum of the tendon vibration (A), mechanical admittance of the muscle-tendon unit (B), and centre of pressure movement under each leg along with soleus EMG (C). Thin blue lines represent 95% confidence intervals.

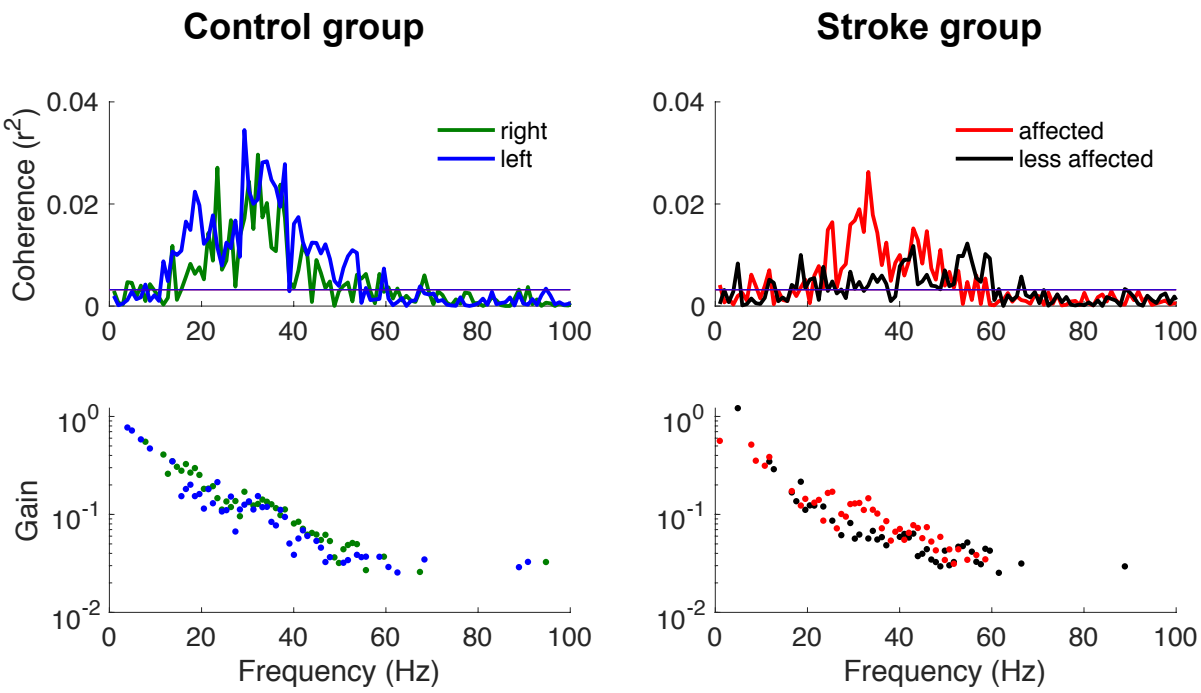

Figure 6-2 Coherence and gain for the control and stroke groups

Coherence (r^2) and gain ($mV/m/s^2$) overlaid for the left and right sides of the control group (n = 8) and the affected and less affected sides of the stroke group (n = 8). Thin blue lines represent 95% confidence intervals.

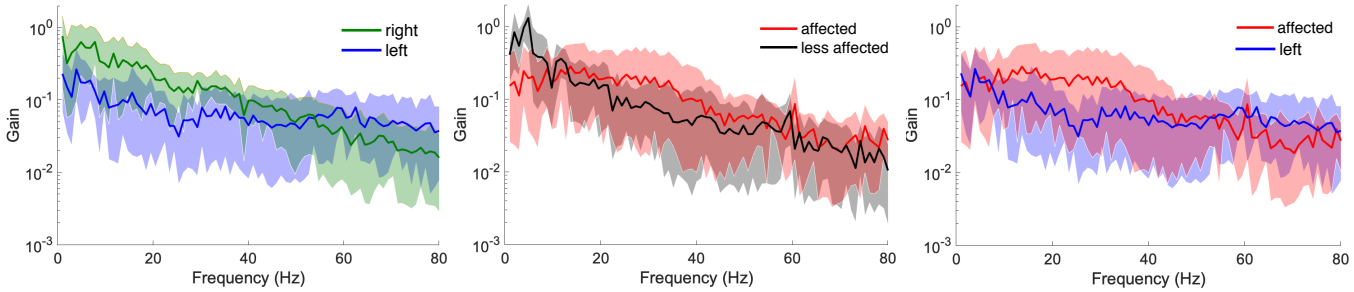

Figure 6-3 Comparison of gain in the stroke and control groups

Comparison of gain (mV/m/s^2) between the right and left sides of the control group (n = 8), affected and less affected sides of the stroke group (n = 8), and affected side of the stroke group and left side of the control group. The left side was chosen for comparison since this was the affected side in 7/8 participants in the chronic stroke group. Shaded areas represent 95% confidence intervals.

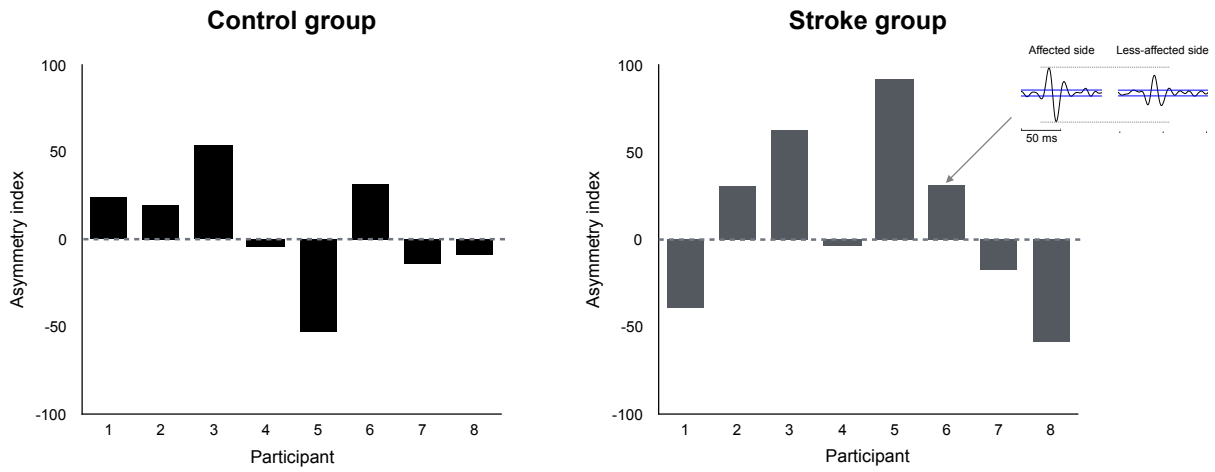

Figure 6-4 Asymmetry in responses for participants in the control and stroke groups

Asymmetry between soleus responses (peak-to-peak cross-covariance; r) measured on the right and left sides for participants in the control group, and affected and less affected sides of participants in the stroke group. Note: positive values indicate larger responses on the right side of participants in the control group, and on the affected side of participants in the stroke group (demonstrated in the inset).

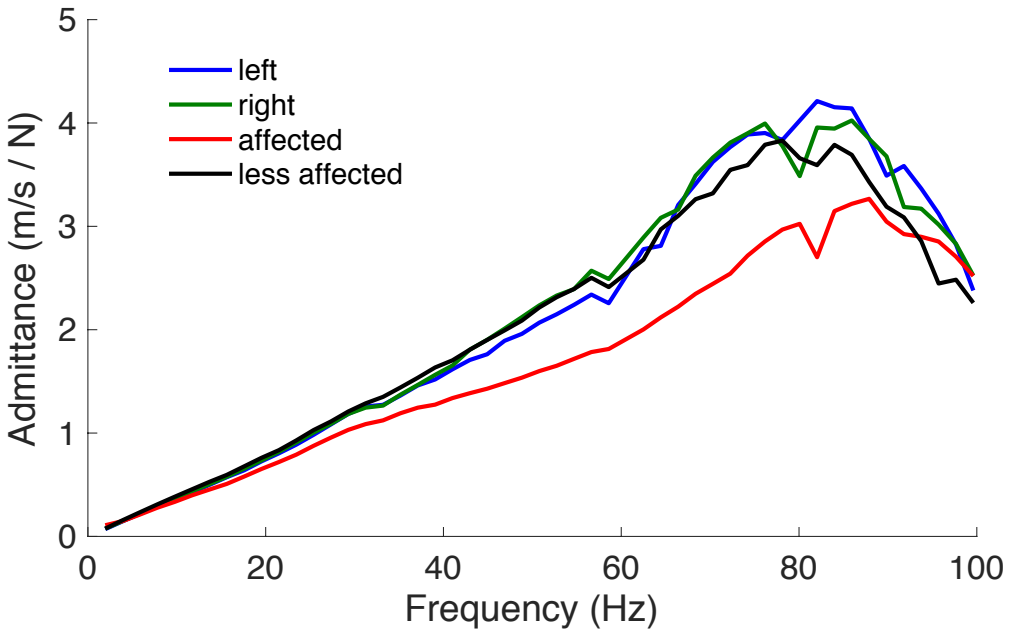

Figure 6-5 Mechanical admittance in the control and stroke groups

Mechanical admittance (m/s/N) across frequencies for the probe against the Achilles tendon for the right and left sides of the control group (n = 8) and the affected and less affected sides of the chronic stroke group (n = 8).

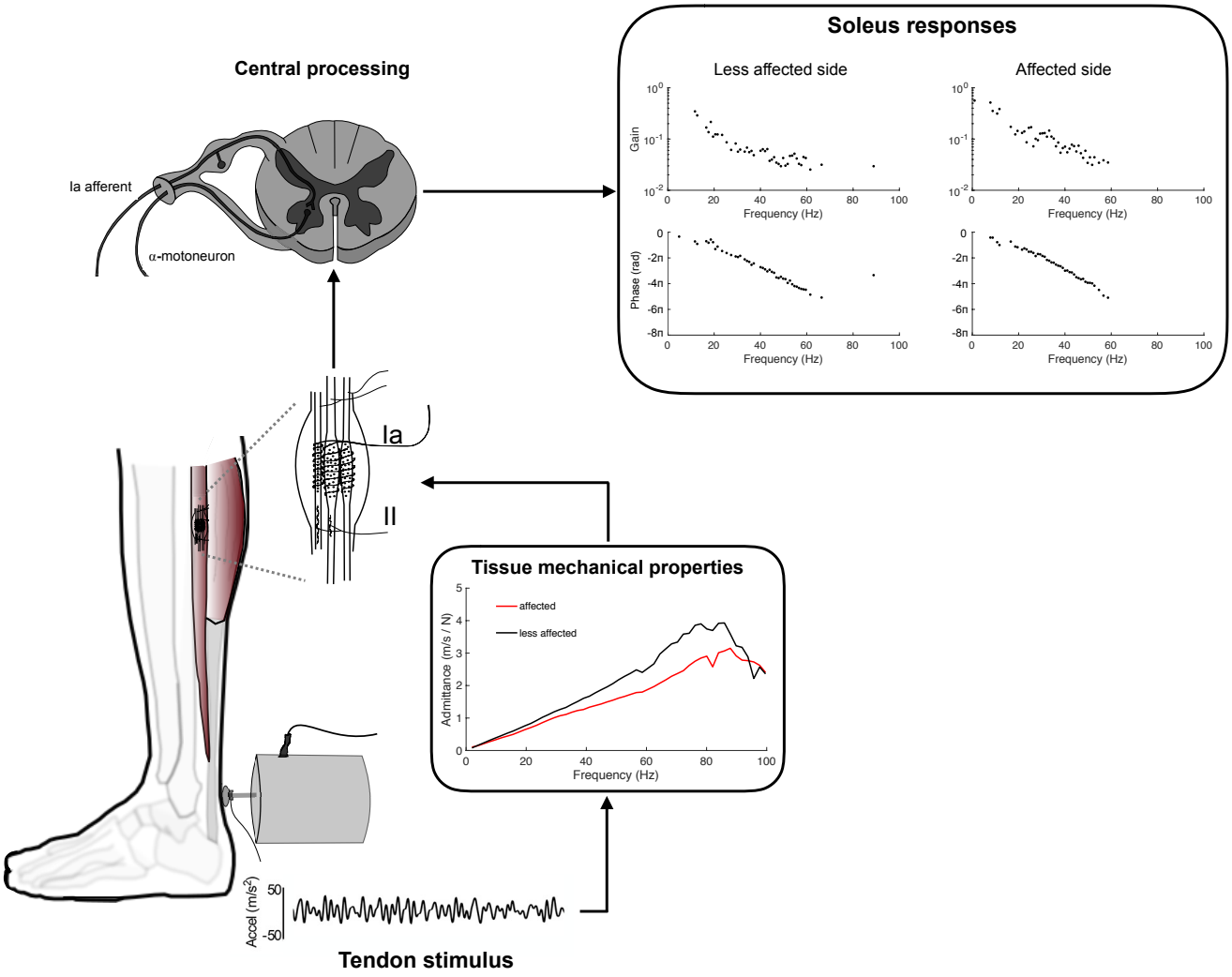

Figure 6-6 Schematic of changes to proprioceptive responses post-stroke

Schematic of the stages involved in determining the transfer functions from tendon vibration to soleus muscle activity. The mechanical stimulus is transmitted to muscle spindles to activate afferents that send signals to the spinal cord. The spinal cord processes this information and sends signals to the muscle. Chronic stroke likely influences the transmission of stimuli through the tissue due to changes in stiffness and strain behaviour, as well as processing in the spinal cord due to changes in descending drive.

Chapter 7: General discussion

7.1 Synthesis of findings

Proprioceptive feedback is critical for the control of movement and posture (Cole and Sedgwick, 1992). In this thesis, a series of five studies were designed to provide information about the characteristics of lower limb responses to proprioceptive perturbations during standing in healthy young adults, middle aged and old adults, and chronic stroke survivors.

To examine responses evoked by proprioceptive perturbations, a stimulus trigger-averaging approach is typically used; this involves delivering multiple transient stimuli and averaging the muscle or cortical activity over time following the stimuli. In the first study of this thesis, we developed an innovative methodology to examine the frequency characteristics of lower limb muscle responses to proprioceptive perturbations during standing. We applied a continuous tendon vibration that contained a broad frequency bandwidth (10-115 Hz) and examined the muscle and cortical responses using a linear correlation analysis. This enabled us to examine response characteristics across a range of frequencies that are generated during every day activities (e.g., walking; Simon et al., 1981), and that muscle spindles are capable of transmitting (Fallon and Macefield, 2007).

Importantly, we found that the noisy stimulus did not noticeably perturb standing balance and provided consistent response measures with relatively short trial durations (<60 s). This made our approach ideal to probe how response characteristics differ in populations with balance deficits such as old adults and stroke survivors (examined in

Chapters 5 and 6). Due to the continuous nature of the stimulus, this noisy vibration approach is also ideal to examine interactions with other sensory inputs by examining the time-varying response following a secondary stimulus; e.g., the cutaneous electrical stimuli used in Chapter 4. This approach allowed us to examine how cutaneous feedback from the foot interacted with the proprioceptive response with a much higher time resolution than has been possible using the condition-test stimulus approach.

Results from the first study of this thesis suggested there may be differences in response characteristics between the three triceps surae muscles, with larger responses in the soleus relative to the medial gastrocnemius, and minimal responses in the lateral gastrocnemius. However, these findings were based on surface EMG recordings, and therefore could be confounded by muscle cross-talk and differences in background activation. This led us to conduct the second study of this thesis, where we compared responses between single motor units at a controlled activation level between soleus and medial gastrocnemius. Here we found soleus single motor units showed stronger coherence across a broad frequency bandwidth relative to medial gastrocnemius single motor units. In this study, we further addressed some methodological considerations for the use of a linear correlation analysis; we delivered sinusoidal vibration at different frequencies up to 100 Hz and examined whether soleus and medial gastrocnemius motor units showed non-linear phase locking with the stimulus. We found that while motor units modulated their firing rate throughout the sine wave cycles at frequencies as high as 100 Hz (the highest frequency we examined), they demonstrated minimal phase locking behaviour.

Cutaneous and proprioceptive afferents from the lower limb both provide important sensory information for the control of balance. In Chapter 4, our data revealed an interesting and probably functional interaction between foot sole cutaneous feedback and proprioceptive feedback. When we electrically stimulated skin under the heel, we found the soleus vibration responses became suppressed. In contrast, when we electrically stimulated skin under the metatarsals, the soleus vibration responses became enhanced. These findings suggest there is some integration within two important somatosensory channels (cutaneous and spindle) that likely has a function in the control of balance. Specifically, cutaneous feedback from the heels during a backward lean could serve to dampen the stretch response in the soleus muscle since there is a greater risk of falling backward, and vice versa during a forward lean or a forward perturbation. While the mechanisms behind this interaction require further investigation, we were able to provide some evidence that they require a strong enough cutaneous stimulus to change α-motoneuron pool excitability, and are likely not due to changes in presynaptic inhibition or fusimotor drive.

The final two studies of this thesis took steps toward understanding how proprioceptive responses are influenced by ageing and chronic stroke. Impaired mobility and increased risk of falls are associated with both ageing and chronic stroke, and the evaluation of proprioceptive pathways may help us understand some mechanisms underlying impaired balance and mobility. In a large sample of healthy adults between 18 and 82 yrs old, we found there was a progressive decline in the amplitude and scaling of the vibration response. There was also a decrease in coherence and gain across a broad

bandwidth between young and middle aged, and between middle aged and old adults. These age-related changes in proprioceptive responses are likely due to impaired mechanotransduction by muscle spindles and processing in the spinal cord, and potentially changes in tissue mechanical properties. Finally, on the affected side of chronic hemiparetic stroke participants, we found changes in mechanical properties of the muscle-tendon unit through examining mechanical admittance, changes in the control of postural adjustments, along with a tendency for altered characteristics of the soleus response to noisy Achilles tendon vibration. These results obtained from a small sample of chronic stroke survivors suggest there could be frequency dependent changes in tissue properties along with changes in central processing that influence responses to proprioceptive perturbations and the control of balance.

7.2 Cortical evoked responses to tendon vibration

In the first study of this thesis (Chapter 2), we recorded EEG across the sensorimotor cortex using a three electrode configuration and examined coherence between Achilles tendon vibration and cortical activity. Vibration-EEG coherence was not significant in all participants in this study (absent in two participants). When present, vibration-EEG coherence was relatively weak and primarily found within the γ-band. The time delay of the EEG response (cross-covariance) aligned with the latency of the earliest evoked potentials to tendon taps that we also examined in this experiment (both ~50 ms). EEG responses in the time domain (cross-covariance) were oscillatory, and there were no

responses at longer time delays that would correspond to later stages of cortical processing of sensory information.

The weak EEG responses to tendon vibration could be due to our minimalistic electrode configuration or filtering of ascending sensory information to disrupt the linear correlation between the stimulus and cortical response. Ascending sensory information passes through multiple relays before reaching the somatosensory cortex, and thus may become filtered at each relay. There is also the possibility that pathways imposing different delays cause interference. For instance, muscle spindle activity has been shown to be coherent with EMG (Baker et al., 2006); thus, spindle activity could be induced by the muscle contraction in response to vibration (in addition to the vibration directly). This would create a longer latency feedback pathway to cortex that could result in some cancellation with the proprioceptive input generated by the vibration directly. However, despite the finding that spindles show coherence with EMG, Witham et al, (2010) found using directed coherence in monkeys that oscillatory activity primarily flows from somatosensory regions of cortex to muscle rather than the other direction. Therefore, interference from spindle activity generated by muscle contraction may be minimal.

With our scalp electrode configuration, we were able to obtain clear evoked potentials to tendon taps in all participants; therefore, our recording setup cannot fully explain the weak vibration-EEG coherence we observed. However, future work should explore whether a more complete scalp recording array and other analysis techniques might overcome some of the limitations of using vibration-EEG coherence to examine the transmission of proprioceptive information to cortex.

7.3 Facilitation of coherence evoked by common fibular nerve stimuli

In Chapter 4, we examined how foot sole cutaneous stimuli influenced the soleus vibration responses and found heel stimuli suppressed and metatarsal stimuli enhanced vibration-EMG coherence and cross-correlations. We then sought to examine what mechanisms might be responsible for this interaction; to that end, we devised experiments to explore potential roles of presynaptic inhibition, and α- and γ- motoneuron excitability.

We expected that stimulation of group I afferents in the deep branch of the common fibular (CF) nerve would evoke a suppression of vibration-EMG coherence due to presynaptic inhibition of Ia afferent terminals from the triceps surae muscles. Characterizing the effects of presynaptic inhibition on the vibration response could help elucidate whether this mechanism has the potential to mediate an interaction between cutaneous stimuli and proprioceptive evoked responses. Surprisingly, we saw no evidence of presynaptic inhibition from CF nerve stimuli; instead, we saw an early and prolonged facilitation of the vibration response. While this finding suggests presynaptic inhibition from PAD does not mediate the effects we saw with cutaneous stimuli, it poses another question of what mediates this facilitation from CF nerve input.

A theory has been proposed that PAD may not strictly serve a role in gating sensory information (Li et al., 2017). Presynaptic inhibition in the spinal cord is thought to result from activation of GABA receptors, which open chloride channels. Chloride efflux depolarizes the afferent, which lowers the amplitude of the invading action

potential. This ultimately causes less calcium influx, less neurotransmitter release, and a smaller EPSP (reviewed in Willis, 2006). However, a common feature of long and highly branched afferents is the presence of conduction block, or failure of the action potential to propagate through all branch points leaving silent branches. Li et al., (2017) proposed that PAD could have a *facilatory* effect because axon depolarization could prevent branch point failure and therefore increase the transmission of sensory information to α-motoneurons. GABA receptors were found to be preferentially located at afferent branch points (Lucas-Osma et al., 2018), which suggests they could play a role in the regulation of transmission through the highly branched Ia afferents.

Previous studies have investigated the function of presynaptic inhibition in the context of ageing, pathology, and control of voluntary movement (Faist et al., 1994; Capaday et al., 1995; Morita et al., 1995, 2001; Iles 1996; Baudry et al., 2012). Recent information that suggests more nuanced roles of PAD could shift research questions and methodologies to reflect potential implications of conduction block (Wall and McMahon, 1994; Li et al., 2017) and the intermittent nature of neural transmission (Barron and Matthews, 1939).

7.4 Cutaneous-fusimotor interactions

In Chapter 4, we also aimed to examine whether cutaneous interactions with the fusimotor system might mediate the change in vibration-EMG coherence following foot sole stimuli. In animals, fusimotor neurons were shown to respond to cutaneous stimuli, and at a lower threshold than corresponding α-motoneurons (Eldred and Hagbarth, 1954;

Appelberg et al., 1977). Thus, we expected that if we reduced the stimulus current to below the threshold to evoke an EMG response (reflecting a change in α-motoneuron excitability) and still observed a change in coherence, this could implicate a change in the activity of fusimotor neurons. However, results showed this was not the case – we were unable to see changes in coherence in the absence of an overt response in surface EMG (i.e., a cutaneous reflex). These findings argue against a selective role of cutaneous-fusimotor interactions. It is possible that in humans, fusimotor neurons are more under the influence of higher centres rather than sensory input. In non-human primates, it was shown that ~15% of corticospinal tract cells originate in area 3a of the somatosensory cortex and make monosynaptic connections to motoneurons in the ventral horn of the spinal cord (Rathelot and Strick, 2006). It was postulated that these projections might serve to regulate γ-motoneuron activity (Rathelot and Strick, 2006), since microstimulation of this region did not evoke movement (Widener and Cheney, 1997).

7.5 Heteronymous responses to proprioceptive stimuli

Spindle afferents branch to provide excitatory input to synergistic muscles as well as muscles that act at other joints. These connections to α-motoneurons of heteronymous muscles coordinate responses to a proprioceptive perturbation across joints. One limitation of the studies in this thesis is that they focused solely on homonymous responses – the activation of triceps surae muscles in response to stimulation of their own intramuscular receptors via perturbations applied to the Achilles tendon. It has been

shown that Achilles tendon vibration during standing in healthy adults evokes responses in the quadriceps, hamstring, and erector spinae muscles (as long as those muscles have background activity) (Eschelmuller et al., 2019). In the study described in Chapter 5, we also recorded vastus lateralis activity and observed an increase in response amplitude (peak-to-peak cross-covariance) with age. However, we did not control for background activation of vastus lateralis; therefore, future research should investigate the influence of age on heteronymous responses while controlling for postural and muscle activation variables.

After a stroke, muscle synergies in both the upper and lower limbs become more pronounced (Bruunstrom, 1970). In the upper limbs, a flexion synergy typically emerges, while in the lower limbs, an extensor synergy typically emerges (Sanchez and Dewald, 2014). The synergy in the upper limbs also manifests as abnormal heteronymous responses evoked by a proprioceptive perturbation at the elbow (shoulder adduction torque paired with elbow flexion torque) (Sangani et al., 2007). Future research should examine whether abnormal heteronymous responses to proprioceptive perturbations are evoked in the lower limbs (reflecting the extensor synergy) while these muscles are engaged in the control of posture and balance. The characteristics of responses to proprioceptive perturbations in heteronymous muscles could provide insight into mechanisms underlying the expression of synergies that might impose constraints to voluntary movement (Sanchez and Dewald, 2014).

7.6 Further opening up the feedback loop

Throughout the experiments contained in this thesis, we examined the linear correlations between the stimulus (acceleration) applied to the Achilles tendon and the surface EMG or spiking activity of single motor units of plantar flexor muscles. Results showed a linear phase slope (reflecting a fixed time delay) and gain that peaked ~10 Hz and then decreased as a function of frequency. This feedback loop could be divided into two stages, 1) the transfer of the tendon stimulus to spike activity of spindle afferents, and 2) the transfer of spindle activity to α-motoneuron activity. How these two stages of processing independently contribute to the changes associated with ageing and chronic stroke are still unknown. Future work could determine these intermediate stages by examining the input-output relationship between vibration and spindle afferent activity recorded through microneurography, and examining or inferring the input-output relationship between afferent and efferent activity.

7.7 How techniques developed in this thesis might advance the field

Similar to tendon taps, noisy tendon vibration provides information about short latency (~40 ms) responses evoked by muscle spindle afferents. One advantage of noisy tendon vibration is it provides a means to probe proprioceptive pathways in a more subtle way without generating a noticeable disturbance to balance. Furthermore, frequency information can be obtained, which can provide useful mechanistic information due to the frequency dependent effects of certain mechanisms such as presynaptic inhibition and short-term synaptic plasticity (Rudomin and Schmidt, 1999; Regehr, 2010). In contrast,

tendon taps are more unpleasant, create a noticeable disturbance to balance, and require averaging over a large number of stimuli to obtain reliable responses. If the use of a continuous noisy stimulus and correlation analysis approach is adopted into research and clinical examinations, it could improve the ability to assess and monitor proprioceptive responses in disorders associated with spasticity and loss of somatosensory function, such as stroke, multiple sclerosis, spinal cord injury, and peripheral neuropathy.

A continuous stimulus method can also improve the ability to examine time varying processes. For instance, in Chapter 4, we examined how vibration responses varied following cutaneous stimuli, as well as how vibration responses varied following CF nerve stimuli. In future research, this approach could be used to examine other sensory interactions (e.g., vestibular and proprioceptive) or time varying changes in the triceps surae vibration response prior to motor tasks such as voluntary dorsiflexion. Previously, the examination of sensory interactions has been tedious since it involves the repeated delivery of condition and test stimuli at many defined condition-test intervals to build the profile of the interaction over time. The improved temporal resolution obtained with the time-dependent correlation approach may be useful to understand aspects of motor control in healthy adults and changes that occur after an injury to the nervous system.

7.8 Concluding remarks

Collectively, the studies contained within this thesis present novel data on the characteristics of responses evoked by proprioceptive perturbations in engaged postural muscles. Responses were found to differ between triceps surae muscles, and were tuned

by cutaneous information from the foot sole. Furthermore, responses were found to be altered by ageing and chronic stroke. This information can be important to guide clinical assessments and monitor rehabilitation, as well as inform the development of neuroprostheses. The ideas presented and approaches used in this thesis will help progress our understanding of how somatosensory information is processed, as well as how future experimental and clinical tests are conducted and interpreted.

Bibliography

Ada L, Vattanasilp W, O'Dwyer NJ, Crosbie J. Does spasticity contribute to walking dysfunction after stroke? *J Neurol Neurosurg Psychiatry*. 1998;64:628-635.

Afzal T, Chardon MK, Rymer WZ, Suresh NL. Stretch reflex excitability in contralateral limbs of stroke survivors is higher than in matched controls. *J Neuroeng Rehabil*. 2019;16:154-019-0623-8.

Allum JH, Carpenter MG, Honegger F, Adkin AL, Bloem BR. Age-dependent variations in the directional sensitivity of balance corrections and compensatory arm movements in man. *J Physiol*. 2002;542:643-663.

Alnaes E, Jansen JK, Rudjord T. Fusimotor activity in the spinal cat. *Acta Physiol Scand*. 1965;63:197-212.

Alway SE, MacDougall JD, Sale DG, Sutton JR, McComas AJ. Functional and structural adaptations in skeletal muscle of trained athletes. *J Appl Physiol (1985)*. 1988;64:1114-1120.

Amjad AM, Halliday DM, Rosenberg JR, Conway BA. An extended difference of coherence test for comparing and combining several independent coherence estimates: theory and application to the study of motor units and physiological tremor. *J Neurosci Methods*. 1997;73:69-79.

Angulo-Kinzler RM, Mynark RG, Koceja DM. Soleus H-reflex gain in elderly and young adults: modulation due to body position. *J Gerontol A Biol Sci Med Sci*. 1998;53:M120-5.

Aniss AM, Diener HC, Hore J, Gandevia SC, Burke D. Behavior of human muscle receptors when reliant on proprioceptive feedback during standing. *J Neurophysiol*. 1990;64:661-670.

Aniss AM, Gandevia SC, Burke D. Reflex responses in active muscles elicited by stimulation of low-threshold afferents from the human foot. *J Neurophysiol*. 1992;67:1375-1384.

Aniss AM, Gandevia SC, Burke D. Reflex changes in muscle spindle discharge during a voluntary contraction. *J Neurophysiol*. 1988;59:908-921.

Appelberg B, Johansson H, Kalistratov G. The influence of group II muscle afferents and low threshold skin afferents on dynamic fusimotor neurones to the triceps surae of the cat. *Brain Res*. 1977;132:153-158.

Baker SN, Chiu M, Fetz EE. Afferent encoding of central oscillations in the monkey arm. *J Neurophysiol*. 2006;95:3904-3910.

Bakheit AM, Maynard VA, Curnow J, Hudson N, Kodapala S. The relation between Ashworth scale scores and the excitability of the alpha motor neurones in patients with post-stroke muscle spasticity. *J Neurol Neurosurg Psychiatry*. 2003;74:646-648.

Banks RW. An allometric analysis of the number of muscle spindles in mammalian skeletal muscles. *J Anat*. 2006;208:753-768.

Barbieri G, Gissot AS, Nougier V, Perennou D. Achilles tendon vibration shifts the center of pressure backward in standing and forward in sitting in young subjects. *Neurophysiol Clin*. 2013;43:237-242.

Barron DH, Matthews BHC. Intermittent conduction in the spinal cord. *J Physiol (Lond)* 1939;85:73–103

Baudry S. Aging Changes the contribution of spinal and corticospinal pathways to control balance. *Exerc Sport Sci Rev*. 2016;44:104-109.

Baudry S, Collignon S, Duchateau J. Influence of age and posture on spinal and corticospinal excitability. *Exp Gerontol*. 2015;69:62-69.

Baudry S, Duchateau J. Age-related influence of vision and proprioception on Ia presynaptic inhibition in soleus muscle during upright stance. *J Physiol*. 2012;590:5541-5554.

Bauer M, Oostenveld R, Peeters M, Fries P. Tactile spatial attention enhances gamma-band activity in somatosensory cortex and reduces low-frequency activity in parieto-occipital areas. *J Neurosci*. 2006;26:490-501.

Bent LR, Lowrey CR. Single low-threshold afferents innervating the skin of the human foot modulate ongoing muscle activity in the upper limbs. *J Neurophysiol*. 2013;109:1614-1625.

Bergego C, Pierrot-Deseilligny E, Mazieres L. Facilitation of transmission in Ib pathways by cutaneous afferents from the contralateral foot sole in man. *Neurosci Lett*. 1981;27:297-301.

Bewick GS. Synaptic-like vesicles and candidate transduction channels in mechanosensory terminals. *J Anat*. 2015;227:194-213.

Binder MD, Kroin JS, Moore GP, Stuart DG. The response of Golgi tendon organs to single motor unit contractions. *J Physiol*. 1977;271:337-349.

Binder MD, Powers RK, Heckman CJ. Nonlinear input-output functions of motoneurons. *Physiology (Bethesda)*. 2020;35:31-39.

Blouin JS, Dakin CJ, van den Doel K, Chua R, McFadyen BJ, Inglis JT. Extracting phase-dependent human vestibular reflexes during locomotion using both time and frequency correlation approaches. *J Appl Physiol (1985)*. 2011;111:1484-1490.

Bloem BR, Allum JH, Carpenter MG, Verschuuren JJ, Honegger F. Triggering of balance corrections and compensatory strategies in a patient with total leg proprioceptive loss. *Exp Brain Res*. 2002;142:91-107.

Blum KP, Lamotte D'Incamps B, Zytnicki D, Ting LH. Force encoding in muscle spindles during stretch of passive muscle. *PLoS Comput Biol*. 2017;13:e1005767.

Boxer PA, Morales FR, Chase MH. Alterations of group Ia-motoneuron monosynaptic EPSPs in aged cats. *Exp Neurol*. 1988;100:583-595.

Braun C, Haug M, Wiech K, Birbaumer N, Elbert T, Roberts LE. Functional organization of primary somatosensory cortex depends on the focus of attention. *Neuroimage*. 2002;17:1451-1458.

Brunnstrom S. Movement therapy in hemiplegia: A neurophysiological approach. Harper & Row, New York 1970.

Burgess PR, Clark FJ. Characteristics of knee joint receptors in the cat. *J Physiol*. 1969;203:317-335.

Burke D, Gandevia SC, McKeon B. The afferent volleys responsible for spinal proprioceptive reflexes in man. *J Physiol*. 1983;339:535-552.

Burke D, Hagbarth KE, Lofstedt L. Muscle spindle activity in man during shortening and lengthening contractions. *J Physiol*. 1978;277:131-142.

Burke D, Hagbarth KE, Lofstedt L, Wallin BG. The responses of human muscle spindle endings to vibration during isometric contraction. *J Physiol*. 1976;261:695-711.

Burke D, Hagbarth KE, Lofstedt L, Wallin BG. The responses of human muscle spindle endings to vibration of non-contracting muscles. *J Physiol*. 1976;261:673-693.

Burke D, Wissel J, Donnan GA. Pathophysiology of spasticity in stroke. *Neurology*. 2013;80:S20-6.

Burne JA, Carleton VL, O'Dwyer NJ. The spasticity paradox: movement disorder or disorder of resting limbs? *J Neurol Neurosurg Psychiatry*. 2005;76:47-54.

Capaday C, Lavoie BA, Comeau F. Differential effects of a flexor nerve input on the human soleus H-reflex during standing versus walking. *Can J Physiol Pharmacol*. 1995;73:436-449.

Capogrosso M, Milekovic T, Borton D, et al. A brain-spine interface alleviating gait deficits after spinal cord injury in primates. *Nature*. 2016;539:284-288.

Cathers I, O'Dwyer N, Neilson P. Dependence of stretch reflexes on amplitude and bandwidth of stretch in human wrist muscle. *Exp Brain Res*. 1999;129:278-287.

Cathers I, O'Dwyer N, Neilson P. Tracking performance with sinusoidal and irregular targets under different conditions of peripheral feedback. *Exp Brain Res*. 1996;111:437-446.

Cattaert D, El Manira A. Shunting versus inactivation: analysis of presynaptic inhibitory mechanisms in primary afferents of the crayfish. *J Neurosci*. 1999;19:6079-6089.

Ceyte H, Cian C, Zory R, Barraud PA, Roux A, Guerraz M. Effect of Achilles tendon vibration on postural orientation. *Neurosci Lett*. 2007;416:71-75.

Chardon MK, Suresh NL, Dhaher YY, Rymer WZ. In-vivo study of passive musculotendon mechanics in chronic hemispheric stroke survivors. *IEEE Trans Neural Syst Rehabil Eng*. 2020;28:1022-1031.

Chung SG, Van Rey EM, Bai Z, Rogers MW, Roth EJ, Zhang LQ. Aging-related neuromuscular changes characterized by tendon reflex system properties. *Arch Phys Med Rehabil*. 2005;86:318-327.

Clair JM, Okuma Y, Misiaszek JE, Collins DF. Reflex pathways connect receptors in the human lower leg to the erector spinae muscles of the lower back. *Exp Brain Res*. 2009;196:217-227.

Cole JD, Sedgwick EM. The perceptions of force and of movement in a man without large myelinated sensory afferents below the neck. *J Physiol*. 1992;449:503-515.

Connell LA, Davey NJ, Ellaway PH. The degree of short-term synchrony between alpha- and gamma-motoneurones coactivated during the flexion reflex in the cat. *J Physiol*. 1986;376:47-61.

Crone C, Nielsen J. Methodological implications of the post activation depression of the soleus H-reflex in man. *Exp Brain Res*. 1989;78:28-32.

Crone C, Nielsen J, Petersen N, Ballegaard M, Hultborn H. Disynaptic reciprocal inhibition of ankle extensors in spastic patients. *Brain*. 1994;117 (Pt 5): 1161-1168.

Cronin NJ, Carty CP, Barrett RS. Triceps surae short latency stretch reflexes contribute to ankle stiffness regulation during human running. *PLoS One*. 2011;6:e23917.

Curtis DR, Eccles JC. Synaptic action during and after repetitive stimulation. *J Physiol*. 1960;150:374-398.

Dai C, Suresh NL, Suresh AK, Rymer WZ, Hu X. Altered motor unit discharge coherence in paretic muscles of stroke survivors. *Front Neurol*. 2017;8:202.

Dakin CJ, Heroux ME, Luu BL, Inglis JT, Blouin JS. Vestibular contribution to balance control in the medial gastrocnemius and soleus. *J Neurophysiol*. 2016;115:1289-1297.

Dakin CJ, Inglis JT, Blouin JS. Short and medium latency muscle responses evoked by electrical vestibular stimulation are a composite of all stimulus frequencies. *Exp Brain Res*. 2011;209:345-354.

Dakin CJ, Luu BL, van den Doel K, Inglis JT, Blouin JS. Frequency-specific modulation of vestibular-evoked sway responses in humans. *J Neurophysiol*. 2010;103:1048-1056.

Dakin CJ, Son GM, Inglis JT, Blouin JS. Frequency response of human vestibular reflexes characterized by stochastic stimuli. *J Physiol*. 2007;583:1117-1127.

Dalton BH, Blouin JS, Allen MD, Rice CL, Inglis JT. The altered vestibular-evoked myogenic and whole-body postural responses in old men during standing. *Exp Gerontol*. 2014;60:120-128.

Dalton BH, Harwood B, Davidson AW, Rice CL. Triceps surae contractile properties and firing rates in the soleus of young and old men. *J Appl Physiol (1985)*. 2009;107:1781-1788.

Dalton BH, McNeil CJ, Doherty TJ, Rice CL. Age-related reductions in the estimated numbers of motor units are minimal in the human soleus. *Muscle Nerve*. 2008;38:1108-1115.

D'Amico JM, Condliffe EG, Martins KJ, Bennett DJ, Gorassini MA. Recovery of neuronal and network excitability after spinal cord injury and implications for spasticity. *Front Integr Neurosci*. 2014;8:36.

Davidson AG, Buford JA. Bilateral actions of the reticulospinal tract on arm and shoulder muscles in the monkey: stimulus triggered averaging. *Exp Brain Res*. 2006;173:25-39.

Davis JR, Horslen BC, Nishikawa K, et al. Human proprioceptive adaptations during states of height-induced fear and anxiety. *J Neurophysiol*. 2011;106:3082-3090.

Delabastita T, Bogaerts S, Vanwanseele B. Age-related changes in Achilles tendon stiffness and impact on functional activities: A systematic review and meta-analysis. *J Aging Phys Act*. 2018:1-12.

Deshpande N, Simonsick E, Metter EJ, Ko S, Ferrucci L, Studenski S. Ankle proprioceptive acuity is associated with objective as well as self-report measures of balance, mobility, and physical function. *Age (Dordr)*. 2016;38:53-016-9918-x. Epub 2016 May 4.

deVries HA, Wiswell RA, Romero GT, Heckathorne E. Changes with age in monosynaptic reflexes elicited by mechanical and electrical stimulation. *Am J Phys Med*. 1985;64:71-81.

Dimitriou M, Edin BB. Human muscle spindles act as forward sensory models. *Curr Biol*. 2010;20:1763-1767.

Duysens J, Tax AA, van der Doelen B, Trippel M, Dietz V. Selective activation of human soleus or gastrocnemius in reflex responses during walking and running. *Exp Brain Res*. 1991;87:193-204.

Dyer JO, Maupas E, de Andrade Melo S, Bourbonnais D, Fleury J, Forget R. Transmission in heteronymous spinal pathways is modified after stroke and related to motor incoordination. *PLoS One*. 2009;4:e4123.

Dyer JO, Maupas E, Melo Sde A, Bourbonnais D, Forget R. Abnormal coactivation of knee and ankle extensors is related to changes in heteronymous spinal pathways after stroke. *J Neuroeng Rehabil*. 2011;8:41-0003-8-41.

Earles D, Vardaxis V, Koceja D. Regulation of motor output between young and elderly subjects. *Clin Neurophysiol*. 2001;112:1273-1279.

Eccles JC, Schmidt RF, Willis WD. Presynaptic inhibition of the spinal monosynaptic reflex pathway. *J Physiol*. 1962;161:282-297.

Eldred E, Hagbarth KE. Facilitation and inhibition of gamma efferents by stimulation of certain skin areas. *J Neurophysiol*. 1954;17:59-65.

Elias LA, Watanabe RN, Kohn AF. Spinal mechanisms may provide a combination of intermittent and continuous control of human posture: predictions from a biologically based neuromusculoskeletal model. *PLoS Comput Biol*. 2014;10:e1003944.

Enríquez-Denton M, Morita H, Christensen LO, Petersen N, Sinkjaer T, Nielsen JB. Interaction between peripheral afferent activity and presynaptic inhibition of ia afferents in the cat. *J Neurophysiol*. 2002;88:1664-1674.

Erimaki S, Christakos CN. Coherent motor unit rhythms in the 6-10 Hz range during time-varying voluntary muscle contractions: neural mechanism and relation to rhythmical motor control. *J Neurophysiol*. 2008;99:473-483.

Eschelmuller, G., Mildren, R.L., Blouin, J-S., Carpenter, M.G., Inglis, J.T., 2019. Heteronymous muscle responses to noisy achilles tendon vibration during standing. J. Exercise, Movement, and Sport (SCAPPS refereed abstracts repository). 51, 20–20.

Faist M, Mazevet D, Dietz V, Pierrot-Deseilligny E. A quantitative assessment of presynaptic inhibition of Ia afferents in spastics. Differences in hemiplegics and paraplegics. *Brain*. 1994;117 (Pt 6):1449-1455.

Fallon JB, Bent LR, McNulty PA, Macefield VG. Evidence for strong synaptic coupling between single tactile afferents from the sole of the foot and motoneurons supplying leg muscles. *J Neurophysiol*. 2005;94:3795-3804.

Fallon JB, Macefield VG. Vibration sensitivity of human muscle spindles and Golgi tendon organs. *Muscle Nerve*. 2007;36:21-29.

Ferlinc A, Fabiani E, Velnar T, Gradisnik L. The importance and role of proprioception in the elderly: a short review. *Mater Sociomed*. 2019;31:219-221.

Fink AJ, Croce KR, Huang ZJ, Abbott LF, Jessell TM, Azim E. Presynaptic inhibition of spinal sensory feedback ensures smooth movement. *Nature*. 2014;509:43-48.

Fitzpatrick R, Rogers DK, McCloskey DI. Stable human standing with lower-limb muscle afferents providing the only sensory input. *J Physiol*. 1994;480 (Pt 2):395-403.

Florman JE, Duffau H, Rughani AI. Lower motor neuron findings after upper motor neuron injury: insights from postoperative supplementary motor area syndrome. *Front Hum Neurosci*. 2013;7:85.

Fornari MC, Kohn AF. High frequency tendon reflexes in the human soleus muscle. *Neurosci Lett*. 2008;440:193-196.

Frank K, Fuortes MGF Presynaptic and postsynaptic inhibition of monosynaptic reflexes. *Fed. Proc.* 1957;16:39-40.

Frascarelli M, Brusa A, Fricci GF. Evoked potentials obtained with tendon percussion in hemiplegic patients. *Electromyogr Clin Neurophysiol*. 1993;33:157-160.

Fritz J, Shamma S, Elhilali M, Klein D. Rapid task-related plasticity of spectrotemporal receptive fields in primary auditory cortex. *Nat Neurosci*. 2003;6:1216-1223.

Fung J, Barbeau H. Effects of conditioning cutaneomuscular stimulation on the soleus H-reflex in normal and spastic paretic subjects during walking and standing. *J Neurophysiol*. 1994;72:2090-2104.

Gandevia SC, Wilson L, Cordo PJ, Burke D. Fusimotor reflexes in relaxed forearm muscles produced by cutaneous afferents from the human hand. *J Physiol*. 1994;479 (Pt 3):499-508.

Gao F, Grant TH, Roth EJ, Zhang LQ. Changes in passive mechanical properties of the gastrocnemius muscle at the muscle fascicle and joint levels in stroke survivors. *Arch Phys Med Rehabil*. 2009;90:819-826.

Garland SJ, Pollock CL, Ivanova TD. Could motor unit control strategies be partially preserved after stroke? *Front Hum Neurosci*. 2014;8:864.

Ghanim Z, Lamy JC, Lackmy A, et al. Effects of galvanic mastoid stimulation in seated human subjects. *J Appl Physiol (1985)*. 2009;106:893-903.

Gioux M, Petit J. Effects of immobilizing the cat peroneus longus muscle on the activity of its own spindles. *J Appl Physiol (1985)*. 1993;75:2629-2635.

Gorassini MA, Bennett DJ, Yang JF. Self-sustained firing of human motor units. *Neurosci Lett*. 1998;247:13-16.

Grey MJ, Klinge K, Crone C, et al. Post-activation depression of soleus stretch reflexes in healthy and spastic humans. *Exp Brain Res*. 2008;185:189-197.

Hagbarth KE, Nordin M, Bongiovanni LG. After-effects on stiffness and stretch reflexes of human finger flexor muscles attributed to muscle thixotropy. *J Physiol*. 1995;482 (Pt 1):215-223.

Hagbarth KE, Wallin G, Lofstedt L. Muscle spindle responses to stretch in normal and spastic subjects. *Scand J Rehabil Med*. 1973;5:156-159.

Hagbarth KE, Wallin G, Lofstedt L, Aquilonius SM. Muscle spindle activity in alternating tremor of Parkinsonism and in clonus. *J Neurol Neurosurg Psychiatry*. 1975;38:636-641.

Halliday DM, Rosenberg JR, Amjad AM, Breeze P, Conway BA, Farmer SF. A framework for the analysis of mixed time series/point process data--theory and application to the study of physiological tremor, single motor unit discharges and electromyograms. *Prog Biophys Mol Biol*. 1995;64:237-278.

Hammerstad JP, Elliott K, Mak E, Schulzer M, Calne S, Calne DB. Tendon jerks in Parkinson's disease. *J Neural Transm Park Dis Dement Sect*. 1994;8:123-130.

Haridas C, Zehr EP, Misiaszek JE. Adaptation of cutaneous stumble correction when tripping is part of the locomotor environment. *J Neurophysiol*. 2008;99:2789-2797.

Heckman CJ, Binder MD. Analysis of effective synaptic currents generated by homonymous Ia afferent fibers in motoneurons of the cat. *J Neurophysiol*. 1988;60:1946-1966.

Heckman CJ, Lee RH, Brownstone RM. Hyperexcitable dendrites in motoneurons and their neuromodulatory control during motor behavior. *Trends Neurosci*. 2003;26:688-695.

Henry M, Baudry S. Age-related changes in leg proprioception: implications for postural control. *J Neurophysiol*. 2019;122:525-538.

Hepple RT, Rice CL. Innervation and neuromuscular control in ageing skeletal muscle. *J Physiol*. 2016;594:1965-1978.

Heroux ME, Brown HJ, Inglis JT, Siegmund GP, Blouin JS. Motor units in the human medial gastrocnemius muscle are not spatially localized or functionally grouped. *J Physiol*. 2015;593:3711-3726.

Heroux ME, Dakin CJ, Luu BL, Inglis JT, Blouin JS. Absence of lateral gastrocnemius activity and differential motor unit behavior in soleus and medial gastrocnemius during standing balance. *J Appl Physiol (1985)*. 2014;116:140-148.

Horslen BC, Murnaghan CD, Inglis JT, Chua R, Carpenter MG. Effects of postural threat on spinal stretch reflexes: evidence for increased muscle spindle sensitivity? *J Neurophysiol*. 2013;110:899-906.

Hu X, Suresh NL, Chardon MK, Rymer WZ. Contributions of motoneuron hyperexcitability to clinical spasticity in hemispheric stroke survivors. *Clin Neurophysiol*. 2015;126:1599-1606.

Hulliger M, Matthews PB, Noth J. Static and dynamic fusimotor action on the response of Ia fibres to low frequency sinusoidal stretching of widely ranging amplitude. *J Physiol*. 1977;267:811-838.

Hultborn H, Brownstone RB, Toth TI, Gossard JP. Key mechanisms for setting the input-output gain across the motoneuron pool. *Prog Brain Res*. 2004;143:77-95.

Hultborn H, Illert M, Nielsen J, Paul A, Ballegaard M, Wiese H. On the mechanism of the post-activation depression of the H-reflex in human subjects. *Exp Brain Res*. 1996;108:450-462.

Hultborn H, Meunier S, Morin C, Pierrot-Deseilligny E. Assessing changes in presynaptic inhibition of I a fibres: a study in man and the cat. *J Physiol*. 1987;389:729-756.

Hunt CC. The reflex activity of mammalian small-nerve fibres. *J Physiol*. 1951;115:456-469.

Ihara A, Hirata M, Yanagihara K, et al. Neuromagnetic gamma-band activity in the primary and secondary somatosensory areas. *Neuroreport*. 2003;14:273-277.

Iles JF. Evidence for cutaneous and corticospinal modulation of presynaptic inhibition of Ia afferents from the human lower limb. *J Physiol*. 1996;491 (Pt 1):197-207.

Jankelowitz SK, Colebatch JG. The acoustic startle reflex in ischemic stroke. *Neurology*. 2004;62:114-116.

Jankowska E. On the distribution of information from muscle spindles in the spinal cord; how much does it depend on random factors? *J Anat*. 2015;227:184-193.

Jimenez I, Rudomin P, Solodkin M, Vyklicky L. Specific and nonspecific mechanisms involved in generation of PAD of group Ia afferents in cat spinal cord. *J Neurophysiol*. 1984;52:921-940.

Johnson SW, Lynn PA, Miller JS, Reed GA. Identification of the stretch reflex using pseudorandom excitation: electromyographic response to displacement of the human forearm. *Med Biol Eng Comput*. 1981;19:195-207.

Jones JP, Palmer LA. An evaluation of the two-dimensional Gabor filter model of simple receptive fields in cat striate cortex. *J Neurophysiol*. 1987;58:1233-1258.

Kajikawa Y, Hackett TA. Entropy analysis of neuronal spike train synchrony. *J Neurosci Methods*. 2005;149:90-93.

Kallio J, Sogaard K, Avela J, Komi PV, Selanne H, Linnamo V. Motor unit firing behaviour of soleus muscle in isometric and dynamic contractions. *PLoS One*. 2013;8:e53425.

Karacan I, Cakar HI, Sebik O, et al. A new method to determine reflex latency induced by high rate stimulation of the nervous system. *Front Hum Neurosci*. 2014;8:536.

Karamanidis K, Arampatzis A. Mechanical and morphological properties of different muscle-tendon units in the lower extremity and running mechanics: effect of aging and physical activity. *J Exp Biol*. 2005;208:3907-3923.

Kavounoudias A, Roll R, Roll JP. Foot sole and ankle muscle inputs contribute jointly to human erect posture regulation. *J Physiol*. 2001;532:869-878.

Kavounoudias A, Roll R, Roll JP. Specific whole-body shifts induced by frequency-modulated vibrations of human plantar soles. *Neurosci Lett*. 1999;266:181-184.

Kavounoudias A, Roll R, Roll JP. The plantar sole is a 'dynamometric map' for human balance control. *Neuroreport*. 1998;9:3247-3252.

Kawashima N, Nakazawa K, Yamamoto SI, Nozaki D, Akai M, Yano H. Stretch reflex excitability of the anti-gravity ankle extensor muscle in elderly humans. *Acta Physiol Scand*. 2004;180:99-105.

Kearney RE, Hunter IW. System identification of human stretch reflex dynamics: tibialis anterior. *Exp Brain Res*. 1984;56:40-49.

Kearney RE, Hunter IW. System identification of human triceps surae stretch reflex dynamics. *Exp Brain Res*. 1983;51:117-127.

Kennedy PM, Inglis JT. Distribution and behaviour of glabrous cutaneous receptors in the human foot sole. *J Physiol*. 2002;538:995-1002.

Keshner EA, Allum JH, Honegger F. Predictors of less stable postural responses to support surface rotations in healthy human elderly. *J Vestib Res*. 1993;3:419-429.

Kim GH, Suzuki S, Kanda K. Age-related physiological and morphological changes of muscle spindles in rats. *J Physiol*. 2007;582:525-538.

Kirk EA, Gilmore KJ, Stashuk DW, Doherty TJ, Rice CL. Human motor unit characteristics of the superior trapezius muscle with age-related comparisons. *J Neurophysiol*. 2019;122:823-832.

Knikou M. Plantar cutaneous afferents normalize the reflex modulation patterns during stepping in chronic human spinal cord injury. *J Neurophysiol*. 2010;103:1304-1314.

Knikou M. Plantar cutaneous input modulates differently spinal reflexes in subjects with intact and injured spinal cord. *Spinal Cord*. 2007;45:69-77.

Knikou M, Conway BA. Modulation of soleus H-reflex following ipsilateral mechanical loading of the sole of the foot in normal and complete spinal cord injured humans. *Neurosci Lett*. 2001;303:107-110.

Koceja DM, Markus CA, Trimble MH. Postural modulation of the soleus H reflex in young and old subjects. *Electroencephalogr Clin Neurophysiol*. 1995;97:387-393.

Koceja DM, Mynark RG. Comparison of heteronymous monosynaptic Ia facilitation in young and elderly subjects in supine and standing positions. *Int J Neurosci*. 2000;103:1-17.

Krutki P, Jankowska E, Edgley SA. Are crossed actions of reticulospinal and vestibulospinal neurons on feline motoneurons mediated by the same or separate commissural neurons? *J Neurosci*. 2003;23:8041-8050.

Lamy JC, Wargon I, Mazevet D, Ghanim Z, Pradat-Diehl P, Katz R. Impaired efficacy of spinal presynaptic mechanisms in spastic stroke patients. *Brain*. 2009;132:734-748.

Lance JW. The control of muscle tone, reflexes, and movement: Robert Wartenberg Lecture. *Neurology*. 1980;30:1303-1313.

Leao RN, Burne JA. Continuous wavelet transform in the evaluation of stretch reflex responses from surface EMG. *J Neurosci Methods*. 2004;133:115-125.

Leksell L. The action potential and excitatory effects of the small ventral root fibres to skeletal muscle. *Acta Physiol Scand.* 1945;10:Suppl. 31.

Levin MF, Hui-Chan C. Are H and stretch reflexes in hemiparesis reproducible and correlated with spasticity? *J Neurol*. 1993;240:63-71.

Lexell J, Downham DY. The occurrence of fibre-type grouping in healthy human muscle: a quantitative study of cross-sections of whole vastus lateralis from men between 15 and 83 years. *Acta Neuropathol*. 1991;81:377-381.

Li S, Chang SH, Francisco GE, Verduzco-Gutierrez M. Acoustic startle reflex in patients with chronic stroke at different stages of motor recovery: a pilot study. *Top Stroke Rehabil*. 2014;21:358-370.

Li S, Francisco GE. New insights into the pathophysiology of post-stroke spasticity. *Front Hum Neurosci*. 2015;9:192.

Li Y, Lucas-Osma AM, Black S, Fenrich KK, Stephens MJ, Sanelli L, Lin S, Fouad K, Goroassini MA, Bennett DJ. Presynaptic facilitation of the monosynaptic reflex in humans and rats. *Society for Neuroscience*, Nov 15, 2017; 679.12/DD4.

Lin SI, Woollacott MH. Postural muscle responses following changing balance threats in young, stable older, and unstable older adults. *J Mot Behav*. 2002;34:37-44.

Liu JX, Eriksson PO, Thornell LE, Pedrosa-Domellof F. Fiber content and myosin heavy chain composition of muscle spindles in aged human biceps brachii. *J Histochem Cytochem*. 2005;53:445-454.

Loram ID, Maganaris CN, Lakie M. Paradoxical muscle movement in human standing. *J Physiol*. 2004;556:683-689.

Lorentzen J, Kirk H, Fernandez-Lago H, et al. Treadmill training with an incline reduces ankle joint stiffness and improves active range of movement during gait in adults with cerebral palsy. *Disabil Rehabil*. 2017;39:987-993.

Lowrey CR, Bent LR. Modulation of the soleus H-reflex following galvanic vestibular stimulation and cutaneous stimulation in prone human subjects. *Muscle Nerve*. 2009;40:213-220.

Lucas-Osma AM, Li Y, Lin S, et al. Extrasynaptic alpha$_5$GABA$_A$ receptors on proprioceptive afferents produce a tonic depolarization that modulates sodium channel function in the rat spinal cord. *J Neurophysiol*. 2018;120:2953-2974.

Lundberg A, Malmgren K, Schomburg ED. Cutaneous facilitation of transmission in reflex pathways from Ib afferents to motoneurones. *J Physiol*. 1977;265:763-780.

Maeda N, Kato J, Shimada T. Predicting the probability for fall incidence in stroke patients using the Berg Balance Scale. *J Int Med Res*. 2009;37:697-704.

Maki BE, Perry SD, Norrie RG, McIlroy WE. Effect of facilitation of sensation from plantar foot-surface boundaries on postural stabilization in young and older adults. *J Gerontol A Biol Sci Med Sci*. 1999;54:M281-7.

Mansfield A, Aqui A, Danells CJ, et al. Does perturbation-based balance training prevent falls among individuals with chronic stroke? A randomised controlled trial. *BMJ Open*. 2018;8:e021510-2018-021510.

Marigold DS, Eng JJ. Altered timing of postural reflexes contributes to falling in persons with chronic stroke. *Exp Brain Res*. 2006;171:459-468.

Marigold DS, Eng JJ, Inglis JT. Modulation of ankle muscle postural reflexes in stroke: influence of weight-bearing load. *Clin Neurophysiol*. 2004;115:2789-2797.

Marsden CD, Merton PA, Morton HB. Servo action in the human thumb. *J Physiol*. 1976;257:1-44.

Matthews PB. Spindle and motoneuronal contributions to the phase advance of the human stretch reflex and the reduction of tremor. *J Physiol*. 1997;498 (Pt 1):249-275.

Matthews PB. The simple frequency response of human stretch reflexes in which either short- or long-latency components predominate. *J Physiol*. 1994;481 (Pt 3): 777-798.

Matthews PB. Interaction between short- and long-latency components of the human stretch reflex during sinusoidal stretching. *J Physiol*. 1993;462:503-527.

Matthews PB. Observations on the automatic compensation of reflex gain on varying the pre-existing level of motor discharge in man. *J Physiol*. 1986;374:73-90.

Matthews PB. The relative unimportance of the temporal pattern of the primary afferent input in determining the mean level of motor firing in the tonic vibration reflex. *J Physiol*. 1975;251:333-361.

Matthews PB, Stein RB. The sensitivity of muscle spindle afferents to small sinusoidal changes of length. *J Physiol*. 1969;200:723-743.

Mauguiére F. Somatosensory evoked potentials: normal responses, abnormal waveforms and clinical applications in neurological diseases. In: *Electroencephalography: Basic Principles, Clinical Applications, and Related Fields* (4th ed.), edited by Niedermeyer E, Lopez da Silva F, New York: William and Wilkins, 1999;p. 1014-1058.

McPherson JG, Ellis MD, Heckman CJ, Dewald JP. Evidence for increased activation of persistent inward currents in individuals with chronic hemiparetic stroke. *J Neurophysiol*. 2008;100:3236-3243.

Meyer PF, Oddsson LI, De Luca CJ. The role of plantar cutaneous sensation in unperturbed stance. *Exp Brain Res*. 2004;156:505-512.

Mezzarane RA, Nakajima T, Zehr EP. After stroke bidirectional modulation of soleus stretch reflex amplitude emerges during rhythmic arm cycling. *Front Hum Neurosci*. 2014;8:136.

Mildren RL, Hare CM, Bent LR. Cutaneous afferent feedback from the posterior ankle contributes to proprioception. *Neurosci Lett*. 2017;636:145-150.

Mildren RL, Peters RM, Carpenter MG, Blouin JS, Inglis JT. Soleus single motor units show stronger coherence with Achilles tendon vibration across a broad bandwidth

relative to medial gastrocnemius units while standing. *J Neurophysiol*. 2019;122:2119-2129.

Mildren RL, Peters RM, Hill AJ, Blouin JS, Carpenter MG, Inglis JT. Frequency characteristics of human muscle and cortical responses evoked by noisy Achilles tendon vibration. *J Appl Physiol (1985)*. 2017;122:1134-1144.

Mildren RL, Strzalkowski ND, Bent LR. Foot sole skin vibration perceptual thresholds are elevated in a standing posture compared to sitting. *Gait Posture*. 2016;43:87-92.

Miles TS, Turker KS, Le TH. Ia reflexes and EPSPs in human soleus motor neurones. *Exp Brain Res*. 1989;77:628-636.

Miller DM, Baker JF, Rymer WZ. Ascending vestibular drive is asymmetrically distributed to the inferior oblique motoneuron pools in a subset of hemispheric stroke survivors. *Clin Neurophysiol*. 2016;127:2022-2030.

Miller DM, Klein CS, Suresh NL, Rymer WZ. Asymmetries in vestibular evoked myogenic potentials in chronic stroke survivors with spastic hypertonia: evidence for a vestibulospinal role. *Clin Neurophysiol*. 2014;125:2070-2078.

Miller DM, Rymer WZ. Sound-evoked biceps myogenic potentials reflect asymmetric vestibular drive to spastic muscles in chronic hemiparetic stroke survivors. *Front Hum Neurosci*. 2017;11:535.

Mima T, Hallett M. Corticomuscular coherence: a review. *J Clin Neurophysiol*. 1999;16:501-511.

Misiaszek JE. The H-reflex as a tool in neurophysiology: its limitations and uses in understanding nervous system function. *Muscle Nerve*. 2003;28:144-160.

Miwa T, Miwa Y, Kanda K. Dynamic and static sensitivities of muscle spindle primary endings in aged rats to ramp stretch. *Neurosci Lett*. 1995;201:179-182.

Morales FR, Boxer PA, Fung SJ, Chase MH. Basic electrophysiological properties of spinal cord motoneurons during old age in the cat. *J Neurophysiol*. 1987;58:180-194.

Morgan DL, Prochazka A, Proske U. Action of single dynamic fusimotor neurones on cat soleus Ia afferents during muscle shortening. *Exp Brain Res*. 1985;58:56-61.

Morita H, Crone C, Christenhuis D, Petersen NT, Nielsen JB. Modulation of presynaptic inhibition and disynaptic reciprocal Ia inhibition during voluntary movement in spasticity. *Brain*. 2001;124:826-837.

Morita H, Petersen N, Christensen LO, Sinkjaer T, Nielsen J. Sensitivity of H-reflexes and stretch reflexes to presynaptic inhibition in humans. *J Neurophysiol*. 1998;80:610-620.

Morita H, Shindo M, Yanagawa S, Yoshida T, Momoi H, Yanagisawa N. Progressive decrease in heteronymous monosynaptic Ia facilitation with human ageing. *Exp Brain Res*. 1995;104:167-170.

Morse CI, Thom JM, Birch KM, Narici MV. Changes in triceps surae muscle architecture with sarcopenia. *Acta Physiol Scand*. 2005;183:291-298.

Mottram CJ, Heckman CJ, Powers RK, Rymer WZ, Suresh NL. Disturbances of motor unit rate modulation are prevalent in muscles of spastic-paretic stroke survivors. *J Neurophysiol*. 2014;111:2017-2028.

Murnaghan CD, Squair JW, Chua R, Inglis JT, Carpenter MG. Cortical contributions to control of posture during unrestricted and restricted stance. *J Neurophysiol*. 2014;111:1920-1926.

Mynark RG. Reliability of the soleus H-reflex from supine to standing in young and elderly. *Clin Neurophysiol*. 2005;116:1400-1404.

Mynark RG, Koceja DM. Down training of the elderly soleus H reflex with the use of a spinally induced balance perturbation. *J Appl Physiol (1985)*. 2002;93:127-133.

Nakajima T, Sakamoto M, Tazoe T, Endoh T, Komiyama T. Location specificity of plantar cutaneous reflexes involving lower limb muscles in humans. *Exp Brain Res*. 2006;175:514-525.

Nardone A, Corna S, Turcato AM, Schieppati M. Afferent control of walking: are there distinct deficits associated to loss of fibres of different diameter? *Clin Neurophysiol*. 2014;125:327-335.

Nardone A, Siliotto R, Grasso M, Schieppati M. Influence of aging on leg muscle reflex responses to stance perturbation. *Arch Phys Med Rehabil*. 1995;76:158-165.

Nguyen DAT, Lewis RHC, Gandevia SC, Butler JE, Hudson AL. Discharge properties of human diaphragm motor units with ageing. *J Physiol*. 2019;597:5079-5092.

Nichols TR, Houk JC. Improvement in linearity and regulation of stiffness that results from actions of stretch reflex. *J Neurophysiol*. 1976;39:119-142.

Obata H, Kawashima N, Akai M, Nakazawa K, Ohtsuki T. Age-related changes of the stretch reflex excitability in human ankle muscles. *J Electromyogr Kinesiol*. 2010;20:55-60.

O'Dwyer NJ, Ada L, Neilson PD. Spasticity and muscle contracture following stroke. *Brain*. 1996;119 (Pt 5):1737-1749.

Perez MA, Soteropoulos DS, Baker SN. Corticomuscular coherence during bilateral isometric arm voluntary activity in healthy humans. *J Neurophysiol*. 2012;107:2154-2162.

Peters RM, Dalton BH, Blouin JS, Inglis JT. Precise coding of ankle angle and velocity by human calf muscle spindles. *Neuroscience*. 2017;349:98-105.

Pierrot-Deseilligny E, Bergego C, Katz R, Morin C. Cutaneous depression of Ib reflex pathways to motoneurones in man. *Exp Brain Res*. 1981;42:351-361.

Pierrot-Deseilligny E, Burke D. The circuitry of the human spinal cord. *Cambridge University Press*. 2012.

Pollock CL, Hunt MA, Vieira TM, Gallina A, Ivanova TD, Garland SJ. Challenging standing balance reduces the asymmetry of motor control of postural sway poststroke. *Motor Control*. 2019;23:327-343.

Prochazka A, Hulliger M, Zangger P, Appenteng K. 'Fusimotor set': new evidence for alpha-independent control of gamma-motoneurones during movement in the awake cat. *Brain Res*. 1985;339:136-140.

Proske U. The role of muscle proprioceptors in human limb position sense: a hypothesis. *J Anat*. 2015;227:178-183.

Proske U, Gandevia SC. The proprioceptive senses: their roles in signaling body shape, body position and movement, and muscle force. *Physiol Rev*. 2012;92:1651-1697.

Rathelot JA, Strick PL. Muscle representation in the macaque motor cortex: an anatomical perspective. *Proc Natl Acad Sci U S A*. 2006;103:8257-8262.

Regehr WG. Short-term presynaptic plasticity. *Cold Spring Harb Perspect Biol*. 2012;4:a005702.

Roll R, Kavounoudias A, Roll JP. Cutaneous afferents from human plantar sole contribute to body posture awareness. *Neuroreport*. 2002;13:1957-1961.

Rosenberg JR, Amjad AM, Breeze P, Brillinger DR, Halliday DM. The Fourier approach to the identification of functional coupling between neuronal spike trains. *Prog Biophys Mol Biol*. 1989;53:1-31.

Rossi A, Mazzocchio R. Cutaneous control of group I pathways from ankle flexors to extensors in man. *Exp Brain Res*. 1988;73:8-14.

Rothwell JC. Control of human voluntary movement. *Springer Science & Business Media.* 1994;New York USA.

Rudomin P, Schmidt RF. Presynaptic inhibition in the vertebrate spinal cord revisited. *Exp Brain Res*. 1999;129:1-37.

Sabbahi MA, Sedgwick EM. Age-related changes in monosynaptic reflex excitability. *J Gerontol*. 1982;37:24-32.

Sakai ST, Davidson AG, Buford JA. Reticulospinal neurons in the pontomedullary reticular formation of the monkey (Macaca fascicularis). *Neuroscience*. 2009;163:1158-1170.

Sanchez N, Dewald JP. Constraints imposed by the lower extremity extensor synergy in chronic hemiparetic stroke: Preliminary findings. *Conf Proc IEEE Eng Med Biol Soc*. 2014;2014:5804-5807.

Sangani SG, Starsky AJ, McGuire JR, Schmit BD. Multijoint reflex responses to constant-velocity volitional movements of the stroke elbow. *J Neurophysiol*. 2009;102:1398-1410.

Sangani SG, Starsky AJ, McGuire JR, Schmit BD. Multijoint reflexes of the stroke arm: neural coupling of the elbow and shoulder. *Muscle Nerve*. 2007;36:694-703.

Sawacha Z, Carraro E, Contessa P, Guiotto A, Masiero S, Cobelli C. Relationship between clinical and instrumental balance assessments in chronic post-stroke hemiparesis subjects. *J Neuroeng Rehabil*. 2013;10:95-0003-10-95.

Sayenko DG, Vette AH, Kamibayashi K, Nakajima T, Akai M, Nakazawa K. Facilitation of the soleus stretch reflex induced by electrical excitation of plantar cutaneous afferents located around the heel. *Neurosci Lett*. 2007;415:294-298.

Sayenko DG, Vette AH, Obata H, Alekhina MI, Akai M, Nakazawa K. Differential effects of plantar cutaneous afferent excitation on soleus stretch and H-reflex. *Muscle Nerve*. 2009;39:761-769.

Scaglioni G, Narici MV, Maffiuletti NA, Pensini M, Martin A. Effect of ageing on the electrical and mechanical properties of human soleus motor units activated by the H reflex and M wave. *J Physiol*. 2003;548:649-661.

Schepens B, Drew T. Descending signals from the pontomedullary reticular formation are bilateral, asymmetric, and gated during reaching movements in the cat. *J Neurophysiol*. 2006;96:2229-2252.

Schneider AD, Cullen KE, Chacron MJ. In vivo conditions induce faithful encoding of stimuli by reducing nonlinear synchronization in vestibular sensory neurons. *PLoS Comput Biol*. 2011;7:e1002120.

Semmler JG, Kornatz KW, Dinenno DV, Zhou S, Enoka RM. Motor unit synchronisation is enhanced during slow lengthening contractions of a hand muscle. *J Physiol*. 2002;545:681-695.

Sherrington CS. Man on his nature. *Cambridge University Press.* 1940; New York, NY.

Sherrington CS. The integrative action of the nervous system. *Yale University Press.* 1906; New Haven, CT.

Simoes C, Jensen O, Parkkonen L, Hari R. Phase locking between human primary and secondary somatosensory cortices. *Proc Natl Acad Sci U S A*. 2003;100:2691-2694.

Simon SR, Paul IL, Mansour J, Munro M, Abernethy PJ, Radin EL. Peak dynamic force in human gait. *J Biomech*. 1981;14:817-822.

Simonsen EB, Alkjaer T, Raffalt PC. Reflex response and control of the human soleus and gastrocnemius muscles during walking and running at increasing velocity. *Exp Brain Res*. 2012;219:163-174.

Singer JC, Mansfield A, Danells CJ, McIlroy WE, Mochizuki G. The effect of post-stroke lower-limb spasticity on the control of standing balance: Inter-limb spatial and temporal synchronisation of centres of pressure. *Clin Biomech (Bristol, Avon)*. 2013;28:921-926.

Sohtaoglu M, E Kiziltan M, Gunduz A, Bozluolcay M. Startle responses after different stimulus modalities differ in stroke. *Neurophysiol Clin*. 2016;46:193-199.

Son J, Hu X, Suresh NL, Rymer WZ. Prolonged time course of population excitatory postsynaptic potentials in motoneurons of chronic stroke survivors. *J Neurophysiol*. 2019;122:176-183.

Soyuer F, Ozturk A. The effect of spasticity, sense and walking aids in falls of people after chronic stroke. *Disabil Rehabil*. 2007;29:679-687.

Stenroth L, Peltonen J, Cronin NJ, Sipila S, Finni T. Age-related differences in Achilles tendon properties and triceps surae muscle architecture in vivo. *J Appl Physiol (1985)*. 2012;113:1537-1544.

Strzalkowski ND, Mildren RL, Bent LR. Thresholds of cutaneous afferents related to perceptual threshold across the human foot sole. *J Neurophysiol*. 2015;114:2144-2151.

Suresh AK, Hu X, Powers RK, Heckman CJ, Suresh NL, Rymer WZ. Changes in motoneuron afterhyperpolarization duration in stroke survivors. *J Neurophysiol*. 2014;112:1447-1456.

Suresh NL, Ellis MD, Moore J, Heckman H, Rymer WZ. Excitatory synaptic potentials in spastic human motoneurons have a short rise-time. *Muscle Nerve*. 2005;32:99-103.

Swallow M. Fibre size and content of the anterior tibial nerve of the foot. *J Neurol Neurosurg Psychiatry*. 1966;29:205-213.

Swash M, Fox KP. The effect of age on human skeletal muscle. Studies of the morphology and innervation of muscle spindles. *J Neurol Sci*. 1972;16:417-432.

Takakusaki K, Kohyama J, Matsuyama K, Mori S. Medullary reticulospinal tract mediating the generalized motor inhibition in cats: parallel inhibitory mechanisms acting on motoneurons and on interneuronal transmission in reflex pathways. *Neuroscience*. 2001;103:511-527.

ten Bruggencate G, Lundberg A. Facilitatory interaction in transmission to motoneurones from vestibulospinal fibres and contralateral primary afferents. *Exp Brain Res*. 1974;19:248-270.

Tian M, Herbert RD, Hoang P, Gandevia SC, Bilston LE. Myofascial force transmission between the human soleus and gastrocnemius muscles during passive knee motion. *J Appl Physiol (1985)*. 2012;113:517-523.

Ting LH, Chiel HJ, Trumbower RD, et al. Neuromechanical principles underlying movement modularity and their implications for rehabilitation. *Neuron*. 2015;86:38-54.

Tokuno CD, Carpenter MG, Thorstensson A, Garland SJ, Cresswell AG. Control of the triceps surae during the postural sway of quiet standing. *Acta Physiol (Oxf)*. 2007;191:229-236.

Tomlinson BE, Irving D. The numbers of limb motor neurons in the human lumbosacral cord throughout life. *J Neurol Sci*. 1977;34:213-219.

Tucker KJ, Tuncer M, Turker KS. A review of the H-reflex and M-wave in the human triceps surae. *Hum Mov Sci*. 2005;24:667-688.

Turker KS, Yang J, Scutter SD. Tendon tap induces a single long-lasting excitatory reflex in the motoneurons of human soleus muscle. *Exp Brain Res*. 1997;115:169-173.

Vallbo AB. Muscle spindle response at the onset of isometric voluntary contractions in man. Time difference between fusimotor and skeletomotor effects. *J Physiol*. 1971;218:405-431.

van Wezel BM, Ottenhoff FA, Duysens J. Dynamic control of location-specific information in tactile cutaneous reflexes from the foot during human walking. *J Neurosci*. 1997;17:3804-3814.

van Wezel BM, van Engelen BG, Gabreels FJ, Gabreels-Festen AA, Duysens J. Abeta fibers mediate cutaneous reflexes during human walking. *J Neurophysiol*. 2000;83:2980-2986.

Vaughan SK, Stanley OL, Valdez G. Impact of Aging on Proprioceptive Sensory Neurons and Intrafusal Muscle Fibers in Mice. *J Gerontol A Biol Sci Med Sci*. 2017;72:771-779.

Vette AH, Sayenko DG, Jones M, Abe MO, Nakazawa K, Masani K. Ankle muscle co-contractions during quiet standing are associated with decreased postural steadiness in the elderly. *Gait Posture*. 2017;55:31-36.

Vieira D, Silva MB, Melo MC, Soares AB. Effect of myofeedback on the threshold of the stretch reflex response of post-stroke spastic patients. *Disabil Rehabil*. 2017;39:458-467.

Voerman GE, Gregoric M, Hermens HJ. Neurophysiological methods for the assessment of spasticity: the Hoffmann reflex, the tendon reflex, and the stretch reflex. *Disabil Rehabil*. 2005;27:33-68.

Voss H. Tabulation of the absolute and relative muscular spindle numbers in human skeletal musculature. *Anat Anz*. 1971;129:562-572.

Wall PD, McMahon SB. Long range afferents in rat spinal cord. III. Failure of impulse transmission in axons and relief of the failure after rhizotomy of dorsal roots. *Philos Trans R Soc Lond B Biol Sci*. 1994;343:211-223.

Wang Y, Watanabe K, Chen L. Effect of plantar cutaneous inputs on center of pressure during quiet stance in older adults. *J Exerc Sci Fit*. 2016;14:24-28.

Warnica MJ, Weaver TB, Prentice SD, Laing AC. The influence of ankle muscle activation on postural sway during quiet stance. *Gait Posture*. 2014;39:1115-1121.

Widener GL, Cheney PD. Effects on muscle activity from microstimuli applied to somatosensory and motor cortex during voluntary movement in the monkey. *J Neurophysiol*. 1997;77:2446-2465.

Willis WD. John Eccles' studies of spinal cord presynaptic inhibition. *Prog Neurobiol*. 2006;78:189-214.

Wilson LR, Gandevia SC, Inglis JT, Gracies J, Burke D. Muscle spindle activity in the affected upper limb after a unilateral stroke. *Brain*. 1999;122 (Pt 11):2079-2088.

Witham CL, Wang M, Baker SN. Corticomuscular coherence between motor cortex, somatosensory areas and forearm muscles in the monkey. *Front Syst Neurosci*. 2010;4:10.3389/fnsys.2010.00038. eCollection 2010.

Woollacott MH, Nashner LM. Inhibition of the achilles tendon reflex by antagonist long-latency postural responses in humans. *Exp Neurol*. 1982;75:420-439.

Yang Y, Xiao J, Song W. Post-activation depression of the lower extremities in stroke patients with spasticity and spastic equinovarus deformity. *Arq Neuropsiquiatr*. 2015;73:493-498.

Yavuz SU, Mrachacz-Kersting N, Sebik O, Berna Unver M, Farina D, Turker KS. Human stretch reflex pathways reexamined. *J Neurophysiol*. 2014;111:602-612.

Zaback M, Horslen BC, Cleworth TW, et al. Influence of emotional stimuli on lower limb cutaneous reflexes during human gait. *Neurosci Lett*. 2018;664:123-127.

Zehr EP, Komiyama T, Stein RB. Cutaneous reflexes during human gait: electromyographic and kinematic responses to electrical stimulation. *J Neurophysiol*. 1997;77:3311-3325.

Zehr EP, Loadman PM. Persistence of locomotor-related interlimb reflex networks during walking after stroke. *Clin Neurophysiol*. 2012;123:796-807.

Zehr EP, Nakajima T, Barss T, et al. Cutaneous stimulation of discrete regions of the sole during locomotion produces "sensory steering" of the foot. *BMC Sports Sci Med Rehabil*. 2014;6:33-1847-6-33. eCollection 2014.

Zhan Y, Halliday D, Jiang P, Liu X, Feng J. Detecting time-dependent coherence between non-stationary electrophysiological signals--a combined statistical and time-frequency approach. *J Neurosci Methods*. 2006;156:322-332.

Zhang C, Goto N, Suzuki M, Ke M. Age-related reductions in number and size of anterior horn cells at C6 level of the human spinal cord. *Okajimas Folia Anat Jpn*. 1996;73:171-177.

Zhao H, Ren Y, Roth EJ, Harvey RL, Zhang LQ. Concurrent deficits of soleus and gastrocnemius muscle fascicles and Achilles tendon post stroke. *J Appl Physiol (1985)*. 2015;118:863-871.

Zuur AT, Lundbye-Jensen J, Leukel C, et al. Contribution of afferent feedback and descending drive to human hopping. *J Physiol*. 2010;588:799-807.